The Dissertation Committee for Norman Randall Horn Certifies that this is the approved version of the following dissertation:

Carbon Dioxide Plasticization and Conditioning of Thin Glassy Polymer Films Monitored by Gas Permeability and Optical Methods

Committee:

Don Paul, Supervisor

Chris Biewlawski

Christopher J. Ellison

Benny Freeman

Isaac Sanchez

Carbon Dioxide Plasticization and Conditioning of Thin Glassy Polymer Films Monitored by Gas Permeability and Optical Methods

by

Norman Randall Horn, B.S.Ch.E., B.S.Ch., M.S.E.

Dissertation

Presented to the Faculty of the Graduate School of

The University of Texas at Austin

in Partial Fulfillment

of the Requirements

for the Degree of

Doctor of Philosophy

The University of Texas at Austin

May, 2012

Dedication

To Katelyn and my family,

With thanks to God,

Soli Deo Gloria

Acknowledgements

Earning a doctoral degree never occurs in a vacuum; many people are involved in manners both great and small. As I look back on my own journey, I recall so many wonderful people that shaped my experience as a Ph.D. student at the University of Texas, and I take much pleasure in recounting their numerous names and contributions to my education and personal life.

My family has always been a constant source of encouragement throughout my education. My mother and father supported my interest in chemistry and engineering from the beginning, and have maintained that support during graduate school. My amazing wife Katelyn, of course, cannot be thanked enough for her love and selfless service in our first years of marriage living in Austin and attending the University of Texas. She has had to put up with the perils and demands of graduate research from a different side of the equation – the one who is left behind while the spouse works late nights and is generally a spoil-sport of the first order.

I would be neglectful if I did not recognize the influence of the University Avenue Church of Christ in my life these past six years. Besides the congregation itself, there are three people in particular worthy of special notice. Elders Hugh Gainey and Jack Wright, both chemical engineers and great men of God, have been stupendous examples to me and I aspire to their success. Eddie Sharp will always be my hero, and I cannot thank him enough for the teaching, friendship, and great memories made over many a cup of coffee.

My research group colleagues have made my time at the University of Texas at Austin a most enjoyable experience. Many thanks to Brandon Rowe, Grant Offord, Tom Murphy, Daniel Miller, Kevin Tung, Lili Cui, Katrina Czenkusch, Rajikiran Tiwari, Zach Smith, and David Sanders. I wish them all the best as they finish their doctorates and embark upon their careers, and I hope all of us have the opportunity to work together again in the future. I am also very thankful for my colleagues throughout the UT Chemical Engineering Department, and wish especially to acknowledge Mark Pond and Ashwin Dalvi for their friendship. The faculty and staff of UT-Austin deserve thanks as well.

Lastly, I want to thank especially Dr. Donald Paul, my supervising professor. Working with him has been a blessing that I did not expect to have when I initially arrived at UT, and I am incredibly grateful for the opportunity. His guidance throughout my graduate career has been absolutely invaluable. Besides his towering intellect, his wisdom in working with students is second to none. He had faith in me when I was not even sure I had faith in myself anymore. If there is anyone deserving of credit for this dissertation, it is Don Paul.

Carbon Dioxide Plasticization and Conditioning of Thin Glassy Polymer Films Monitored by Gas Permeability and Optical Methods

Norman Randall Horn, Ph.D.

The University of Texas at Austin, 2012

Supervisor: Don Paul

This research project investigated physical aging and carbon dioxide plasticization behavior of glassy polymer films. Recent studies have shown that thin glassy polymer films undergo physical aging more rapidly than thick films. This suggests that thickness may also play a role in the plasticization and conditioning responses of thin glassy films in the presence of highly-sorbing penetrants such as CO_2. The effect of film thickness on CO_2 permeation and sorption was studied extensively through carefully defined and controlled methods that provide a basis for future study of plasticization behavior.

Thin films are found to be more sensitive than thick films to CO_2 exposure, undergoing more extensive and rapid plasticization at any pressure. The response of glassy polymers films to CO_2 is not only dependent on thickness, but also on aging time, CO_2 pressure, exposure time, and prior history. Thin films experiencing constant CO_2

exposure for longer periods of time exhibit an initial large increase in CO_2 permeability, which eventually reaches a maximum, followed by a significant decrease in permeability for the duration of the experiment. Thick films, in contrast, do not seem to exhibit this trend for the range of conditions explored. For a series of different polymers, the extent of plasticization response tracks with CO_2 solubility.

There is little data available for gas sorption in thin glassy polymer films. In this work, a novel method involving spectroscopic ellipsometry is used to obtain simultaneously the film thickness and CO_2 sorption capacity for thin glassy polymer films. This allows a more comprehensive look at CO_2 permeability, sorption, and diffusivity as a function of both CO_2 pressure and exposure time. Like the gas permeation data, these experiments suggest that thin film sorption behavior is substantially different than that of thick film counterparts. Dynamic ellipsometry experiments show that refractive index minima, fractional free volume maxima, and CO_2 diffusivity maxima correlate well with observed CO_2 permeability maxima observed for thin Matrimid® films.

These experiments demonstrate that plasticization and physical aging are competing processes. Aging, however, dominates over long time scales. Over time, CO_2 diffusivity is most affected by these competing effects, and the evolution of CO_2 diffusivity is shown to be the main contributing factor to changes in CO_2 permeability at constant pressure.

Table of Contents

List of Tables

List of Figures

Chapter 1: Introduction

1.1 INTRODUCTION

Glassy polymers have long been materials of interest for gas separation membranes because they tend to have favorable permeability-selectivity characteristics relative to many rubbery polymers. However, glassy polymers are non-equilibrium materials and undergo "physical aging," which changes many material properties as the material slowly returns to an equilibrium state. As a result, any practical membrane system made of these materials must take into account how its gas transport properties evolve over time. Physical aging occurs in a similar manner for all glassy polymers, and is marked by changes in material properties such as permeability and modulus. Adding more difficulty, gas separation membranes made from glassy polymers must be very thin (~100 nm) in order to have sufficiently high flux for a practical membrane system, but thin films are known to behave differently than bulk films. Thin films undergo physical aging much more rapidly than bulk films [1–11]. The thickness effect on physical aging is currently not well-understood. A more extensive understanding of the fundamental science behind the aging behavior of thin films less than 1 μm in thickness is needed to facilitate the development of new materials for gas separation membranes.

Gas permeation in glassy polymers usually follows the dual sorption – dual mobility model [12], and effects are generally reversible for reasonable time periods. In certain cases, though, highly soluble penetrants, such as CO_2, tend to swell the polymer, increasing free volume and facilitating molecular motion, which increases the permeability of all species and decreases selectivity [13–18]. This phenomenon, termed "plasticization," understandably adds a further challenge to a membrane separation process with feeds containing any such penetrants. Plasticization is not immediately reversible; the polymer does not return to its original state following the removal of the

plasticizing molecules. This effect is sometimes called "conditioning" [19]. Due to these irreversible effects, plasticization and conditioning effects are strongly dependent on thermal history and experimental conditions.

As more concern has been given to plasticization in industrial membrane applications, the effect of thickness on CO_2 plasticization comes into question. Some researchers have suggested that thickness does indeed play a role [20–40], but systematic studies of the effect of thickness in more realistic process conditions have never been performed. Additionally, studies of gas sorption of thin films are very infrequent and, thus, knowledge of the dynamic relationship between gas permeability, sorption, and diffusivity is quite limited.

1.2 GOALS AND FOCUS OF THIS DISSERTATION

The focus of this research was to improve the fundamental understanding of physical aging and CO_2 plasticization behavior that affect the performance of glassy polymer films. The effect of film thickness on CO_2 permeation and sorption was studied extensively through carefully defined and controlled methods that provide a basis for future study of plasticization behavior. These issues are of fundamental interest and of practical importance for advancing realistic membrane systems.

This dissertation is divided into 7 chapters, including this introduction. Chapter 2 provides background information on membrane separations, glassy polymer materials, physical aging, gas transport processes, and CO_2 plasticization. The materials and experimental techniques used in this research are described in detail in Chapter 3.

Chapter 4 demonstrates conclusively that thick and thin films respond quite differently to CO_2 plasticization, using Matrimid® as a model polymer. In addition to

being dependent upon thickness, plasticization in thin films is also affected by aging time, prior history, CO_2 pressure, and exposure time. At longer exposure times unusual CO_2 permeation behavior was observed. Instead of the expected permeability increase and plateau as observed in thick films, thin films exhibit a significant increase in permeability followed by a significant decrease in permeability for the duration of the experiment.

Chapter 5 expands the study from Chapter 4 to include multiple fundamentally different polymer systems. The methods developed in Chapter 4 are applied to these new polymers to examine the general response of glassy polymers to CO_2. The maximum permeability maximum observed with Matrimid® was also observed in the other polymers studied.

Knowledge of gas sorption behavior in thin films is quite limited. In Chapter 6, a novel method for using ellipsometry to obtain gas sorption data in thin films is presented, and CO_2 sorption in four different types of glassy polymers is investigated. The CO_2 sorption data obtained for Matrimid® is correlated with similar permeation data to develop, for the first time, a definitive look at the relationship between CO_2 permeability, sorption, and diffusivity as a function of both CO_2 pressure and exposure time.

Finally, Chapter 7 presents conclusions from this work and recommendations for future studies of CO_2 plasticization and sorption behavior in glassy polymers that will be relevant to the fields of membrane separation technology and polymer physics.

1.3 REFERENCES

[1] Y. Huang and D. R. Paul, "Physical aging of thin glassy polymer films monitored by gas permeability," *Polymer*, vol. 45, pp. 8377-8393, 2004.

[2] Y. Huang and D. R. Paul, "Experimental methods for tracking physical aging of thin glassy polymer films by gas permeation," *Journal of Membrane Science*, vol. 244, pp. 167-178, 2004.

[3] Y. Huang and D. R. Paul, "Physical Aging of Thin Glassy Polymer Films Monitored by Optical Properties," *Macromolecules*, vol. 39, no. 4, pp. 1554-1559, 2006.

[4] Y. Huang, X. Wang, and D. R. Paul, "Physical aging of thin glassy polymer films: Free volume interpretation," *Journal of Membrane Science*, vol. 277, no. 1-2, pp. 219-229, 2006.

[5] Y. Huang and D. R. Paul, "Effect of Film Thickness on the Gas-Permeation Characteristics of Glassy Polymer Membranes," *Industrial and Engineering Chemistry Research*, vol. 46, no. 8, pp. 2342-2347, 2007.

[6] M. S. McCaig and D. R. Paul, "Effect of film thickness on the changes in gas permeability of a glassy polyarylate due to physical aging. Part I. Experimental Observations," *Polymer*, vol. 41, pp. 629-637, 2000.

[7] M. S. McCaig, D. R. Paul, and J. W. Barlow, "Effect of film thickness on the changes in gas permeability of a glassy polyarylate due to physical aging. Part II. Mathematical Model," *Polymer*, vol. 41, pp. 639-648, 2000.

[8] P. H. Pfromm and W. J. Koros, "Accelerated physical ageing of thin glassy polymer films: evidence from gas transport measurements," *Polymer*, vol. 36, no. 12, pp. 2379-2387, 1995.

[9] B. W. Rowe, B. D. Freeman, and D. R. Paul, "Physical aging of ultrathin glassy polymer films tracked by gas permeability," *Polymer*, vol. 50, no. 23, pp. 5565-5575, 2009.

[10] K. D. Dorkenoo and P. H. Pfromm, "Experimental evidence and theoretical analysis of physical aging in thin and thick amorphous glassy polymer films," *Journal of Polymer Science, Part B: Polymer Physics*, vol. 37, no. 16, pp. 2239-2251, 1999.

[11] K. D. Dorkenoo and P. H. Pfromm, "Accelerated Physical Aging of Thin Poly[1-(trimethylsilyl)-1-propyne] Films," *Macromolecules*, vol. 33, no. 10, pp. 3747-3751, 2000.

[12] W. R. Vieth, J. M. Howell, and J. H. Hsieh, "Dual sorption theory," *Journal of Membrane Science*, vol. 1, pp. 177-220, 1976.

[13] E. S. Sanders, "Penetrant-induced plasticization and gas permeation in glassy polymers," *Journal of Membrane Science*, vol. 37, no. 1, pp. 63–80, 1988.

[14] J. S. Chiou and D. R. Paul, "Effecs of carbon dioxide exposure on gas transport of properties of glassy polymers," *Journal of Membrane Science*, vol. 32, pp. 195-205, 1987.

[15] J. S. Chiou, J. W. Barlow, and D. R. Paul, "Plasticization of Glassy Polymers by CO_2," *Journal of Applied Polymer Science*, vol. 30, no. 6, pp. 2633-2642, 1985.

[16] R. T. Chern and C. N. Provan, "Gas-induced plasticization and the permselectivity of poly(tetrabromophenolphthalein terephthalate) to a mixture of carbon dioxide and methane," *Macromolecules*, vol. 24, no. 9, pp. 2203-2207, 1991.

[17] M. Wessling, S. Schoeman, T. van der Boomgaard, and C. A. Smolders, "Plasticization of gas separation membranes," *Gas Separation and Purification*, vol. 5, no. 4, pp. 222-228, 1991.

[18] W. J. Koros and D. R. Paul, "Sorption and Transport of CO_2 Above and Below the Glass Transition of Poly (Ethylene Terephthalate)," *Polymer Engineering and Science*, vol. 20, no. 1, pp. 14-19, 1980.

[19] A. G. Wonders and D. R. Paul, "Effect of CO_2 exposure history on sorption and transport in polycarbonate," *Journal of Membrane Science*, vol. 5, pp. 63–75, 1979.

[20] A. R. Berens, "Diffusion and relaxation in glassy polymer powders: 1. Fickian diffusion of vinyl chloride in poly (vinyl choride)," *Polymer*, vol. 18, pp. 697-704, 1977.

[21] A. R. Berens and H. B. Hopfenberg, "Diffusion and relaxation in glassy polymer powders: 2. Separation of diffusion and relaxation parameters," *Polymer*, vol. 19, pp. 489-96, 1978.

[22] A. R. Berens and H. B. Hopfenberg, "Induction and measurement of glassy state relaxations by vapor sorption techniques," *Journal of Polymer Science, Part B: Polymer Physics*, vol. 17, pp. 1757-70, 1979.

[23] A. R. Berens, "Analysis of transport behavior in polymer powders," *Journal of Membrane Science*, vol. 3, no. 2-3-4, pp. 247-64, 1978.

[24] A. R. Berens, "Transport of plasticizing penetrants in glassy polymers," *ACS Symposium Series: Barrier Polymer Structures*, vol. 423, pp. 92-110, 1990.

[25] A. R. Berens, "Gravimetric and Volumetric Study of the Sorption of Gases and Vapors in Poly(Vinyl Chloride) Powders," *Polymer Engineering and Science*, vol. 20, no. 1, pp. 95-101, 1980.

[26] M. Wessling, M. L. Lopez, and H. Strathmann, "Accelerated plasticization of thin-film composite membranes used in gas separation," *Separation and Purification Technology*, vol. 24, no. 1-2, pp. 223-233, 2001.

[27] C. Zhou, T.-S. Chung, R. Wang, Y. Liu, and S. H. Goh, "The accelerated CO_2 plasticization of ultra-thin polyimide films and the effect of surface chemical cross-linking on plasticization and physical aging," *Journal of Membrane Science*, vol. 225, no. 1-2, pp. 125-134, 2003.

[28] P. H. Pfromm, "Gas transport properties and aging of thin and thick films made from amorphous glassy polymers," *PhD Thesis, University of Texas at Austin*, 1994.

[29] C. A. Scholes, G. Q. Chen, G. W. Stevens, and S. E. Kentish, "Plasticization of ultra-thin polysulfone membranes by carbon dioxide," *Journal of Membrane Science*, vol. 346, no. 1, pp. 208-214, 2010.

[30] T.-S. Chung, C. Cao, and R. Wang, "Pressure and temperature dependence of the gas-transport properties of dense poly[2,6-toluene-2,2-bis(3,4dicarboxylphenyl)hexafluoropropane diimide] membranes," *Journal of Polymer Science, Part B: Polymer Physics*, vol. 42, no. 2, pp. 354-364, 2004.

[31] J. H. Kim, W. J. Koros, and D. R. Paul, "Physical aging of thin 6FDA-based polyimide membranes containing carboxyl acid groups. Part II. Optical properties," *Polymer*, vol. 47, no. 9, pp. 3104-3111, 2006.

[32] J. H. Kim, W. J. Koros, and D. R. Paul, "Effects of CO_2 exposure and physical aging on the gas permeability of thin 6FDA-based polyimide membranes. Part 2. with crosslinking," *Journal of Membrane Science*, vol. 282, no. 1-2, pp. 32-43, 2006.

[33] J. H. Kim, W. J. Koros, and D. R. Paul, "Effects of CO_2 exposure and physical aging on the gas permeability of thin 6FDA-based polyimide membranes Part 1. Without crosslinking," *Journal of Membrane Science*, vol. 282, no. 1-2, pp. 21-31, 2006.

[34] J. H. Kim, W. J. Koros, and D. R. Paul, "Physical aging of thin 6FDA-based polyimide membranes containing carboxyl acid groups. Part I. Transport properties," *Polymer*, vol. 47, no. 9, pp. 3094–3103, 2006.

[35] A. M. Kratochvil, S. Damle-Mogri, and W. J. Koros, "Effects of Supercritical CO_2 Conditioning on Un-Cross-Linked Polyimide Membranes for Natural Gas Purification," *Macromolecules*, vol. 42, no. 15, pp. 5670-5675, 2009.

[36] A. M. Kratochvil and W. J. Koros, "Effects of Supercritical CO_2 Conditioning on Cross-Linked Polyimide Membranes," *Macromolecules*, vol. 43, no. 10, pp. 4679-4687, 2010.

[37] J. S. Lee, W. C. Madden, and W. J. Koros, "Antiplasticization and plasticization of Matrimid® asymmetric hollow fiber membranes. Part A. Experimental," *Journal of Membrane Science*, vol. 350, no. 1-2, pp. 232-241, 2010.

[38] J. S. Lee, W. C. Madden, and W. J. Koros, "Antiplasticization and plasticization of Matrimid® asymmetric hollow fiber membranes. Part B. Modeling," *Journal of Membrane Science*, vol. 350, no. 1-2, pp. 242-251, 2010.

[39] S. Neyertz, D. Brown, S. Pandiyan, and N. van der Vegt, "Carbon Dioxide Diffusion and Plasticization in Fluorinated Polyimides," *Macromolecules*, vol. 43, no. 18, pp. 7813-7827, 2010.

[40] B. W. Rowe, B. D. Freeman, and D. R. Paul, "Influence of previous history on physical aging in thin glassy polymer films as gas separation membranes," *Polymer*, vol. 51, no. 16, pp. 3784-3792, 2010.

Chapter 2: Background

2.1 MEMBRANE SEPARATIONS

Membranes act as molecular-scale filters that enrich one component of a high pressure gas stream by selectively permeating the other component (Figure 2.1). For instance, the desirable component of a natural gas stream (CH_4) differs in effective diffusion cross-section by only 0.5 Å from the undesirable contaminant (CO_2).

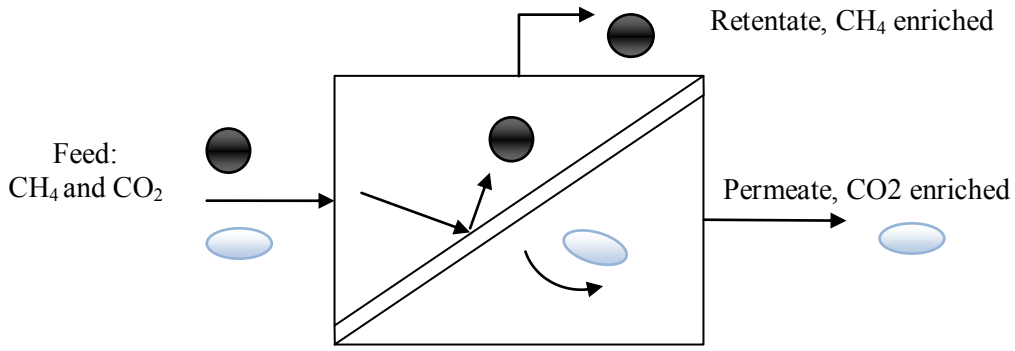

Figure 2.1: Schematic of a membrane-based separation

Matteuci et al. have published a thorough review of the fundamentals of membrane separations [1]. Gas transport in non-porous polymeric membranes occurs via a solution-diffusion mechanism, originally developed in the 19th century by Mitchell [2], Graham [3], and von Wroblewski [4]. According to this model, gas transport involves a two-stage process whereby gas first sorbs into the polymer and then diffuses across the thickness of the membrane.

Gas transport in polymer films is frequently described in terms of permeability, which refers to the pressure- and thickness-normalized molar gas flux of gas through a polymer. Permeability is an intrinsic property for a given polymer/gas pair. An analysis of Fick's first law for a plane polymer film leads to the following relationship for the permeability of a gas in a polymer:

$$P = \left(\frac{C_2 - C_1}{p_2 - p_1}\right) D \quad (2.1)$$

Where C_1 and C_2 are the gas concentrations in the polymer at the downstream and upstream faces of the membrane, respectively, and are in equilibrium with the external pressures p_1 and p_2. When the upstream pressure and concentration are much greater than the corresponding downstream values, the result is simplified:

$$P = (C/p)D \quad (2.2)$$

The C/p term is simply the equilibrium solubility coefficient S of the material, and thus Equation 2 can be further simplified to the well-known result:

$$P = D \times S \quad (2.3)$$

This important result emphasizes that gas permeability relies upon two factors: the thermodynamic term S that describes how much gas is sorbed into the polymer matrix, and the kinetic term D that characterizes how gas molecules move through the polymer once sorbed. A penetrant molecule's diffusion coefficient is dependent upon the size of the diffusing molecule and the local free volume, whereas the solubility coefficient is dependent on thermodynamic properties such as critical temperature and critical volume.

2.2 THE GLASSY STATE, PHYSICAL AGING, AND THE FREE VOLUME CONCEPT

Simon first recognized the non-equilibrium state of glassy materials [5,6]. He proposed that, upon cooling, the molecular structure of an equilibrium liquid was "frozen in" whenever the time-scale of molecular rearrangements was longer than the time-scale

of cooling. The resultant glass has excess thermodynamic quantities, such as volume, enthalpy, or entropy (Figure 2.2). The difference between the excess state and the equilibrium state constitutes a driving force that continually reduces these quantities towards equilibrium, a process termed "physical aging." Aging in polymers, thus, is dependent on the thermal history of the sample. Thermal history can be erased and the aging clock reset by heating the sample above T_g. This basic thermodynamic and kinetic explanation of the glassy state has been generally accepted for many years.

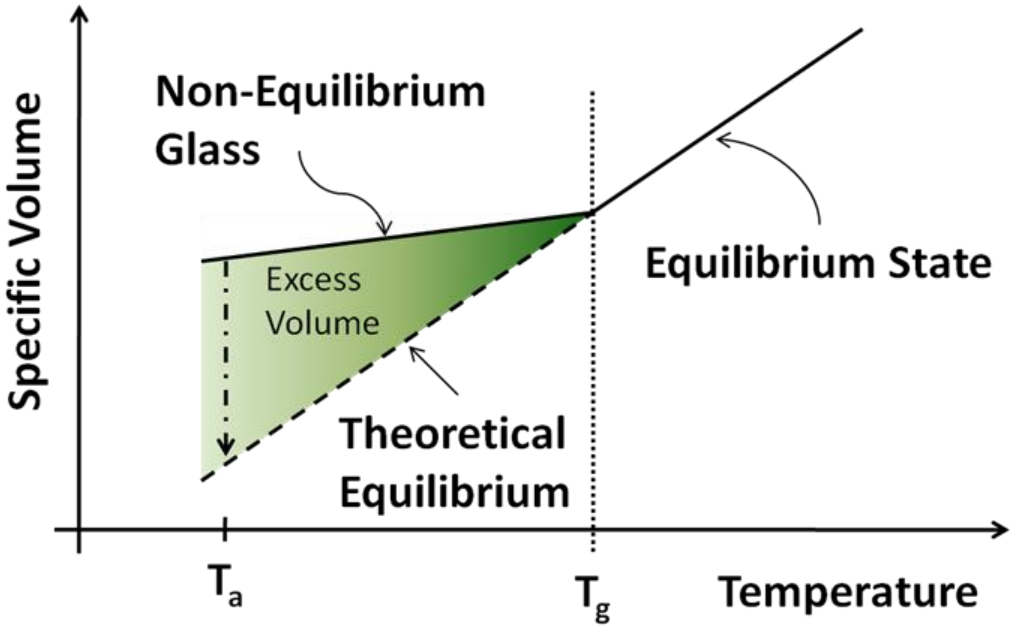

Figure 2.2: Schematic of the origin of physical aging

Struik has published an extensive systematic study of aging phenomenon in over forty polymers, focused on mechanical properties [7]. Hutchinson discusses the mechanisms and kinetics of aging processes, different tools to study aging, and theories for how aging proceeds [8]. In addition to studying thermodynamic properties, much research has investigated the effects of aging on physical properties, including creep rate

and toughness [7], storage modulus and elastic modulus [9], density [10], and yield stress [11].

Much effort has been expended studying thick glassy films under the assumption that the properties of thick films are approximately those of thin films. However, evidence from aging studies supports the contrary. At short aging times, permeability values of thin films tend to be significantly higher than those of thick films. This is believed to be the result of a higher state of free volume in thin films.[18] At longer aging times, permeability values drop well below the corresponding bulk values. These observations have led many to conclude that thin films undergo more rapid physical aging than their thick film counterparts. The rate of physical aging has been shown to increase as film thickness decreases (Figure 2.3). Multiple mechanisms have been proposed to explain these phenomena, but no definitive proof exists at this time. One possible explanation for this effect is that free volume elements diffuse to the surface and escape, while at the same time polymer chains compact closer together via "lattice contraction" [12–14]. Another explanation is that constraints on relaxation times are reduced as glassy films become thinner, and thus the relaxation rate accelerates.

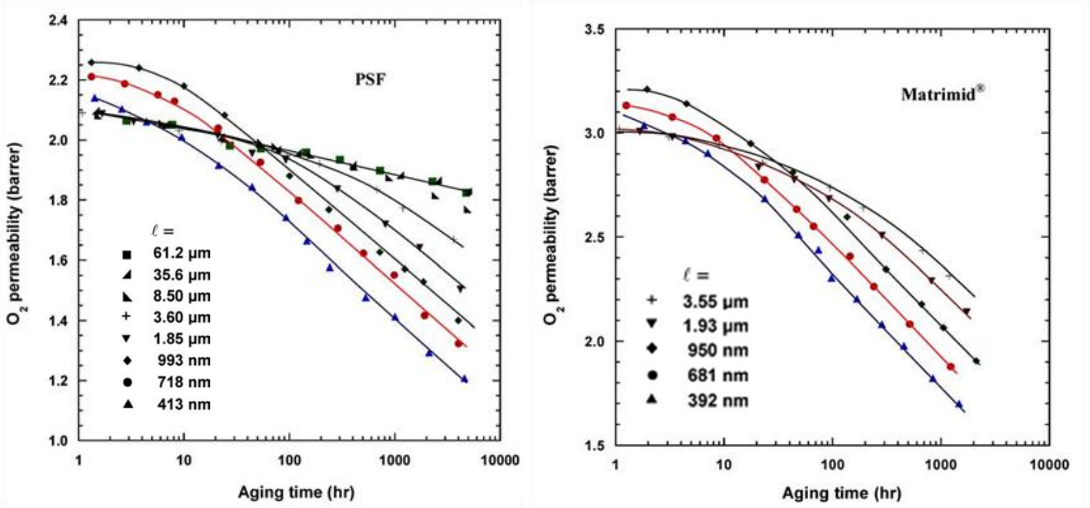

Figure 2.3: Evidence of rapid physical aging in thin glassy films and of aging rate increasing as thickness decreases, from Huang et al. [15].

It seems apparent that the practice of using thick film data as the basis for designing a thin film membrane device is a rough approximation at best. Thin film physical aging is fundamentally different than that of thick films especially with regards to time-dependent behavior, and these materials require careful study to be used appropriately.

2.3 PLASTICIZATION AND CONDITIONING EFFECTS IN POLYMER MEMBRANES

At temperatures greater than the glass transition temperature (T_g), amorphous polymers are nearly always in a state of physical equilibrium, and their gas permeation properties at low sorption levels are characterized by constant permeability, diffusivity, and solubility coefficients. High sorption levels of more soluble gases, such as CO_2, can "plasticize" these polymers, resulting in an increase in permeability and diffusivity with concentration [16]. These effects are reversible upon removal of penetrant, with no

observable time and thickness effects. The gas concentration alone determines the transport properties.

As discussed in Section 2.2, a polymer below T_g is in a non-equilibrium state, but for bulk polymers, i.e., thick films, the rate of progress toward equilibrium, termed physical aging, is very slow. At relatively low penetrant concentrations, permeation usually follows the dual sorption - dual mobility model [17] and the effects of penetrant sorption are mostly reversible over reasonable time periods. However, "plasticization" can occur at high penetrant concentrations owing to increased free volume that facilitates molecular motions and, thereby, increases the permeability of all gas species [18–22]. Once the plasticizer is removed, the polymer may not immediately return to its previous state, an effect sometimes called "conditioning" [23]. Conditioning is not immediately reversible, and all changes depend on the thermodynamic history and experimental conditions.

2.4 THE EFFECT OF THICKNESS UPON CARBON DIOXIDE PERMEATION BEHAVIOR

Most gas separation membranes are made of glassy polymers, and understandably the "plasticization" effect is very important as membrane technology is extended to cases where there are high partial pressures of penetrants that are highly soluble in the polymer, such as natural gas streams with high CO_2 contents. This is a very complex problem for several reasons. Practical membranes must be very thin, ~100 nm, in order to obtain high flux or productivity, but such thin structures are now well known to behave differently than thicker counterparts. For instance, gas transport through glassy polymers is significantly affected by physical aging. Physical aging has been extensively studied in

bulk polymers [7], but films below ~1 micron in thickness exhibit greatly accelerated physical aging relative to the bulk state [12,13,15,24–31]. The reason for the thickness effect in thin films is not well-understood, but there is every reason to expect that thickness also plays a role in plasticization and conditioning behavior. Furthermore, plasticization and physical aging are competitive processes; as plasticization changes the state of the polymer over time, physical aging is perturbed, and vice versa. Consequently, any practical membrane system made from glassy polymers must take into account how gas transport properties evolve over time due to these processes.

Much effort has been expended studying CO_2 transport in thick glassy films, generally under the implicit assumption that the properties of thick films mimic those of thin films [32–36]. There have been a few investigations concerned with CO_2 plasticization in thin films, but systematic studies of this phenomenon are extremely limited. Berens [37–40] and Hopfenberg [41,42] studied gas sorption kinetics in polymer powders and suggested that particle size played some role in transport properties; however, they did not extensively study the size effect with plasticizing molecules. Wessling et al. and Zhou et al. observed accelerated plasticization in composite membranes and polyimide membranes, respectively, with thicknesses varying from 0.5 to 4 μm [43,44]. Zhou suggests that the so-called "plasticization pressure" is thickness dependent, in contrast with Pfromm [45]. Scholes et al. reported significant plasticization for thin films below the plasticization pressure and used an expanded dual-sorption model to fit their data [46]. Chung et al. also observed that the plasticization pressure was inadequate to determine the incipient point of plasticization, but their work focused on thicker films (~50 μm) [47]. Kim et al. described the effects of CO_2 exposure on thin 6FDA-based polyimide membrane systems [48–51]. Kratochvil et al. showed an

unexpected decline in CO_2 permeability and sorption above the supercritical point of CO_2 for uncrosslinked 6F-based polyimide thick membranes, but did not see a decline for crosslinked membranes under similar conditions [52,53]. Lee et al. investigated how highly-sorbing organic vapors contaminants, such as toluene or n-heptane, affect the CO_2/CH_4 separation performance of Matrimid® hollow-fiber membranes [54,55]. Pandiyan, Neyertz, and coworkers performed CO_2 solubility, diffusion, and plasticization simulations consistent with prior experimental results, but the timescale of the simulation was only a few nanoseconds [56,57]. Most recently, Rowe et al. demonstrated that prior CO_2 exposure history plays an unusual role in physical aging behavior in thin polysulfone films [58]. Clearly, there is growing evidence that CO_2 effects on permeation behavior are thickness dependent.

It will be shown in this work that thick and thin films respond quite differently to CO_2 plasticization [59,60]. In addition to seeing thickness dependence, plasticization in thin films is demonstrated to be dependent on aging time, prior history, CO_2 pressure, and exposure time. At longer exposure times unusual CO_2 permeation behavior was observed. Instead of the expected permeability increase and plateau as observed in thick films, thin films exhibit a significant increase in permeability followed by a significant decrease in permeability for the duration of the experiment.

2.5 THE EFFECT OF THICKNESS UPON CARBON DIOXIDE SORPTION BEHAVIOR

As mentioned previously, gas transport in polymers follows the solution-diffusion model, whereby a gas first dissolves into the polymer and then diffuses through the thickness of the polymer. The gas permeability of any polymer film consists of a

solubility component, which is thermodynamic in nature, and a diffusivity component, which is kinetic in nature. They are related by the well-known equation, $P = D \times S$. If two of the terms can be directly measured, then the third can be simply calculated.

Gas permeability can be measured in a number of ways, most notably with constant volume systems [61]. Solubility can be measured by gravimetric methods, such as magnetic suspension balance [62] or Cahn microbalance [39,46,63,64], or by measuring pressure decay in a well-sealed constant volume system [16,65]. Diffusivity can be calculated for transient experiments from the time lag and the well-known equation $D = l^2 / 6\, t_{lag}$. For bulk polymer films, these methods have been widely used and are well-understood.

Gas sorption in thin polymer films, though, is not often investigated for two reasons. First, the time scale of diffusion is very short for thin films, and, thus, it is impossible to estimate sorption from a combination of permeability and time lag experiments. Second, the typical experimental methods for directly measuring sorption in thick films cannot be used with thin films. Pressure decay, magnetic suspension balance, and Cahn microbalance instruments require relatively large quantities of sample so thin films cannot be used in these devices. Quartz crystal microbalances have seen some use for measuring gas sorption in thin polymer films [66–69], but a number of issues have limited its use.

Since the aforementioned methods are not useful for measuring sorption in thin films directly, the effect of thickness on gas sorption of both plasticizing and non-plasticizing gases in glassy polymers has not been explored to any significant extent. Thickness effects have been observed in physical aging [12,26–29] and plasticization

studies [59,60], though, and those results suggest that gas sorption in glassy polymers may also be dependent upon thickness. Tan et al. used x-ray reflectivity to study water sorption in thin polyimide films (l < 100 nm) and observed thickness-dependent swelling [70]. A survey of the literature [63,64,71–75] indicates that the extent of CO_2 sorption for the polyimide Matrimid® varies widely from one report to another, as seen in Figure 2.4. Some of these differences might be attributable to different sample histories, sample preparation procedures, experimental techniques, etc., but it appears film thickness may also be a factor.

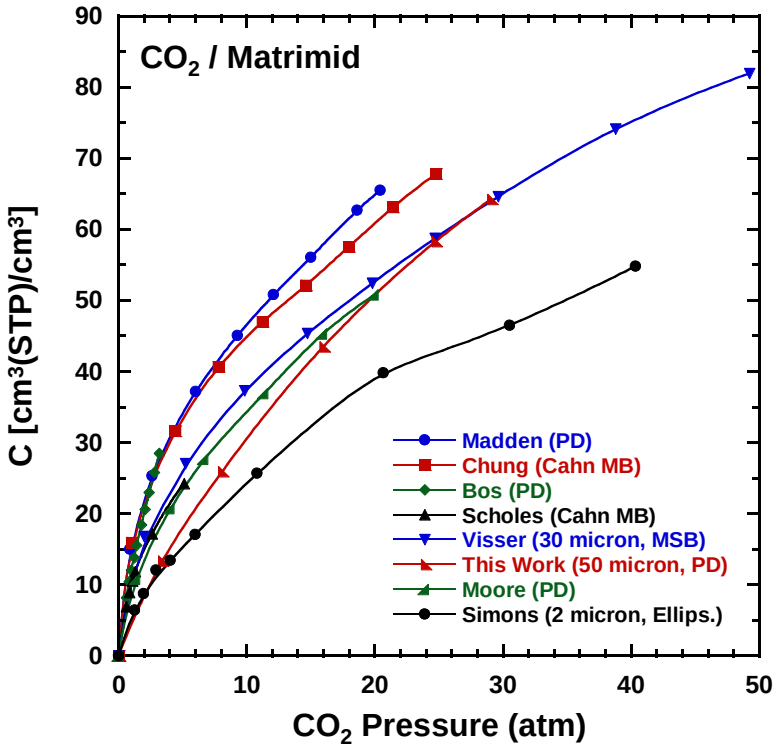

Figure 2.4: Literature data for Matrimid® CO_2 sorption Isotherms obtained from various methods and thicknesses. PD = Pressure Decay, MSB = Magnetic Suspension Balance, MB = Microbalance. [63,64,71–75]

A small number of papers have reported sorption data for thin polymer films using spectroscopic ellipsometry. Ellipsometry is a powerful method for characterizing thin polymer films, but the technique has been underutilized as a tool for obtaining sorption data. Sirard et al. investigated swelling and sorption in thin PDMS films with supercritical CO_2, showing that at high CO_2 pressures (>50 atm) thin PDMS films swell nearly 10% more than bulk PDMS films [76]. Wind et al. observed some differences in the thin film values of dual-sorption model parameters for CO_2 relative to thick films in 6FDA-DAM:DABA and its cyclohexanedimethanol monoester, and substantially different CO_2 sorption at constant pressure for longer exposure times [34,77]. They attributed this difference primarily to the effect of thermal treatments on the films rather than to the effect of thickness itself. Wind noted, though, that the possibility of a fundamental difference between bulk films and thin films could not be ruled out, and suggested studying the effect of thickness as an avenue of future research. Finally, Wind hypothesized that the assumptions of the optical model, such as constant specific refraction, might be too simplistic to capture the subtleties of CO_2 sorption behavior. In contrast, Rowe et al. used ellipsometry to track the effect of relative humidity upon thin films, and their results suggested that a polymer's specific refraction is indeed independent of density and temperature [78]. Even so, Rowe's approach assumed that the equilibrium sorption in thick and thin films was the same when compared at the same density or refractive index and thus did not conclude that sorption behavior differed in thick and thin films. Most recently, Simons et al. found that CO_2 sorption behavior for films ~2-3 μm, measured via ellipsometry, only differed from bulk films in the Langmuir capacity (C_H') parameter of the dual-sorption model; the Henry's law constant (k_d) and Langmuir affinity parameter (b) showed no thickness dependence [72].

Even though there is some evidence in the literature that CO_2 sorption behavior differs between thick and thin glassy polymer films, no systematic study has been done to solidify this conclusion. This work presents a method for measuring gas sorption with spectroscopic ellipsometry to investigate thickness-dependent CO_2 sorption of glassy polymer films. The sorption data is correlated with our previous work demonstrating the effect of thickness on CO_2 permeation of thin glassy polymer films [59] to give a more complete picture of how plasticization proceeds for these materials. To this author's knowledge, this is the first time that CO_2 plasticization has been described in terms of independently obtained permeability and sorption data for thin films, with similar thicknesses and thermal histories, in order to describe CO_2 permeability, sorption, and diffusivity as a function of both pressure and exposure time.

2.6 Determining Thickness, Optical Properties, and Gas Sorption with Variable-Angle Spectroscopic Ellipsometry

Obtaining absolute permeability measurements is only possible if one accurately knows the thickness of the test material. Ellipsometry is a powerful optical method for examining the dielectric properties of thin films (including refractive index) and can characterize film thicknesses ranging from a few angstroms to several micrometers. Optical properties in polymeric materials are also closely related to structural features, and thus can be utilized to track physical aging and plasticization.

Ellipsometry detects changes in the polarization state of light reflected or transmitted from a sample surface. Light with a known polarization state is directed at the surface, and a detector at the reflection end measures the two ellipsometric angles, Ψ and Δ, which describe the change in polarization (Figure 2.5). In a typical experiment, these

values are measured numerous times at a variety of wavelengths and reflection angles, resulting in highly reproducible data. Using mathematical models provided by the instrument's software, the thickness and refractive index of a thin film can be accurately determined. A Woollam M2000-D Spectroscopic Ellipsometer was used in this research.

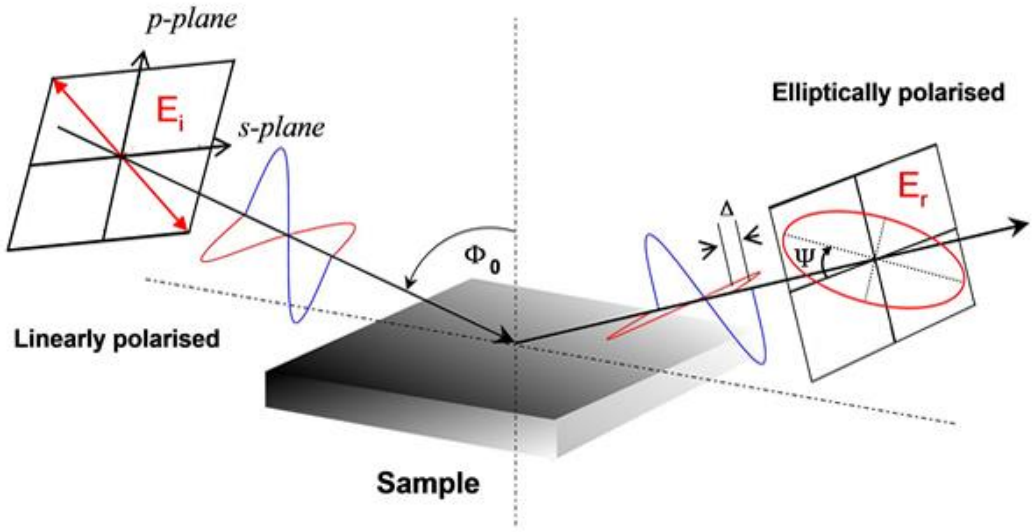

Figure 2.5: Spectroscopic Ellipsometry Schematic

Optical data obtained via ellipsometry can also be used to calculate gas sorption within a polymer film. A major advantage of using ellipsometry for measuring sorption is that the film thickness and refractive index are determined independently of each other; thickness is decoupled from other optical data. After scanning a sample, a polymer's refractive index can be calculated from the well-known Cauchy dispersion equation:

$$n(\lambda) = A + B/\lambda^2 + C/\lambda^4 \qquad (2.4)$$

where A, B, and C are constants fitted from optical data and λ is the wavelength. The Lorentz-Lorenz parameter can be calculated from the refractive index and is related to the mass density of the material by

$$L = \frac{n^2-1}{n^2+2} = q \cdot \rho \tag{2.5}$$

where q is the specific refraction of the material, a constant which can be obtained from bulk values of refractive index and density. For mixed systems of j components, the Lorentz-Lorenz equation becomes

$$\frac{n^2-1}{n^2+2} = \sum q_j \rho_j \tag{2.6}$$

This is sometimes called the Clausius-Mosotti equation [79]. For a two component system of CO_2 and polymer this becomes

$$\frac{\langle n \rangle^2-1}{\langle n \rangle^2+2} = q_{CO_2}\rho_{CO_2} + q_p\rho_p \tag{2.7}$$

where ‹n› is an averaged refractive index for a particular wavelength range. In this study, the wavelength range selected was 450 to 750 nm. For the polymer, q is calculated from known bulk values of density and refractive index. For CO_2, the Virial equation is used to calculate the density [80], and refractive index, which is pressure dependent, is determined from literature values [81].

A mass balance on the polymer film relates the polymer mass concentration of the swollen film to the thickness change due to swelling (assuming constant area due to adhesion).

$$\rho_p = \rho_p \frac{h_0}{h} \tag{2.8}$$

where ρ_p and h_0 are the density and thickness of the polymer before exposure to CO_2, respectively, and h is the thickness of the swollen film. The mass concentration of CO_2 in a polymer film can be estimated with knowledge of h_0, h, CO_2 pressure, and ‹n› by rearranging equation 4:

$$\rho_{CO_2} = \frac{1}{q_{CO_2}}\left(\frac{\langle n\rangle^2-1}{\langle n\rangle^2+2} - q_p\rho_p\frac{h_0}{h}\right) \tag{2.9}$$

The mass concentration can be converted to molar units by dividing by the molecular weight. Concentrations are conventionally reported in the literature in units of cm^3(STP)/cm^3(polymer). A plot of the change in film thickness versus the molar concentration of CO_2, denoted C_{CO2} , can be used to calculate the partial molar volume of CO_2 in the polymer [72].

$$v_{CO_2} = 22400 \cdot \frac{\partial(\Delta h/h_0)}{\partial C_{CO_2}} \tag{2.10}$$

Time-dependent experiments require the use of an "apparent molar volume" instead of the partial molar volume [77]. While partial molar volume describes the differential volume change upon further sorption of gas, apparent molar volume refers to the average volume occupied by the gas on a molar basis.

$$\phi_{v_{CO_2}} = 22400 \cdot \left[\frac{\Delta h/h_0}{C_{CO_2}}\right]_{T,P} \tag{2.11}$$

The fractional free volume of a polymer can be calculated as:

$$f = \frac{V-V_0}{V} = 1 - \rho V_0 \tag{2.12}$$

where $V = 1/\rho$ is the specific volume and V_0 is the occupied volume of the polymer (or mixed system). Maeda [82–84] and Lee [85], following Bondi [86,87], indicate that the occupied volume is closely related to the van der Waals volume, V_{vdw}:

$$V_0 = (1/\rho^*) \cdot V_{vdw} \tag{2.13}$$

where ρ^* is the unitless packing fraction at absolute zero. Van Krevelen [88] estimated that the reciprocal of the packing fraction, $1/\rho^*$, was 1.3, assuming all polymers have the same packing fraction, 1/1.3 = 0.77, at absolute zero. Sanchez and Cho [89] suggested that a more appropriate measure of V_0 was the specific volume at absolute zero, i.e., $V_0 = v_{0°K} = 1/\rho_{0°K}$. The characteristic mass density, $\rho_{0°K}$, can be obtained by extrapolating zero pressure densities to absolute zero. Van Krevelen's approximation should only be used in the absence of known values of packing fraction or characteristic mass density. Values of V_{vdw} and $\rho_{0°K}$ for the polymers of interest in this study are given in Chapter 3, Table 3.2. The packing fraction of CO_2 is 0.76 [87], and the van der Waals volume of CO_2 will be discussed further in section 4.4.

For a mixed system, the occupied volume includes contributions from each component:

$$V_{0,mix} = \sum w_j V_{0,j} = w_{CO_2} V_{0,CO_2} + (1 - w_{CO_2}) V_{0,p} \tag{2.14}$$

where w_j is the weight fraction, calculated from the mass concentrations of polymer and CO_2 as shown previously:

$$w_{CO_2} = \frac{\rho_{CO_2}}{\rho_{CO_2} + \rho_p} = \frac{\rho_{CO_2}}{\rho_{CO_2} + \rho_p \frac{h_0}{h}} \tag{2.15}$$

The denominator of equation 2.15 is also the density used to calculate the free volume of the mixed system. Making the appropriate substitutions in equation 9:

$$f = 1 - \left(\rho_{CO_2} + \rho_p \frac{h_0}{h}\right)\left[w_{CO_2} V_{0,CO_2} + (1 - w_{CO_2}) V_{0,p}\right] \quad (2.16)$$

2.7 REFERENCES

[1] S. Matteucci, Y. Yampolskii, B. D. Freeman, and I. Pinnau, "Transport of Gases and Vapors in Glassy and Rubbery Polymers," in *Materials Science of Membranes for Gas and Vapor Separation*, 2006, pp. 1-48.

[2] J. K. Mitchell, "On the Penetrativeness of Fluids," *Journal of Membrane Science*, vol. 100, pp. 11-16, 1995.

[3] T. Graham, "On the absorption and dialytic separation of gases by colloid septa." *Philosophical Magazine*, vol. 32, pp. 401-420, 1866.

[4] S. von Wroblewski, "Ueber die natur der absorption der gase durch flussigkeiten unter hohen drucken," *Ann. Physik. u. Chem.*, vol. 8, pp. 29-52, 1879.

[5] F. Simon, *Ergeg. Exaxt. Naturw.*, vol. 9, p. 222, 1930.

[6] F. Simon, *Zeitschrift fur anorganische und allgemeine Chemie*, vol. 203, p. 220, 1931.

[7] L. C. E. Struik, *Physical Aging in Amorphous Polymers and Other Materials*, vol. 54, no. 1-2. Amsterdam, The Netherlands: Elsevier Scientific Publishing Company, 1978, p. 234.

[8] J. M. Hutchinson, "Physical Aging of Polymers," *Progress in Polymer Science*, vol. 20, no. 4, pp. 703-760, 1995.

[9] J. S. Royal and J. M. Torkelson, "Physical aging effects on molecular-scale polymer relaxations monitored with mobility-sensitive fluorescent molecules," *Macromolecules*, vol. 26, no. 20, pp. 5331-5335, 1993.

[10] A. D. Drozdov, "The effect of temperature on physical aging of glassy polymers," *Journal of Applied Polymer Science*, vol. 81, no. 13, pp. 3309-3320, 2001.

[11] A. J. Hill, K. J. Heater, and C. M. Agrawal, "The Effects of Physical Aging in Polycarbonate," *Journal of Polymer Science, Part B: Polymer Physics*, vol. 28, no. 3, pp. 387-405, 1990.

[12] M. S. McCaig, D. R. Paul, and J. W. Barlow, "Effect of film thickness on the changes in gas permeability of a glassy polyarylate due to physical aging. Part II. Mathematical Model," *Polymer*, vol. 41, pp. 639-648, 2000.

[13] Y. Huang, X. Wang, and D. R. Paul, "Physical aging of thin glassy polymer films: Free volume interpretation," *Journal of Membrane Science*, vol. 277, no. 1-2, pp. 219-229, 2006.

[14] J. G. Curro, R. R. Lagasse, and R. Simha, "Diffusion model for volume recovery in glasses," *Macromolecules*, vol. 15, no. 6, pp. 1621-1626, 1982.

[15] Y. Huang and D. R. Paul, "Physical aging of thin glassy polymer films monitored by gas permeability," *Polymer*, vol. 45, pp. 8377-8393, 2004.

[16] W. J. Koros and D. R. Paul, "Sorption and Transport of CO_2 Above and Below the Glass Transition of Poly (Ethylene Terephthalate)," *Polymer Engineering and Science*, vol. 20, no. 1, pp. 14-19, 1980.

[17] W. R. Vieth, J. M. Howell, and J. H. Hsieh, "Dual sorption theory," *Journal of Membrane Science*, vol. 1, pp. 177-220, 1976.

[18] E. S. Sanders, "Penetrant-induced plasticization and gas permeation in glassy polymers," *Journal of Membrane Science*, vol. 37, no. 1, pp. 63–80, 1988.

[19] J. S. Chiou and D. R. Paul, "Effecs of carbon dioxide exposure on gas transport of properties of glassy polymers," *Journal of Membrane Science*, vol. 32, pp. 195-205, 1987.

[20] J. S. Chiou, J. W. Barlow, and D. R. Paul, "Plasticization of Glassy Polymers by CO_2," *Journal of Applied Polymer Science*, vol. 30, no. 6, pp. 2633-2642, 1985.

[21] M. Wessling, S. Schoeman, T. van der Boomgaard, and C. A. Smolders, "Plasticization of gas separation membranes," *Gas Separation and Purification*, vol. 5, no. 4, pp. 222-228, 1991.

[22] R. T. Chern and C. N. Provan, "Gas-induced plasticization and the permselectivity of poly(tetrabromophenolphthalein terephthalate) to a mixture of carbon dioxide and methane," *Macromolecules*, vol. 24, no. 9, pp. 2203-2207, 1991.

[23] A. G. Wonders and D. R. Paul, "Effect of CO_2 exposure history on sorption and transport in polycarbonate," *Journal of Membrane Science*, vol. 5, pp. 63–75, 1979.

[24] P. H. Pfromm and W. J. Koros, "Accelerated physical ageing of thin glassy polymer films: evidence from gas transport measurements," *Polymer*, vol. 36, no. 12, pp. 2379-2387, 1995.

[25] K. D. Dorkenoo and P. H. Pfromm, "Accelerated Physical Aging of Thin Poly[1-(trimethylsilyl)-1-propyne] Films," *Macromolecules*, vol. 33, no. 10, pp. 3747-3751, 2000.

[26] M. S. McCaig and D. R. Paul, "Effect of film thickness on the changes in gas permeability of a glassy polyarylate due to physical aging. Part I. Experimental Observations," *Polymer*, vol. 41, pp. 629-637, 2000.

[27] Y. Huang and D. R. Paul, "Experimental methods for tracking physical aging of thin glassy polymer films by gas permeation," *Journal of Membrane Science*, vol. 244, pp. 167-178, 2004.

[28] Y. Huang and D. R. Paul, "Physical Aging of Thin Glassy Polymer Films Monitored by Optical Properties," *Macromolecules*, vol. 39, no. 4, pp. 1554-1559, 2006.

[29] Y. Huang and D. R. Paul, "Effect of Film Thickness on the Gas-Permeation Characteristics of Glassy Polymer Membranes," *Industrial and Engineering Chemistry Research*, vol. 46, no. 8, pp. 2342-2347, 2007.

[30] B. W. Rowe, B. D. Freeman, and D. R. Paul, "Physical aging of ultrathin glassy polymer films tracked by gas permeability," *Polymer*, vol. 50, no. 23, pp. 5565-5575, 2009.

[31] K. D. Dorkenoo and P. H. Pfromm, "Experimental evidence and theoretical analysis of physical aging in thin and thick amorphous glassy polymer films," *Journal of Polymer Science, Part B: Polymer Physics*, vol. 37, no. 16, pp. 2239-2251, 1999.

[32] A. Bos, I. G. M. Pünt, M. Wessling, and H. Strathmann, "CO_2-induced plasticization phenomena in glassy polymers," *Journal of Membrane Science*, vol. 155, no. 1, pp. 67-78, 1999.

[33] A. F. Ismail and W. Lorna, "Penetrant-induced plasticization phenomenon in glassy polymers for gas separation membrane," *Separation and Purification Technology*, vol. 27, no. 3, pp. 173-194, 2002.

[34] J. D. Wind, S. M. Sirard, D. R. Paul, P. F. Green, K. P. Johnston, and W. J. Koros, "Carbon Dioxide-Induced Plasticization of Polyimide Membranes: Pseudo-Equilibrium Relationships of Diffusion, Sorption, and Swelling," *Macromolecules*, vol. 36, no. 17, pp. 6433-6441, 2003.

[35] J. D. Wind, D. R. Paul, and W. J. Koros, "Natural gas permeation in polyimide membranes," *Journal of Membrane Science*, vol. 228, no. 2, pp. 227-236, 2004.

[36] S. Kanehashi, T. Nakagawa, K. Nagai, X. Duthie, S. Kentish, and G. Stevens, "Effects of carbon dioxide-induced plasticization on the gas transport properties of glassy polyimide membranes," *Journal of Membrane Science*, vol. 298, no. 1-2, pp. 147-155, 2007.

[37] A. R. Berens, "Diffusion and relaxation in glassy polymer powders: 1. Fickian diffusion of vinyl chloride in poly (vinyl choride)," *Polymer*, vol. 18, pp. 697-704, 1977.

[38] A. R. Berens, "Analysis of transport behavior in polymer powders," *Journal of Membrane Science*, vol. 3, no. 2-3-4, pp. 247-64, 1978.

[39] A. R. Berens, "Gravimetric and Volumetric Study of the Sorption of Gases and Vapors in Poly(Vinyl Chloride) Powders," *Polymer Engineering and Science*, vol. 20, no. 1, pp. 95-101, 1980.

[40] A. R. Berens, "Transport of plasticizing penetrants in glassy polymers," *ACS Symposium Series: Barrier Polymer Structures*, vol. 423, pp. 92-110, 1990.

[41] A. R. Berens and H. B. Hopfenberg, "Diffusion and relaxation in glassy polymer powders: 2. Separation of diffusion and relaxation parameters," *Polymer*, vol. 19, pp. 489-96, 1978.

[42] A. R. Berens and H. B. Hopfenberg, "Induction and measurement of glassy state relaxations by vapor sorption techniques," *Journal of Polymer Science, Part B: Polymer Physics*, vol. 17, pp. 1757-70, 1979.

[43] M. Wessling, M. L. Lopez, and H. Strathmann, "Accelerated plasticization of thin-film composite membranes used in gas separation," *Separation and Purification Technology*, vol. 24, no. 1-2, pp. 223-233, 2001.

[44] C. Zhou, T.-S. Chung, R. Wang, Y. Liu, and S. H. Goh, "The accelerated CO_2 plasticization of ultra-thin polyimide films and the effect of surface chemical cross-linking on plasticization and physical aging," *Journal of Membrane Science*, vol. 225, no. 1-2, pp. 125-134, 2003.

[45] P. H. Pfromm, "Gas transport properties and aging of thin and thick films made from amorphous glassy polymers," *PhD Thesis, University of Texas at Austin*, 1994.

[46] C. A. Scholes, G. Q. Chen, G. W. Stevens, and S. E. Kentish, "Plasticization of ultra-thin polysulfone membranes by carbon dioxide," *Journal of Membrane Science*, vol. 346, no. 1, pp. 208-214, 2010.

[47] T.-S. Chung, C. Cao, and R. Wang, "Pressure and temperature dependence of the gas-transport properties of dense poly[2,6-toluene-2,2-bis(3,4dicarboxylphenyl) hexafluoropropane diimide] membranes," *Journal of Polymer Science, Part B: Polymer Physics*, vol. 42, no. 2, pp. 354-364, 2004.

[48] J. H. Kim, W. J. Koros, and D. R. Paul, "Physical aging of thin 6FDA-based polyimide membranes containing carboxyl acid groups. Part I. Transport properties," *Polymer*, vol. 47, no. 9, pp. 3094–3103, 2006.

[49] J. H. Kim, W. J. Koros, and D. R. Paul, "Physical aging of thin 6FDA-based polyimide membranes containing carboxyl acid groups. Part II. Optical properties," *Polymer*, vol. 47, no. 9, pp. 3104-3111, 2006.

[50] J. H. Kim, W. J. Koros, and D. R. Paul, "Effects of CO_2 exposure and physical aging on the gas permeability of thin 6FDA-based polyimide membranes Part 1. Without crosslinking," *Journal of Membrane Science*, vol. 282, no. 1-2, pp. 21-31, 2006.

[51] J. H. Kim, W. J. Koros, and D. R. Paul, "Effects of CO_2 exposure and physical aging on the gas permeability of thin 6FDA-based polyimide membranes. Part 2. with crosslinking," *Journal of Membrane Science*, vol. 282, no. 1-2, pp. 32-43, 2006.

[52] A. M. Kratochvil, S. Damle-Mogri, and W. J. Koros, "Effects of Supercritical CO_2 Conditioning on Un-Cross-Linked Polyimide Membranes for Natural Gas Purification," *Macromolecules*, vol. 42, no. 15, pp. 5670-5675, 2009.

[53] A. M. Kratochvil and W. J. Koros, "Effects of Supercritical CO_2 Conditioning on Cross-Linked Polyimide Membranes," *Macromolecules*, vol. 43, no. 10, pp. 4679-4687, 2010.

[54] J. S. Lee, W. C. Madden, and W. J. Koros, "Antiplasticization and plasticization of Matrimid® asymmetric hollow fiber membranes. Part A. Experimental," *Journal of Membrane Science*, vol. 350, no. 1-2, pp. 232-241, 2010.

[55] J. S. Lee, W. C. Madden, and W. J. Koros, "Antiplasticization and plasticization of Matrimid® asymmetric hollow fiber membranes. Part B. Modeling," *Journal of Membrane Science*, vol. 350, no. 1-2, pp. 242-251, 2010.

[56] S. Pandiyan, D. Brown, S. Neyertz, and N. van der Vegt, "Carbon Dioxide Solubility in Three Fluorinated Polyimides Studied by Molecular Dynamics Simulations," *Macromolecules*, vol. 43, no. 5, pp. 2605-2621, 2010.

[57] S. Neyertz, D. Brown, S. Pandiyan, and N. van der Vegt, "Carbon Dioxide Diffusion and Plasticization in Fluorinated Polyimides," *Macromolecules*, vol. 43, no. 18, pp. 7813-7827, 2010.

[58] B. W. Rowe, B. D. Freeman, and D. R. Paul, "Influence of previous history on physical aging in thin glassy polymer films as gas separation membranes," *Polymer*, vol. 51, no. 16, pp. 3784-3792, 2010.

[59] N. R. Horn and D. R. Paul, "Carbon dioxide plasticization and conditioning effects in thick vs. thin glassy polymer films," *Polymer*, vol. 52, no. 7, pp. 1619-1627, 2011.

[60] N. R. Horn and D. R. Paul, "Carbon dioxide plasticization of thin glassy polymer films," *Polymer*, vol. 52, no. 24, pp. 5587-5594, 2011.

[61] W. J. Koros, D. R. Paul, and A. A. Rocha, "Carbon dioxide sorption and transport in polycarbonate," *Journal of Polymer Science, Part B: Polymer Physics*, vol. 14, no. 4, pp. 687–702, 1976.

[62] G. D. Weireld, M. Frère, and R. Jadot, "Automated determination of high-temperature and high-pressure gas adsorption isotherms using a magnetic suspension balance," *Meas. Sci. & Tech.*, vol. 10, no. 2, pp. 117-126, 1999.

[63] C. A. Scholes, W. X. Tao, G. W. Stevens, and S. E. Kentish, "Sorption of methane, nitrogen, carbon dioxide, and water in Matrimid 5218," *Journal of Applied Polymer Science*, vol. 117, no. 2, pp. 2284-2289, 2010.

[64] T.-S. Chung, S. S. Chan, R. Wang, Z. Lu, and C. He, "Characterization of permeability and sorption in Matrimid/C60 mixed matrix membranes," *Journal of Membrane Science*, vol. 211, no. 1, pp. 91-99, 2003.

[65] W. J. Koros, D. R. Paul, M. Fujii, H. B. Hopfenberg, and V. Stannett, "Effect of Pressure on CO_2 Transport in Poly(Ethylene-Terephthalate)," *Journal of Applied Polymer Science*, vol. 21, no. 11, pp. 2899-2904, 1977.

[66] K.-ichi Miura et al., "Solubility and adsorption of high pressure carbon dioxide to polystyrene," *Fluid Phase Equilibria*, vol. 144, no. 1-2, pp. 181-189, 1998.

[67] J. H. Aubert, "Solubility of carbon dioxide in polymers by the quartz crystal microbalance technique," *The Journal of Supercritical Fluids*, vol. 11, no. 3, pp. 163-172, 1998.

[68] C. Zhang, B. P. Cappleman, M. Defibaugh-Chavez, and D. H. Weinkauf, "Glassy polymer-sorption phenomena measured with a quartz crystal microbalance technique," *Journal of Polymer Science, Part B: Polymer Physics*, vol. 41, no. 18, pp. 2109-2118, 2003.

[69] M. Pantoula and C. Panayiotou, "Sorption and swelling in glassy polymer/carbon dioxide systems. Part I--Sorption," *The Journal of Supercritical Fluids*, vol. 37, no. 2, pp. 254-262, 2006.

[70] N. C. B. Tan, W. L. Wu, W. E. Wallace, and G. T. Davis, "Interface effects on moisture absorption in ultrathin polyimide films," *Journal of Polymer Science, Part B: Polymer Physics*, vol. 36, no. 1, pp. 155-162, 1998.

[71] W. C. Madden, D. Punsalan, and W. J. Koros, "Age dependent CO_2 sorption in Matrimid® asymmetric hollow fiber membranes," *Polymer*, vol. 46, no. 15, pp. 5433-5436, 2005.

[72] K. Simons et al., "CO_2 sorption and transport behavior of ODPA-based polyetherimide polymer films," *Polymer*, vol. 51, no. 17, pp. 3907-3917, 2010.

[73] A. Bos, I. Pünt, H. Strathmann, and M. Wessling, "Suppression of gas separation membrane plasticization by homogeneous polymer blending," *AIChE Journal*, vol. 47, no. 5, pp. 1088-1093, 2001.

[74] T. T. Moore and W. J. Koros, "Gas sorption in polymers, molecular sieves, and mixed matrix membranes," *Journal of Applied Polymer Science*, vol. 104, no. 6, pp. 4053–4059, 2007.

[75] T. Visser and M. Wessling, "When Do Sorption-Induced Relaxations in Glassy Polymers Set In?" *Macromolecules*, vol. 40, no. 14, pp. 4992-5000, 2007.

[76] S. M. Sirard, P. F. Green, and K. P. Johnston, "Spectroscopic Ellipsometry Investigation of the Swelling of Poly(Dimethylsiloxane) Thin Films with High Pressure Carbon Dioxide," *Journal of Physical Chemistry B*, vol. 105, no. 4, pp. 766-772, 2001.

[77] J. D. Wind, S. M. Sirard, D. R. Paul, P. F. Green, K. P. Johnston, and W. J. Koros, "Relaxation dynamics of CO_2 diffusion, sorption, and polymer swelling for plasticized polyimide membranes," *Macromolecules*, vol. 36, no. 17, pp. 6442-6448, 2003.

[78] B. W. Rowe, B. D. Freeman, and D. R. Paul, "Effect of Sorbed Water and Temperature on the Optical Properties and Density of Thin Glassy Polymer Films on a Silicon Substrate," *Macromolecules*, vol. 40, no. 8, pp. 2806-2813, 2007.

[79] R. P. Feynman, R. B. Leighton, and M. Sands, *The Feynman Lectures on Physics*. Reading, MA: Addison-Wesley Publishing Company, Inc., 1963.

[80] D. R. Lide, *CRC Handbook of Chemistry and Physics*, 78th ed. New York: CRC Press, 1997.

[81] A. Michels and J. Hamers, "The effect of pressure on the refractive index of CO_2:: The Lorentz-Lorenz formula," *Physica*, vol. 4, no. 10, pp. 995–1006, 1937.

[82] Y. Maeda, *Ph.D. Dissertation, University of Texas at Austin*, 1985.

[83] Y. Maeda and D. R. Paul, "Effect of antiplasticization on gas sorption and transport. III. Free volume interpretation.," *Journal of Polymer Science, Part B: Polymer Physics*, vol. 25, no. 5, pp. 1005-1016, 1987.

[84] Y. Maeda and D. R. Paul, "Selective gas transport in miscible PPO-PS blends.," *Polymer*, vol. 26, no. 13, pp. 2055-2063, 1985.

[85] W. M. Lee, "Selection of barrier materials from molecular structure," *Polymer Engineering and Science*, vol. 20, no. 1, pp. 65-69, 1980.

[86] A. Bondi, "Van der Waals Volumes and Radii," *Journal of Physical Chemistry*, vol. 68, no. 3, pp. 441-451, 1964.

[87] A. Bondi, *Physical Properties of Molecular Crystals, Liquids, and Glasses*. New York: John Wiley & Sons, 1968.

[88] D. W. Van Krevelen, *Properties of Polymers*, 3rd ed. New York: Elsevier, 1990.

[89] I. C. Sanchez and J. Cho, "A universal equation of state for polymer liquids," *Polymer*, vol. 36, no. 15, pp. 2929-2939, 1995.

Chapter 3: Materials and Experimental Methods

3.1 GAS PERMEATION STUDIES

The following sections discuss the materials, procedures, and instruments used for the gas permeation studies presented in Chapters 4 and 5.

3.1.1 Materials

The polymer selected initially to investigate the effect of thickness upon CO_2 plasticization and conditioning behavior in glassy polymers (Chapter 4) was Matrimid® 5218, a thermoplastic polyimide made from the monomers 3,3',4,4'-benzophenone tetracarboxylic dianhydride (BTDA) and diaminophenylindane (DAPI). It has favorable high temperature properties for use in composites and adhesives and is soluble in many common solvents. Matrimid® was chosen because it is a commonly used material for commercial gas separation membranes, has a high T_g (310°C) and, thus, is deep within the glassy state during normal use at ambient conditions, and is known to be plasticized by CO_2 to a significant extent. Matrimid® 5218 was used as received from Huntsman Advanced Materials for this study. It is recommended that polyimides such as Matrimid® be dried in a vacuum oven near 100°C prior to initial use, and kept in a dessicator to avoid uptake of ambient moisture.

Two additional polymers were selected for continued study of CO_2 plasticization of thin glassy polymer films (Chapter 5): a polysulfone made from bisphenol A (PSF), and poly(2,6-dimethyl-1,4-phenylene oxide) (PPO). Along with Matrimid®, these polymers are of interest as industrial separation membrane materials. The bulk properties of the three polymers are presented in Table 3.1. Incidentally, each material is related by

phenyl groups in the repeat unit, but each has fundamentally different structural characteristics leading to different gas transport behavior.

Polymer	ρ (g/cm^3)	T_g (°C)	Refractive Index
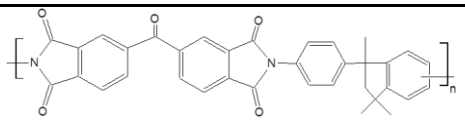 Matrimid® 5218	1.20	310	1.648
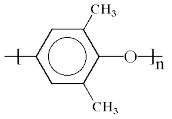 Poly(2,6, dimethyl-1,4-phenylene) oxide (PPO)	1.069	210	1.573
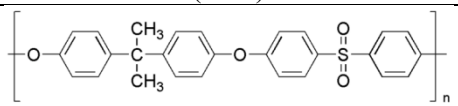 Polysulfone (PSF)	1.240	186	1.633

Table 3.1: Polymer Properties

Figure 3.1 shows CO_2 sorption isotherms at 35°C measured on thick films of the three polymers of interest [1,2]; butyl rubber is included for comparison to a rubbery material. CO_2 solubility for the glassy polymers proceeds in the order of increasing T_g, i.e. PSF < PPO < Matrimid®. Relative plasticization response was expected generally to follow the same order. However, the polymers also have quite different bulk CO_2 diffusivity coefficients. The value for Matrimid® (~1.8 x 10^8 cm^2/s, determined from time lag experiments with thick films) is nearly twice that of PSF (1.0 x 10^8 cm^2/s [3]), likely due to more efficient packing of the relatively more compact backbone of PSF. The CO_2 diffusion coefficient of PPO is an order of magnitude greater than both (17.3 x 10^8 cm^2/s [2]), attesting to its relatively higher state of free volume. This group of polymers has also been compared before in the context of physical aging [4].

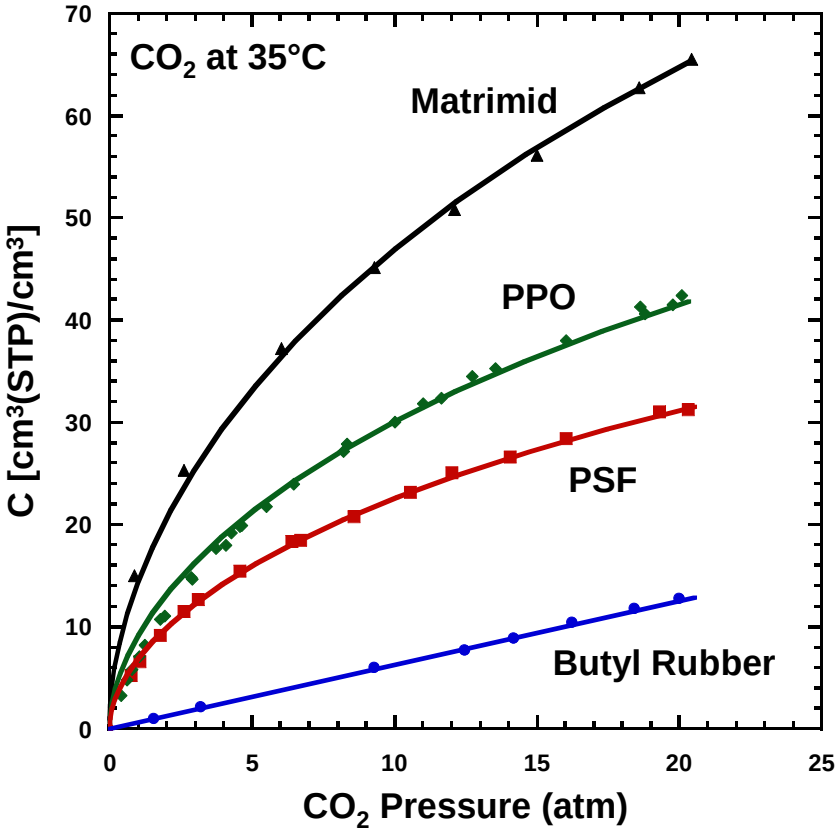

Figure 3.1: CO_2 sorption isotherms for four polymers at 35°C: Matrimid® [5], PSF [6], PPO [6,7], butyl rubber [8,9].

3.1.2 Film Formation

Thick Matrimid® films were prepared by casting solutions of polymer in dichloromethane onto silicon wafers with a steel ring barrier, all within a sealed glove bag to prevent dust particle contamination and to control evaporation of solvent. Film thickness was controlled by varying the polymer concentration from 1-2% by weight, and by varying the diameter of the casting ring. The solution was filtered twice through PTFE microfilters with pore sizes of 0.2 μm and 0.1 μm prior to casting in the glove bag. After

the solvent is fully evaporated from the surface of the film, samples were cut from the deposited thick film and dried in a vacuum oven at 70-80°C for at least three days to remove further any residual solvent in the polymer. A Dektak 6 M stylus profilometer was used to measure the thickness of each film.

Freestanding, single-layer thin films were prepared by spin casting polymer solutions onto silicon wafers; thickness was controlled by varying the concentration of polymer from 3-6 wt.%, and by varying the spin speed from 1200 to 1600 rpm for 90 s. Solvents used were cyclohexanone for Matrimid® and PSF, and chlorobenzene for PPO. The silicon wafers were thoroughly cleaned with water, acetone, and isopropyl alcohol before and after each use. Solutions were filtered three times with PTFE microfilters with pore sizes of 5 μm, 0.2 μm, and 0.1 μm prior to spin coating. Thickness was measured with a variable angle spectroscopic ellipsometer (J.A. Woollam Company, model 2000D), then a secondary coating of rubbery PDMS was spin cast directly onto the glassy layer. (This procedure will be described in more detail in the next section.) Following removal from the silicon wafers, samples were dried in a vacuum oven near 100°C overnight to remove any residual solvent and water.

3.1.3 Application of Poly(dimethylsiloxane) (PDMS) Secondary Coating

Gas transport studies for thin films are often hampered by the presence of microscopic pinhole defects, which allow undesirable convective flow to dominate gas flux and make a film non-selective. A defect fraction of 10^{-6} on an area basis is sufficient to render a film useless for gas separation [10]. However, coating a second layer of a highly-permeable polymer such as poly(dimethylsiloxane) (PDMS) directly on top of the

selective glassy layer (Figure 3.2) can mitigate defects by blocking convective flow [10]. Thus, the effect of defects is directly proportional to the fractional surface area occupied by the defects. At ambient conditions, PDMS is a rubbery polymer whose gas transport properties do not change with time due to physical aging.

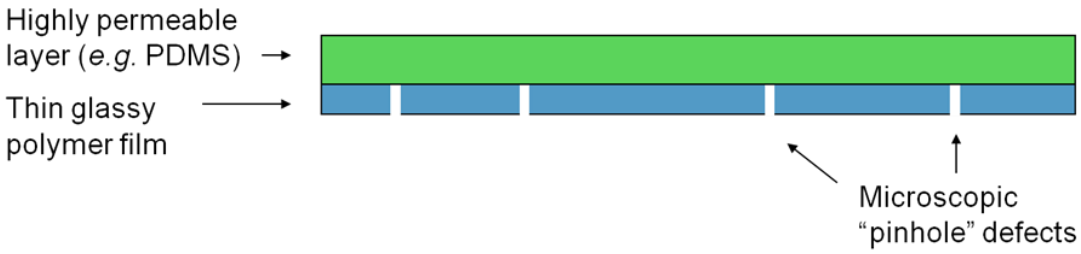

Figure 3.2: Visual representation of layered thin film

A series resistance model is assumed to describe the behavior of the bilayer film:

$$\left(\frac{l}{P}\right)_{composite} = \sum \left(\frac{l}{P}\right)_i \qquad (3.1)$$

However, when calculating the permeability of the selective polymer layer, it is sometimes not required to know the exact thickness of the PDMS layer. For instance, a scaling analysis of the relevant terms for a Matrimid/PDMS film indicates that the l/P of the selective Matrimid® layer is much greater than that of the PDMS layer. In most permeability calculations, therefore, one can ignore the PDMS layer entirely.

Substantial data indicate that while PDMS may affect the absolute permeability of the composite thin film to some extent, the aging behavior of a PDMS-coated thin film is not fundamentally different than that of a non-coated thin film (Figure 3.3). This suggests that no significant interactions between the film layers exist and that the series resistance

model assumption holds. Rowe et al. and Cui et al. have also shown that the rubbery PDMS layer does not appear to affect the physical aging behavior over time [11,12].

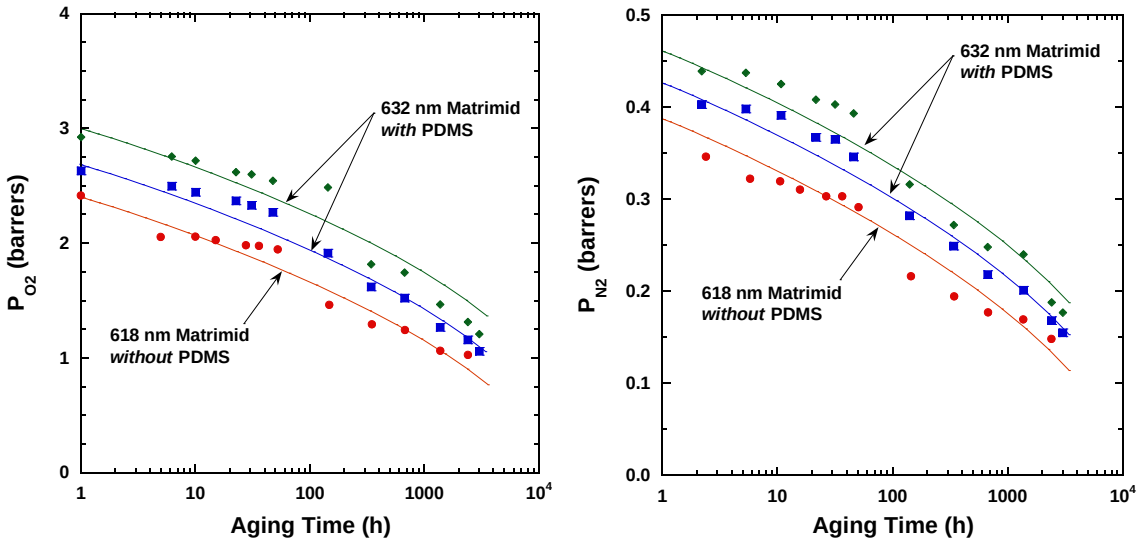

Figure 3.3: O_2 and N_2 permeability for thin Matrimid® films. Aging behavior is the same for thin films with and without PDMS coating.

After spin-coating the glassy thin film layer, the PDMS coating was applied by spin casting a PDMS/cyclohexane solution onto the glassy film at 1000 rpm for 60 s. The wafer was then placed on a hot plate and heated to 110°C for 15 min to crosslink the PDMS film and remove residual solvent. The PDMS solution consisted of Wacker Silicones Corporation Dehesive 940A and cyclohexane in a 2:3 ratio by volume, proprietary catalyst (OL), and crosslinking agent (V24). The thickness of the PDMS layer was ~ 4 μm as measured by a Dektak 6 M stylus profilometer.

3.1.4 Thermal History and Sample Construction

Any polymer film is imbued with a unique thermal history originating from the formation process. Each film, in the freestanding state, was heated to 15°C above its glass transition temperature in a nitrogen rich environment and annealed for 10 min, and upon removal the film was allowed to quench rapidly to room temperature. This treatment erases prior thermal history and relaxes any orientation induced by the film formation process. Thus, all films are given a similar history, allowing legitimate comparison for physical aging.

Finally, the films were masked between two pieces of aluminum tape; thin films were supported by an Anopore™ disc (Figure 3.4). All samples were aged in air at ambient pressure and 35°C. Samples experienced no CO_2 exposure during the initial aging period.

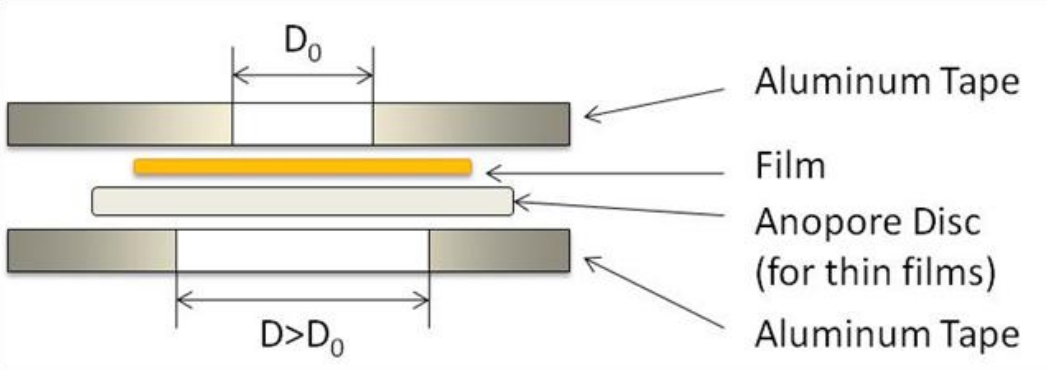

Figure 3.4: Film masking schematic

3.1.5 Gas Permeability Apparatus

In this work, all pure gas permeabilities were measured at 35°C using a standard constant volume, variable pressure apparatus [13]. Mathematically, permeability is defined as the flux of a gas penetrant through a membrane normalized by pressure and by the thickness of the membrane:

$$P_i = \frac{N_i l}{\Delta p_i} \tag{3.2}$$

where P_i is the permeability of gas molecule i, N_i is the flux (molar flow rate per unit membrane area) through the membrane, l is the membrane thickness, and Δp_i is the partial pressure (or fugacity) driving force resulting from a difference in pressure or fugacity between the upstream and downstream. Since the downstream pressure is usually very low (vacuum to ~10 torr) relative to the upstream pressure, Δp_i can be replaced with the upstream pressure or fugacity. The common unit of permeability is the Barrer:

$$1 \text{ Barrer} = 10^{-10} \text{ cm}^3\text{(STP) cm / cm}^2 \text{ s cmHg} \tag{3.3}$$

The ideal selectivity of a membrane describes a membrane's capacity to permeate preferentially certain molecules over others, and is defined as the ratio of the permeability of one penetrant over that of another, i.e.,

$$\alpha_{i/j} = \frac{P_i}{P_j} \tag{3.4}$$

Figure 3.5 depicts a typical permeation cell. All gases used in permeation experiments were provided by Matheson Tri-Gas and were at least 99.99% pure. At higher pressures, the permeation cell upstream metal part connections had a small,

observable leak, which ensured feed gas impurities would not accumulate over long periods of time.

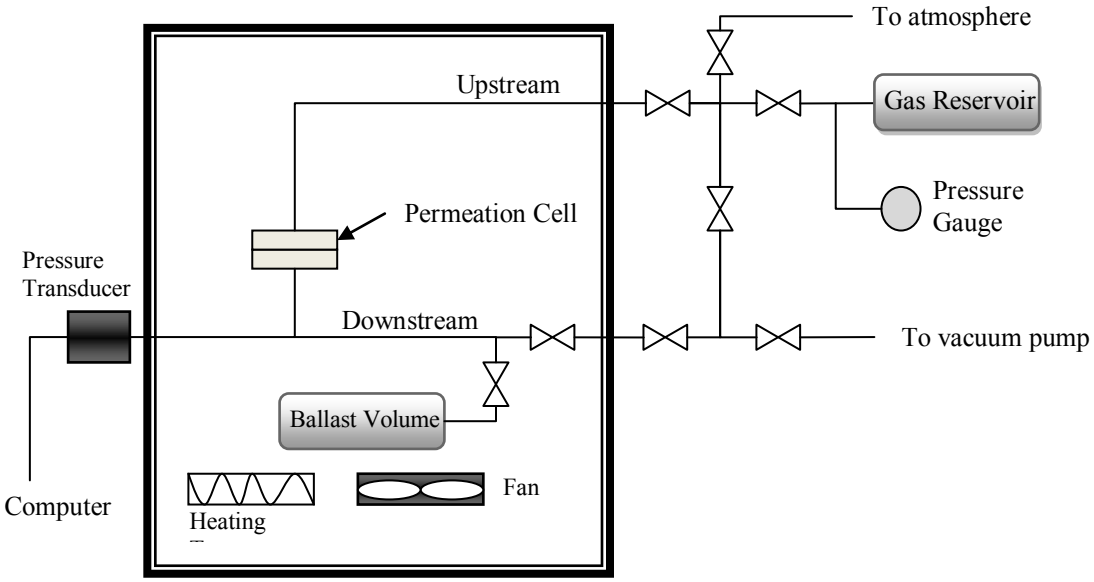

Figure 3.5: Schematic of a constant-volume permeation cell

3.1.6 CO_2 Permeation Experiment Procedures

When conducting experiments on thin glassy films with CO_2, the results are greatly affected by the method chosen. As will be demonstrated throughout this work, CO_2-induced plasticization effects for thin glassy polymer films are pressure, time, and thickness dependent. Thus, many variables must be taken into account: the pressure or concentration of CO_2 a film experiences, the exposure time a film spends at a particular CO_2 pressure, the aging time of the film both before and during CO_2 exposure, the film thickness, and any prior thermal or plasticization history. In this section, four procedures for studying CO_2 permeation behavior are briefly outlined, but the procedures will be

described in each respective results section in Chapters 4 and 5 for maximum clarity. One should additionally keep in mind that CO_2 exposure to a glassy polymer changes the history of the sample. Thus, it is of no value to conduct an experiment involving CO_2 upon a thin film, and then use the same film for a different experiment. The results will not be comparable with other samples. In all of the gas permeation experiments described in this work, every sample is used for a single experiment.

CO_2 Plasticization Pressure Curves

A typical experiment for demonstrating CO_2 plasticization effects in a polymer film involves measuring CO_2 permeability as a function of upstream gas pressure. The literature abounds with polymer gas transport data for gases such as O_2, N_2, and CH_4 that follow the dual-sorption, dual-mobility model, which predicts a slight decrease in permeability with increasing pressure. However, plasticizing penetrants exhibit significant deviations from this behavior. At relatively low CO_2 pressures, the gas permeability of a glassy film decreases with increasing pressure, following the predicted behavior of the dual-mode model. As more CO_2 is sorbed, the polymer is plasticized, which leads to an upward inflection in the gas permeability curve as CO_2 pressure increases, and the minimum in this curve is often called the "plasticization pressure." However, this term is somewhat misleading since plasticization occurs well below this pressure. [14]

In this work, all CO_2 plasticization pressure curves were obtained using a similar sequence of CO_2 pressures. Following an initial aging period with no exposure to CO_2, the films were first exposed to 2 atm of CO_2 at the upstream side of the membrane.

Pressure was incremented by 2 atm until reaching 20 atm, and then incremented by 4 atm until reaching 40 atm. For the thick films presented in Chapter 4, the steady state permeability at each pressure was measured after ~9 min of CO_2 exposure since the time lag for thick Matrimid® films ranges from 60 to 90 s. Films with thickness less than 1 μm, however, reach steady state in a very short time, and, thus, the thin films were held at each pressure for only 3 min.

CO_2 Permeability Hysteresis Experiments

A plasticization pressure curve provides some insight into a polymer's response to CO_2 as pressure is varied but is rather limited in describing the effect of CO_2 exposure for longer times. A modified plasticization pressure curve method was developed to capture these details, following a similar method from Puleo et al. [15]. The method involves four steps:

1. Pressurization from 2 atm to 32 atm CO_2, spending 10 min at each intermediate pressure.
2. Hold at 32 atm CO_2 for 4 hr.
3. Depressurization from 32 atm to 4 atm CO_2, spending 10 min at each intermediate pressure.
4. Hold at 4 atm CO_2 for 12 hr.

This procedure additionally provides some insight into hysteresis effects of gas sorption, which tend to be different for thick and thin glassy polymer films.

Short Time CO_2 Permeation Experiments

In this procedure, CO_2 permeability is tracked for a fixed time with fewer upstream pressure changes. Films were exposed to a sequence of four CO_2 pressures for 2 hr at each pressure: 8 atm, 16 atm, 24 atm, and 32 atm. This particular sequence was initially chosen to include pressures below and above the CO_2 plasticization pressure of Matrimid®, generally accepted to be 12-14 atm.

Long time CO_2 Permeation Experiments

The previously described experiments employ relatively short CO_2 exposure times (<20 hr). Alternatively, one could measure the CO_2 permeability of a film over a long period of time at constant CO_2 pressure. Typically, these experiments were performed on films aged for ~200 h, and the films were exposed to CO_2 at constant pressure for 500-1000 hr. As mentioned above, the particular CO_2 pressures (8 atm, 16 atm, 32 atm) were chosen to include pressures below and above the CO_2 plasticization pressure of Matrimid®.

3.2 GAS SORPTION STUDIES

The following sections discuss the materials, procedures, and instruments used for the gas sorption studies presented in Chapter 6.

3.2.1 Materials

Four polymer systems were investigated in this research: the commercial polyimide Matrimid® 5218, a polysulfone made from bisphenol A (PSF), poly(2,6-dimethyl-1,4-phenylene) oxide (PPO), and a commercial polystyrene designated as Styron 685d. The first three polymers were described in Section 3.1.1. Polystyrene was included for further comparison of fundamentally different polymer types. It also has a lower T_g than the other polymers. The bulk properties of the polymers are presented in Table 3.2, including their van der Waals volumes and density at absolute zero.

Polymer	ρ (gm/cm^3)	T_g (°C)	Refractive Index	V_{vdw} (cm^3/gm)	$\rho_{0°K}$ (gm/cm^3)
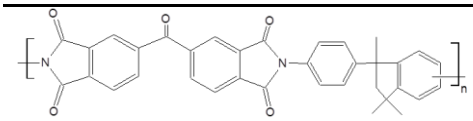 Matrimid® 5218	1.20	310	1.648	0.532[a]	--
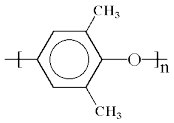 Poly(2,6, dimethyl-1,4-phenylene) oxide (PPO)	1.069	210	1.573	0.588[a]	1.393[c]
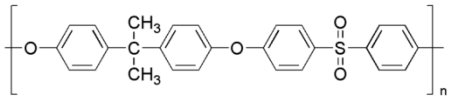 Polysulfone (PSF)	1.24	186	1.633	0.531[a]	1.503[c]
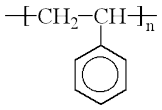 Polystyrene (Styron 685d)	1.05	105	1.586	0.604[b]	1.225[c]

[a] Huang et al. [16]. [b] Van Krevelen [17]. [c] Sanchez and Cho [18].

Table 3.2: Polymer structures and bulk properties

3.2.2 Film Formation

Single-layer thin films were prepared by spin casting polymer solutions onto pre-cut, 1 cm x 1 cm silicon wafers; two to three drops of solution sufficiently covered the wafer without overflowing. It is recommended to measure the SiO_2 thickness of the silicon wafer before spin casting the sample to ensure accuracy. Thickness of the polymer layer was controlled by varying the concentration of polymer from 2-3 wt.% and the spin speed from 1200 to 2100 rpm for 90 s. Solvents used were cyclohexanone for Matrimid® and PSF, chlorobenzene for PPO, and toluene for polystyrene. Following the spin coating, the initial thickness was measured with a variable angle spectroscopic ellipsometer. Samples were dried in a vacuum oven near 100°C overnight to remove any residual solvent and water.

All glassy materials retain a thermal history derived from the film formation process and storage conditions up until testing. Each film was annealed on the silicon substrate at 15°C above its T_g for 10 min (in a nitrogen rich environment) and then rapidly quenched to room temperature to standardize the prior history. Samples were stored at 35°C prior to testing. While these protocols do allow for reasonable comparison of the materials under the varying conditions of CO_2 exposure, it must be noted that annealing on a substrate is different than annealing in the freestanding state. Physical aging for a constrained film such as this may not proceed in exactly the same manner as a freestanding film because the substrate eliminates one of the film's "free surfaces" [19]. Huang observed via ellipsometry that freestanding films tend to decrease in thickness by ~0.8% and increase in density slightly over 6000 h of aging at 35°C [20]. For films annealed on a wafer, however, surface forces will affect this behavior. We observed

slight increases in density with experimentally insignificant changes in thickness over 400 h of aging at 35°C.

3.2.3 Ellipsometer Setup

A spectroscopic ellipsometer made by J.A. Woollam Co. (model 2000D) was used in this research. The CO_2 experiments were conducted with a high-pressure ellipsometry cell made of steel, containing two fused silica windows (Technical Glass Products) at an angle normal to the incident light. A diagram of the cell is presented in Figure 3.6. The windows were sealed with Buna-90 and Teflon o-rings (Buna o-rings were coated with a very thin layer of vacuum grease to improve the seal). The metal window caps were tightened with a torque wrench to control the stresses on the windows; it is desirable to have it tight enough to be well-sealed but not so tight as to overly stress the windows. The torque wrench setting used in these experiments was 180 lb/in^2. It is recommended that the silicon wafer with polymer film be taped (using the same aluminum tape from gas permeability experiments) to the metal stage in the cell to ensure it does not move around when gas rapidly enters the cell. The cell was connected to a transducer to monitor the pressure, a CO_2 cylinder with >99.99% purity (Praxair), and a house vacuum line. Pressure was controlled with the gas regulator connected to the cylinder. Temperature was controlled at 35°C using four cartridge heaters (0.25 in diameter, 3 in long, Omega) and a PID controller (Omega) to within 1°C. The cell was always allowed to equilibrate at 35°C for at least 15 minutes before calibration and testing. The ellipsometer angle and wavelength range were set to 70° and at least 450 to 900 nm, respectively. This wavelength range was selected to maximize the amount of

data for calculating the optical parameters while avoiding wavelengths where absorbance is known to occur (< 450 nm).

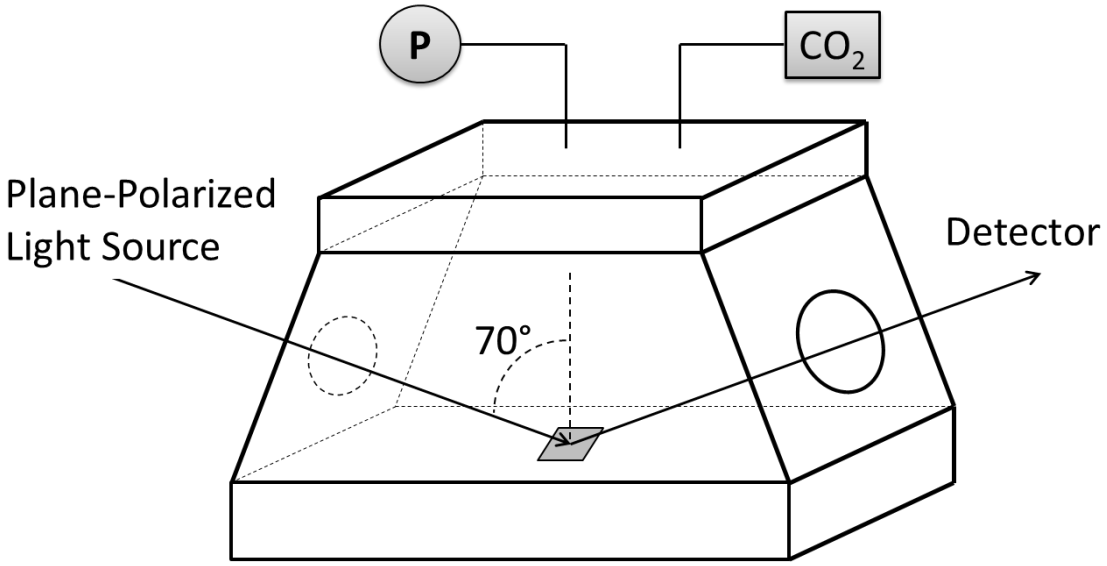

Figure 3.6: Schematic of high-pressure ellipsometry cell

3.2.4 Calibration Procedures

A significant part of conducting high-pressure ellipsometry experiments is compensating for the birefringence of the windows that seal the cell. Even non-birefringent windows can become birefringent owing to strain induced by the high pressure of gas inside the cell. Without accounting for window effects, large errors of as much as 30% can be introduced into refractive index measurements [21]. The WVASE32 software included with the ellipsometer was used to characterize both the "in-plane" and "out-of-plane" window effects. The "out-of-plane" corrections were determined independently with the ellipsometer calibration algorithm. The "in-plane" window effects

cause offsets in the Δ ellipsometric angle and must either be measured separately or be included as adjustable parameters in the ellipsometer model. This procedure has been used previously by Sirard et al. [22].

3.2.5 Sorption Isotherm Experimental Procedure

Samples were tested before exposure to CO_2 at room temperature and ambient conditions to establish a baseline for the measurements. Following cell temperature equilibration, the sample was placed in the cell and the calibration algorithm was run at 35°C and atmospheric air to check the "in-plane" window effects before CO_2 exposure. The sample was scanned again to estimate initial values for the delta offsets at ~1 atm and to observe any difference in the film's properties due to the temperature increase. These differences were generally small, but this additional scan helps determine the best initial conditions possible for maximum accuracy in the data analysis. Following this scan at 35°C, the vacuum line was opened for 3-5 min to remove as much air as possible.

Upon initial exposure to CO_2, the vacuum line was left open for 15 s to purge any remaining air. The pressurization scheme included 1, 2, and 4 atm CO_2, then proceeded in increments of 4 atm up to 32 atm CO_2. The film equilibrates very quickly owing to its short time scale of diffusion, but pressure fluctuations typically require additional equilibration time before acquiring data (about 1 min). At each pressure, the calibration algorithm was run (with the sample still in the cell) to account for the "in-plane" window effects, and then a spectroscopic scan of the sample was performed. This procedure follows, in general, that of Sirard et al. [22]. After scanning at the maximum pressure, the pressure was then decremented to 24, 16, 8, and 2 atm to observe any CO_2 sorption

hysteresis for the film. A final spectroscopic scan outside the cell at room temperature and atmospheric pressure was performed following the exposure to CO_2.

The optical data were fitted with a four-layer optical model as diagrammed in Figure 3.7. The model contained a silicon substrate layer, native oxide layer, a polymer/CO_2 layer, and an "ambient" CO_2 layer. Setting the topmost layer to "ambient" in the model options instructs the analysis program to treat the layer as the ambient CO_2 surroundings of the polymer layer rather than as an additional solid layer. The refractive index of CO_2 was determined by interpolating from literature data [23] and was assumed to be constant for the wavelength range, temperature, and pressure conditions of this study. The polymer/CO_2 layer was modeled with the Cauchy dispersion equation. The fit parameters included the film thickness, Cauchy parameters *A*, *B*, and *C*, and delta offsets.

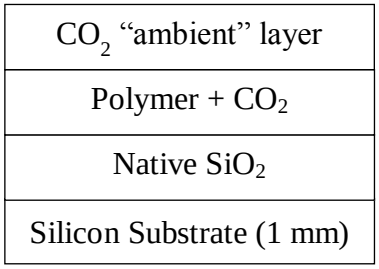

Figure 3.7: Four-layer optical model used by the WVASE32 ellipsometer program to analyze optical data

3.2.6 Constant Pressure Experimental Procedure

With a well-controlled high-pressure ellipsometry cell, one can construct a sorption isotherm with a variety of pressure points in a relatively short time. However, the effect of CO_2 on glassy polymers is known to be time-dependent, and a simple procedure was designed to obtain dynamic ellipsometric data for longer exposure times. In short, the ellipsometer is programmed to probe the polymer film every minute over the course of 100 h with constant CO_2 exposure.

As in the sorption isotherm procedure, samples were tested before exposure to CO_2 at room temperature and ambient conditions. To calibrate the ellipsometer, a standard silicon wafer with a ~50 nm SiO_2 thermal oxide layer was placed in the cell at 35°C and the cell was evacuated for 5 min. Next, the cell was pressurized with CO_2 at the pressure of interest and the calibration algorithm was run to determine the "in-plane" window effects at that pressure. Initial delta offset values were obtained from an additional spectroscopic scan on the silicon wafer following the calibration algorithm. The cylinder was then closed and the standard silicon wafer replaced with the sample film wafer. After evacuating the cell for 3-5 min, the cylinder was opened and the system purged for 15 s. The opening of the cylinder is considered to be time zero for CO_2 exposure. Data collection always began within 1 min of opening the cylinder. Since plasticization is best understood on a logarithmic time scale, spectroscopic scans were taken every 10 s for the first 6 to 10 min using the ellipsometer's dynamic scanning mode. Then, the ellipsometer was set to scan the film once every minute for the next 100 h.

The dynamic ellipsometric data was analyzed with the same four-layer model described in section 3.5, with the initial conditions for the film and delta offsets determined from the scans before the dynamic experiment. The "point-by-point" analysis routine included with WVASE32 would fit the model to the data taken for the first time slice, and then use those results as the initial guess values for the next time slice. Upon completion of the program, values for the film thickness, optical constants, and delta offsets were catalogued for each time the ellipsometer had scanned the sample.

Over the course of 100 h of CO_2 exposure, there is invariably some variation in pressure within the cell that cannot be controlled due to imperfect sealing. However, these fluctuations are typically within ±0.1 atm, and thus we assume in the analysis protocol that the pressure is constant over the duration of the experiment so that the molar density and refractive index of CO_2 can be considered constant in the calculations of the optical model. While this simplifying assumption is not strictly valid, the errors associated with it are relatively low (<0.01% for CO_2 refractive index, <1% for CO_2 molar density, and <0.1% for CO_2 concentration in the polymer film), so we believe it is justifiable.

3.3 REFERENCES

[1] J. S. McHattie, W. J. Koros, and D. R. Paul, "Gas transport properties of polysulphones: 1. Role of symmetry of methyl group placement on bisphenol rings," *Polymer*, vol. 32, no. 5, pp. 840-850, 1991.

[2] R. T. Chern, F. R. Sheu, L. Jia, V. T. Stannett, and H. B. Hopfenberg, "Transport of gases in unmodified and arylbrominated 2,6-dimethyl- 1,4-poly (phenylene oxide)," *Journal of Membrane Science*, vol. 35, no. 1, pp. 103-115, 1987.

[3] A. Higuchi, T. Nakajima, A. Morisato, M. Ando, K. Nagai, and T. Nakagawa, "Estimation of diffusion and permeability coefficients of CO_2 in polymeric membranes by FTIR method," *Journal of Polymer Science, Part B: Polymer Physics*, vol. 34, no. 13, pp. 2153-2160, 1996.

[4] Y. Huang and D. R. Paul, "Physical aging of thin glassy polymer films monitored by gas permeability," *Polymer*, vol. 45, pp. 8377-8393, 2004.

[5] W. C. Madden, D. Punsalan, and W. J. Koros, "Age dependent CO_2 sorption in Matrimid® asymmetric hollow fiber membranes," *Polymer*, vol. 46, no. 15, pp. 5433-5436, 2005.

[6] Y. Maeda, *Ph.D. Dissertation, University of Texas at Austin*, 1985.

[7] Y. Maeda and D. R. Paul, "Effect of antiplasticization on gas sorption and transport. II. Poly(phenylene oxide)," *Journal of Polymer Science, Part B: Polymer Physics*, vol. 25, no. 5, pp. 981-1003, 1987.

[8] D. R. Paul, in *Comprehensive Membrane Science and Technology, Volume 1*, E. Drioli and L. Giorno, Eds. Oxford: Academic Press, 2010, pp. 75-90.

[9] W. J. Koros, "Personal communication," *Personal communication*, 1978.

[10] J. Henis and M. K. Tripodi, "The developing technology of gas separating membranes," *Science*, vol. 220, no. 4592, pp. 11-17, 1983.

[11] B. W. Rowe, B. D. Freeman, and D. R. Paul, "Physical aging of ultrathin glassy polymer films tracked by gas permeability," *Polymer*, vol. 50, no. 23, pp. 5565-5575, 2009.

[12] L. Cui, W. Qiu, D. R. Paul, and W. J. Koros, "Physical aging of 6FDA-based polyimide membranes monitored by gas permeability," *Polymer*, vol. 52, pp. 3374-3380, 2011.

[13] W. J. Koros, D. R. Paul, and A. A. Rocha, "Carbon dioxide sorption and transport in polycarbonate," *Journal of Polymer Science, Part B: Polymer Physics*, vol. 14, no. 4, pp. 687–702, 1976.

[14] C. A. Scholes, G. Q. Chen, G. W. Stevens, and S. E. Kentish, "Plasticization of ultra-thin polysulfone membranes by carbon dioxide," *Journal of Membrane Science*, vol. 346, no. 1, pp. 208-214, 2010.

[15] A. C. Puleo, N. Muruganandam, and D. R. Paul, "Gas sorption and transport in substituted polystyrenes," *Journal of Polymer Science, Part B: Polymer Physics*, vol. 27, no. 11, pp. 2385-2406, 1989.

[16] Y. Huang, X. Wang, and D. R. Paul, "Physical aging of thin glassy polymer films: Free volume interpretation," *Journal of Membrane Science*, vol. 277, no. 1-2, pp. 219-229, 2006.

[17] D. W. Van Krevelen, *Properties of Polymers*, 3rd ed. New York: Elsevier, 1990.

[18] I. C. Sanchez and J. Cho, "A universal equation of state for polymer liquids," *Polymer*, vol. 36, no. 15, pp. 2929-2939, 1995.

[19] B. W. Rowe, S. J. Pas, A. J. Hill, R. Suzuki, B. D. Freeman, and D. R. Paul, "A variable energy positron annihilation lifetime spectroscopy study of physical aging in thin glassy polymer films," *Polymer*, vol. 50, no. 25, pp. 6149-6156, 2009.

[20] Y. Huang and D. R. Paul, "Physical Aging of Thin Glassy Polymer Films Monitored by Optical Properties," *Macromolecules*, vol. 39, no. 4, pp. 1554-1559, 2006.

[21] B. J. Stagg and T. T. Charalampopoulos, "A method to account for window birefringence effects on ellipsometry analysis," *Journal of Physics D: Applied Physics*, vol. 26, no. 11, pp. 2028-35, 1993.

[22] S. M. Sirard, P. F. Green, and K. P. Johnston, "Spectroscopic Ellipsometry Investigation of the Swelling of Poly(Dimethylsiloxane) Thin Films with High Pressure Carbon Dioxide," *Journal of Physical Chemistry B*, vol. 105, no. 4, pp. 766-772, 2001.

[23] A. Michels and J. Hamers, "The effect of pressure on the refractive index of CO_2:: The Lorentz-Lorenz formula," *Physica*, vol. 4, no. 10, pp. 995–1006, 1937.

Chapter 4: Carbon Dioxide Plasticization and Conditioning Effects in Thick vs. Thin Glassy Polymer Films

---

This chapter has been adapted with permission from an article published in Polymer, 2011, 52, (7), 1619-1627.

4.1 SUMMARY

Recent studies have shown that thin glassy polymer films undergo physical aging more rapidly than thick films. This suggests that thickness may also play a role in the plasticization and conditioning responses of thin glassy films in the presence of highly-sorbing penetrants such as CO_2. In this chapter, a carefully designed systematic study explores the effect of thickness upon the CO_2 plasticization and conditioning phenomena in Matrimid®, a polyimide commonly used in commercial gas separation membranes. Thin films are found to be more sensitive than thick films to CO_2 exposure, undergoing more extensive and rapid plasticization at any pressure. The response of glassy polymers films to CO_2 is not only dependent on thickness, but also on aging time, CO_2 pressure, exposure time, and prior history. Finally, thin films experiencing constant CO_2 exposure for longer periods of time exhibit an initial large increase in CO_2 permeability, which eventually reaches a maximum, followed by a significant decrease in permeability for the duration of the experiment. Thick films, in contrast, do not seem to exhibit this trend for the range of conditions explored.

4.2 CO_2 Permeation Behavior for Short Exposure Times

4.2.1 CO_2 Plasticization Pressure Curves

Plasticization is frequently depicted in the literature with plots showing the CO_2 permeability of a glassy polymer passing through a minimum, the so-called "plasticization pressure," as pressure increases. Figure 1 displays such curves for a thick (~20 μm) and thin (~180 nm) Matrimid® film. The films were first aged for 100 hr at 35°C. In each experiment, the films were first exposed to 2 atm of CO_2 at the upstream side of the membrane. Pressure was incremented by 2 atm until reaching 20 atm, and then incremented by 4 atm until reaching 40 atm. Since the time lag for Matrimid® films with thickness of 15 to 35 μm ranges from 60 to 90 s, the steady-state permeability at each pressure was measured after ~9 min of CO_2 exposure by monitoring the downstream pressure for ~60 s. The pressure was then immediately increased to the next set point. A film with thickness less than 1 μm, however, reaches steady state in a very short time, and, thus, the thin film was held at each pressure for only 3 min.

The thick film's plasticization pressure curve (Figure 1) had the expected shape with a minimum at ~14 atm CO_2, which is consistent with the literature. The CO_2 permeability decreased by 22% from 2 atm to 14 atm, but the initial value was recovered by 36 atm. In contrast, the thin film's apparent plasticization pressure is ~6 atm, and CO_2 permeability decreased by only 6% from 2 atm to 6 atm. The permeability returned to its initial value by 14 atm and continued to increase markedly as pressure increased. At 40 atm, the permeability is nearly twice the initial value at 2 atm. The difference in shape of the curves suggests that the thin film experiences substantially more plasticization in short amounts of time, even at lower pressures.

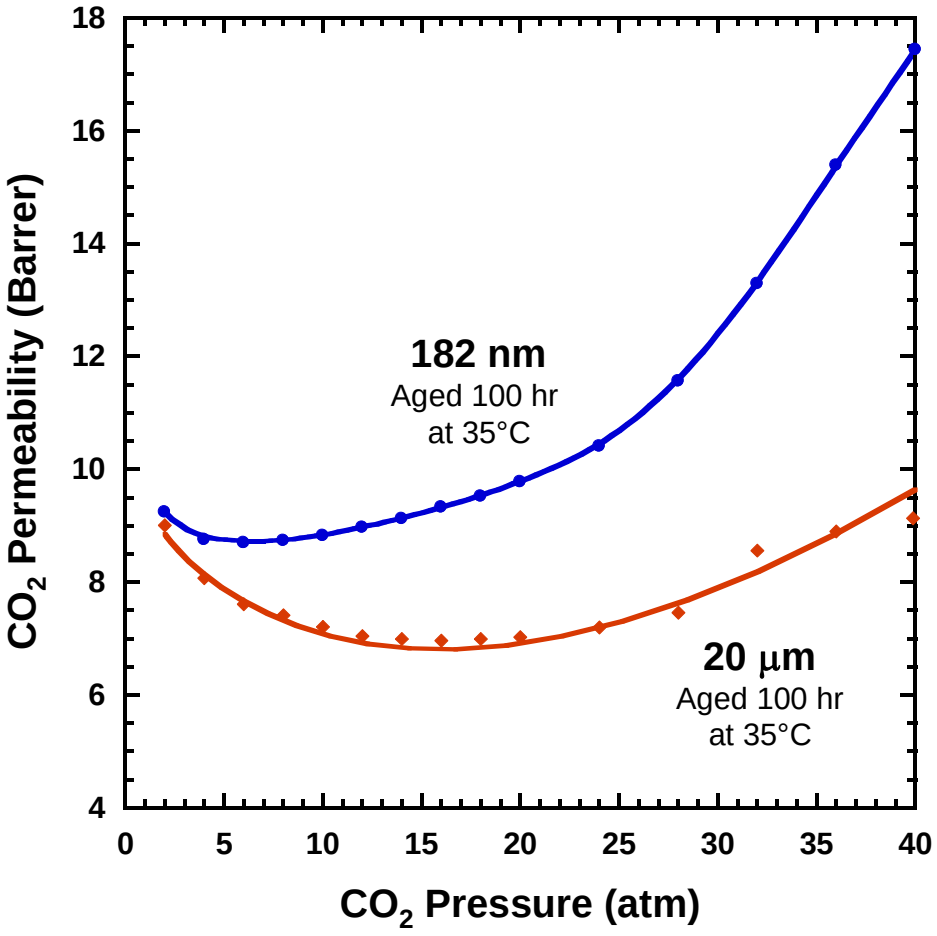

Figure 4.1: CO_2 plasticization pressure curves for thin and thick films with identical prior thermal history. The thin and thick films spent 3 and 10 min, respectively, at each intermediate pressure.

4.2.2 Effect of Thickness on CO_2 Permeability Hysteresis

A plasticization pressure curve provides some insight into a polymer's response to CO_2 as pressure is varied but is rather limited in describing the effect of CO_2 exposure for longer times. A modified plasticization pressure curve method was developed to capture these details, following a similar method from Puleo et al. [1]. The method involves four steps:

1. Pressurization from 2 atm to 32 atm CO_2, spending 10 min at each intermediate pressure.
2. Hold at 32 atm CO_2 for 4 hr.
3. Depressurization from 32 atm to 4 atm CO_2, spending 10 min at each intermediate pressure.
4. Hold at 4 atm CO_2 for 12 hr.

This procedure was applied identically to a thick (~15 μm) and thin (~160 nm) Matrimid® film, each aged for 100 hr at 35°C. Permeability was measured multiple times for the thin film during the pressurization stage (at 2, 5, and 9 min) and depressurization stage (at 5 and 9 min). However, only one measurement was made at each pressure for the thick film, since the thick film's time lag is orders of magnitude greater than that of the thin film. More frequent measurements for thin films allow effects of CO_2 at short exposure times to become more evident.

Figure 4.2 shows CO_2 permeability versus both pressure and time for the procedure described above. For the thick film, the pressurization step resembles the

plasticization pressure curve in Figure 4.1, but the plasticization pressure appears to have shifted to a higher pressure (~16-20 atm) and the film does not return to its initial permeability as quickly. This behavior is attributed to the greater incremental increases in pressure involved in the different procedure. Permeability increased in the 4 hr hold step at 32 atm by 6.2%. The permeability continued to increase during the depressurization step, a phenomenon also observed in thick polystyrene [1], cellulose acetate [2], and polycarbonate [3] films. The polymer begins to relax toward its original state as penetrant is removed, but does not have sufficient time for significant relaxation and the dilated structure allows for greater gas flux. During the 12 hr hold step at 4 atm the permeability decreases and approaches the curve generated during the pressurization cycle.

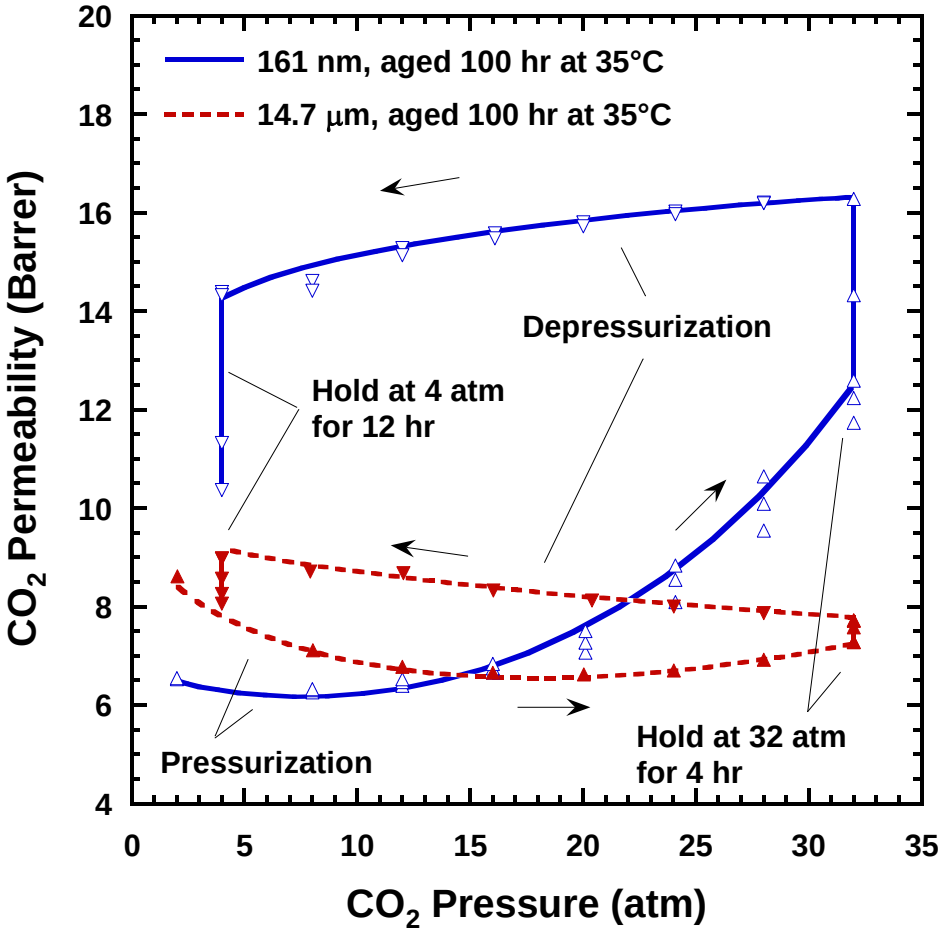

Figure 4.2: CO_2 permeability hysteresis for thin and thick films with identical prior thermal history. Each film proceeds through four steps: 1. Pressurization from 2 atm to 32 atm, spending 10 min at each intermediate pressure; 2. Hold at 32 atm for 4 hr; 3. Depressurization from 32 atm to 4 atm, spending 10 min at each intermediate pressure; 4. Hold at 4 atm for 12 hr.

The thin film reasonably follows the shape of the plasticization pressure curve from Figure 4.1, but the different procedure results in slightly different permeability values at each pressure. At 20 atm in the pressurization step, measureable increases in permeability were observed within 10 min of exposure time. At 32 atm, permeability increased nearly 10% within 10 min of exposure time, and over the 4 hr hold period at 32 atm increased 40%. Unlike the thick film, the permeability decreased during the depressurization step. This decrease is attributed to thin films having shorter relaxation times than thick films. Permeability continued to decrease significantly throughout the 12 hr hold step at 4 atm CO_2, but did not return to the regressed curve for the pressurization step.

4.2.3 Short Time CO_2 Permeation Experiments

The experiments in the previous sections show that thick and thin films respond differently to CO_2 under conditions of varying pressure and time. In this section, CO_2 permeability is tracked for a fixed time with fewer upstream pressure changes. Thick (~35 μm) and thin (~180 nm) Matrimid® films, each aged for 100 hr at 35°C, were exposed to a sequence of four CO_2 pressures for 2 hr at each pressure: 8 atm, 16 atm, 24 atm, and 32 atm. This particular sequence was chosen to include pressures below and above the CO_2 plasticization pressure of Matrimid®, generally accepted to be 12-14 atm.

The responses of the thick and thin films tested with this procedure (Figure 4.3) are quite different. Taking the first data point from each pressure for the thick film, one could construct a rudimentary plasticization pressure curve sufficiently consistent with prior observations. The thin film, however, exhibits a significant departure from behavior

observed with previous methods. Much greater changes take place over short time periods, and the effect becomes more pronounced as pressure increases. For example, the CO_2 permeability for the thin film increased 38% from start to finish, while for the thick film the increase was 15%.

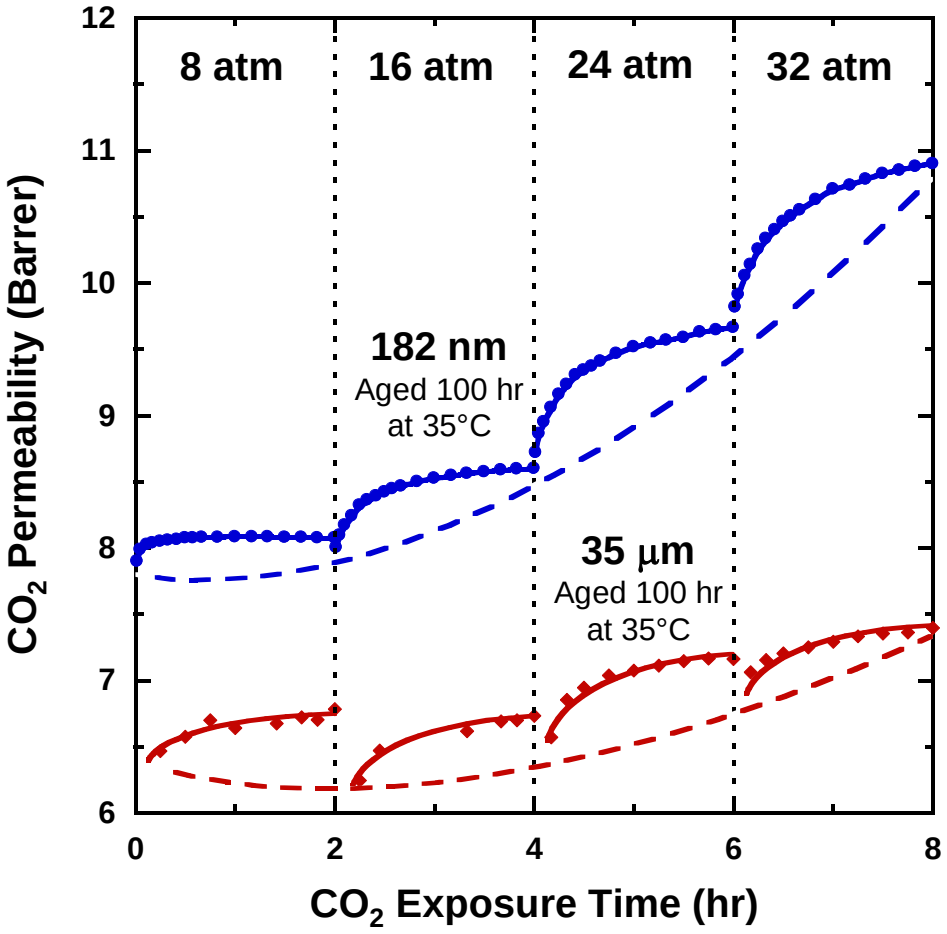

Figure 4.3: Short time experiments for thin and thick films with identical prior thermal history.

4.2.4 Effect of Aging Time on Plasticization Pressure and CO_2 Permeability

Gas sorption and permeability in glassy polymers is directly related to the free volume, and free volume decreases as the polymer ages. Thus, physical aging should have an effect on how a polymer plasticizes in the presence of CO_2. A series of thick (~15-20 μm) and thin (~180 nm) films were prepared and aged at 35°C. At set aging times a film was exposed to CO_2 according to the plasticization pressure curve procedure outlined in Section 4.2.1. More thin films were tested so that the effect of aging time could be more clearly seen.

Figure 4.4 shows results of thick and thin films using the plasticization pressure curve procedure at different aging times. The three thick films, aged 100, 500, and 1000 hr before testing, show little discernible difference between their plasticization pressure curves. This is attributed to the very slow physical aging of bulk glassy polymers; thus, aging does not seem to play a significant role in the plasticization response of bulk polymers. The thin films were aged 3, 100, 250, 500, and 1000 hr before testing. As aging time increased, the plasticization pressure curve shifts to lower permeability and appears to flatten out. The effect of aging is more pronounced at short aging times. For instance, the downward shift of permeability from 3 hr to 250 hr aging is much greater than the shift from 250 hr to 500 hr, or from 500 hr to 1000 hr aging. This is a result of the more rapid aging rate and higher free volume state of thin films at short aging times. The plasticization pressure appears to decrease slightly with increased aging time. Furthermore, films aged for shorter amounts of time had greater relative changes in permeability as pressure was varied.

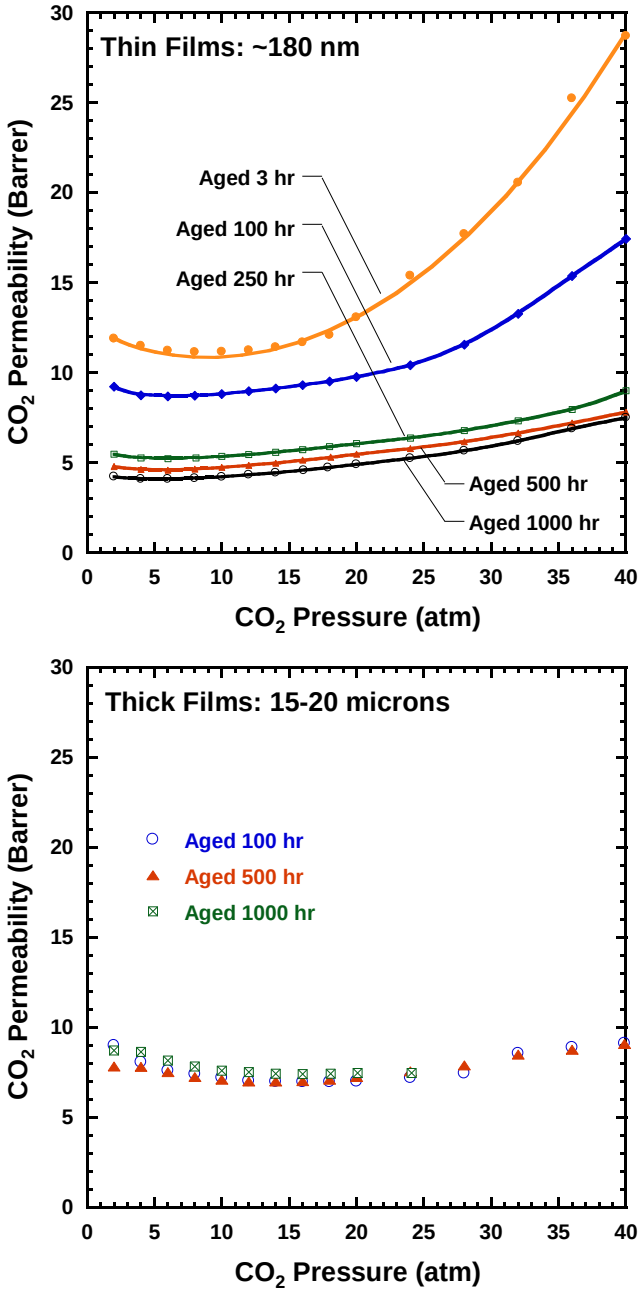

Figure 4.4: Effect of aging time on plasticization pressure and CO_2 permeability for thin and thick films. Each data set represents a unique film aged in the absence of CO_2 until the specified aging time. The thin and thick films spent 3 and 10 min, respectively, at each intermediate pressure.

4.2.5 CO_2 Conditioning Effects

In addition to being plasticized by CO_2, glassy polymers can display rather long term changes associated with the CO_2 exposure, often called conditioning effects, once the CO_2 is removed. To document such behavior, the permeabilities of O_2, N_2, and CH_4 were measured for two thick (~20 μm) and two thin (~160 nm) films before and after CO_2 exposure, while the films were aging at 35°C. After aging for 100 hr, thick and thin films were exposed to CO_2 using the modified plasticization pressure curve method: each film experienced a pressurization step, a hold step at 32 atm CO_2, a depressurization step, and a hold step at 4 atm CO_2. Further details can be found in Section 4.2.2. The remaining films did not experience any CO_2 exposure and serves as the "base case." Upon completion of the CO_2 exposure period, the permeabilities of O_2, N_2, and CH_4 were tracked until the films had aged 200 hr at 35°C.

Figure 4.5 includes permeability data for O_2, N_2, and CH_4 and selectivities calculated for O_2/N_2 and N_2/CH_4. The pure gas permeabilities of the thin films were all initially greater than those of the thick films, but even after aging 100 hr the thin films showed significant decreases in permeability and the relative positions of the thick and thin films had reversed. Following CO_2 exposure, thick and thin film gas permeabilities increased considerably, but the thin film increased to a greater extent for each gas. Despite having shorter relaxation times the thin film did not return to the base case permeability within the time period of this experiment. The thick film, however, appeared close to returning to the base case after aging 200 hr. The general behavior of the pure gas selectivities was consistent with predictions insofar as conditioning caused each selectivity to decrease, but it is difficult to discern any difference due to thickness within the limits of these observations.

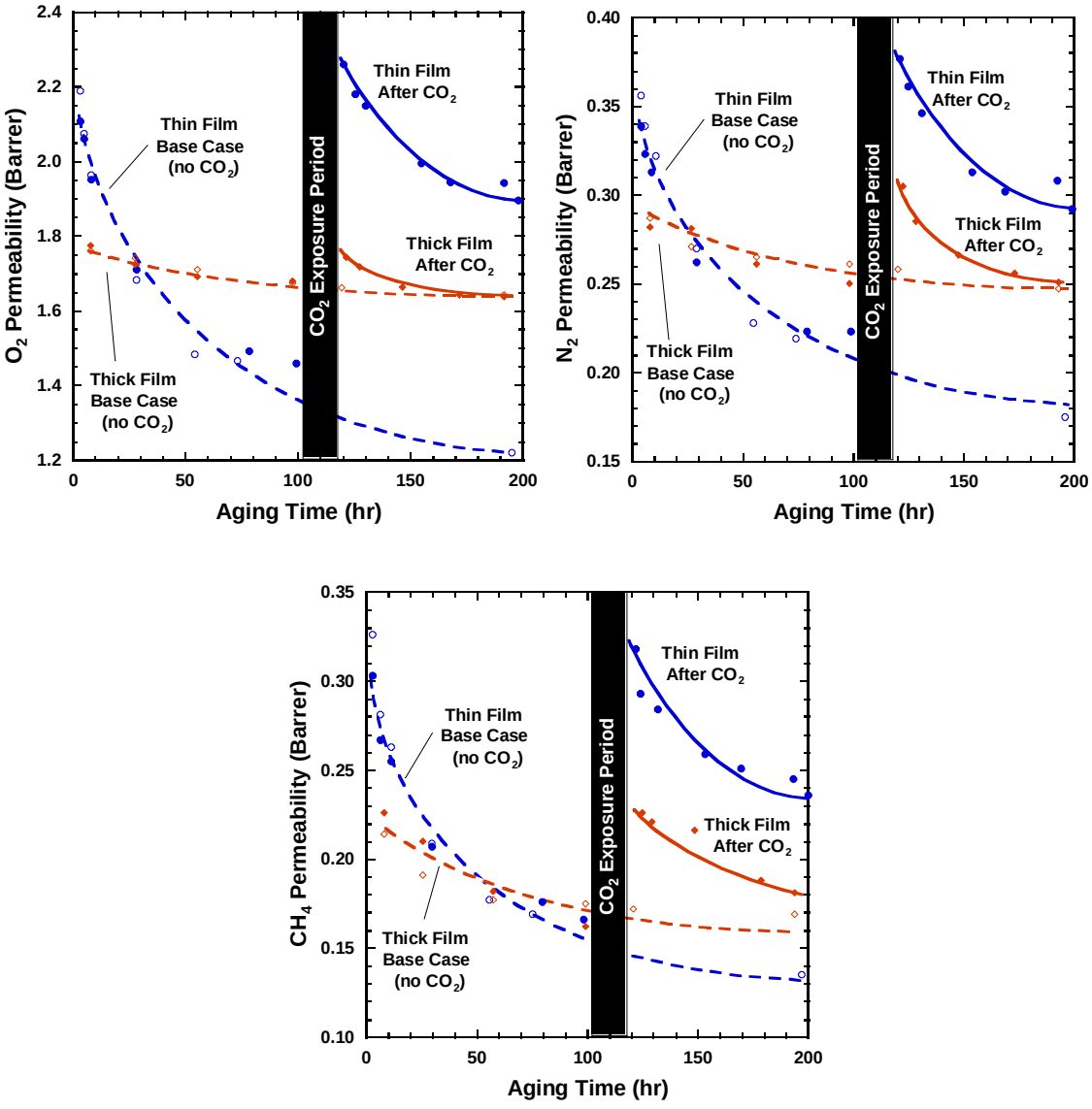
O2 Permeability (Barrer)
Aging Time (hr)
Thin Film Base Case (no CO2)
Thick Film Base Case (no CO2)
CO2 Exposure Period
Thin Film After CO2
Thick Film After CO2
N2 Permeability (Barrer)
Aging Time (hr)
Thin Film Base Case (no CO2)
Thick Film Base Case (no CO2)
CO2 Exposure Period
Thin Film After CO2
Thick Film After CO2
CH4 Permeability (Barrer)
Aging Time (hr)
Thin Film Base Case (no CO2)
Thick Film Base Case (no CO2)
CO2 Exposure Period
Thin Film After CO2
Thick Film After CO2

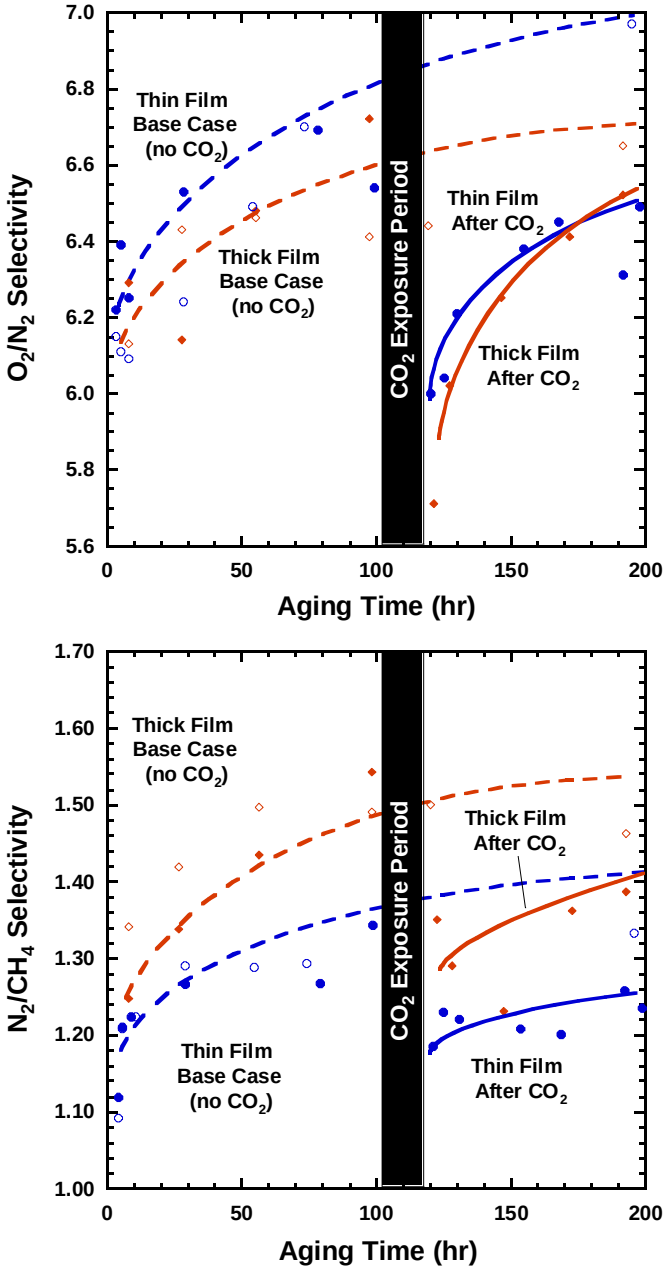

Figure 4.5: CO_2 conditioning effects. (◊) Thin film base case, (♦) thin film with CO_2 exposure, (○) thick film base case, (●) thick film with CO_2 exposure. The CO_2 exposure period followed the procedure outlined in Section 4.2.2.

4.3 CO_2 Permeation Behavior for Long Exposure Times

The experiments described above employ relatively short CO_2 exposure times (<20 hr). Most previous research in the literature tends to focus on thick films, shorter CO_2 exposure periods, and lower CO_2 pressures. However, such experiments could mask the effect that exposure to CO_2 might have for longer periods of time or at higher pressures. Further experiments were performed to explore these possibilities. Three thin films, all 200-220 nm thick, were aged for 200 hr at 35°C. The films were then exposed to CO_2 at constant pressure for 500 hr, and CO_2 permeability was tracked throughout the exposure period. Similar to the experiments described in Section 4.2.3, the particular CO_2 pressures (8 atm, 16 atm, 32 atm) were chosen to include pressures below and above the CO_2 plasticization pressure of Matrimid®.

The literature suggests that such experiments will exhibit significant increases in CO_2 permeability, asymptotically approaching a maximum. In contrast, these thin films behaved quite differently. As expected, the CO_2 permeability of each film, depicted in Figure 4.6, increased significantly with time. However, after each film reached a permeability maximum, the trend reversed and the permeability decreased. At higher pressures, the permeability maximum occurred at shorter times and decreased to a greater extent by 500 hr of CO_2 exposure. The permeability drop indicates that aging is the dominant process even though CO_2 is still present in the film. To our knowledge, such behavior has not previously been described in the literature for gas transport processes, since most experiments of this kind are performed at moderate pressures, with thicker films, and for less than 100 hr of CO_2 exposure, all conditions where this phenomenon is not as prominent. This behavior even occurs below the plasticization pressure of Matrimid®, further confirming that significant plasticization does indeed take place in

thin glassy films at any CO_2 pressure. Another interesting result is that each film has approximately the same maximum relative permeability, with lower CO_2 pressures requiring more time to reach the maximum. This similarity could be due to each film having aged the same amount of time before being tested. Following CO_2 exposure, O_2, N_2, and CH_4 permeability were measured for each film. All permeability coefficients were below the respective values measured before CO_2 exposure, which is consistent with the hypothesis that physical aging out-competed plasticization at long CO_2 exposure times in these thin films.

The effect of aging time and thickness on CO_2 response at long exposure times was investigated using the same procedure. Figure 4.7 shows permeation data for three films tested at 32 atm CO_2 for up to 1000 hr. Included here is data for a 220 nm film, aged 200 hr at 35°C, from Figure 4.6. A second film, 202 nm thick, was aged 800 hr at 35°C before CO_2 exposure, while a third film, 20 μm thick, was aged 200 hr at 35°C before CO_2 exposure.

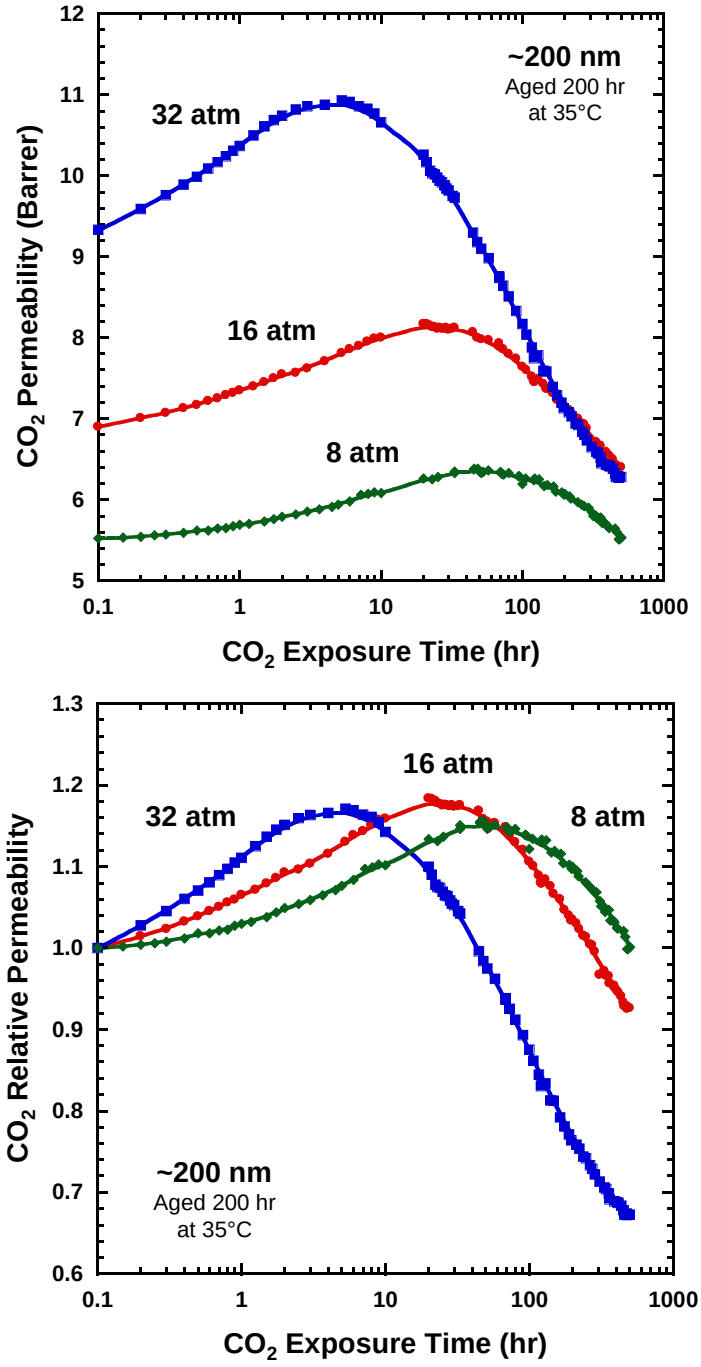

Figure 4.6: Effect of long-time CO_2 exposure at constant pressure for thin films with identical thickness and prior thermal history.

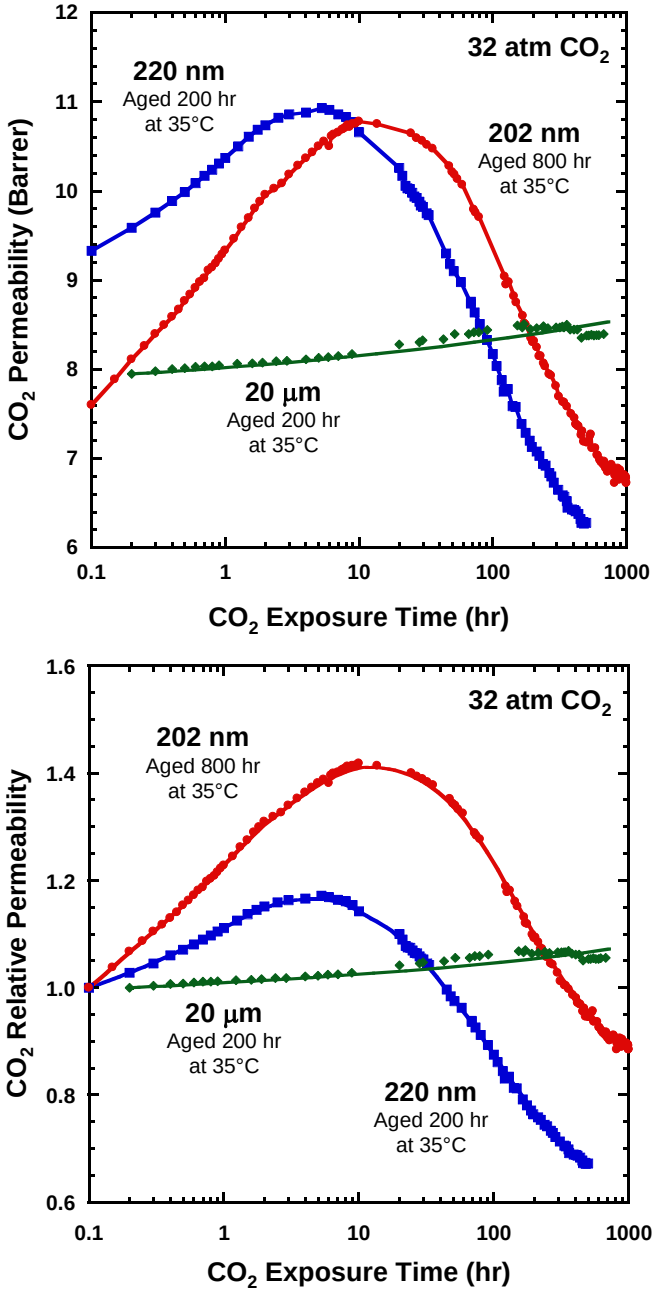

Figure 4.7: Effect of aging time and thickness on long-time CO_2 exposure behavior.

Physical aging is a densification process resulting in a loss of free volume over time. Therefore, relative to a ~200 nm film aged 200 hr at 35°C, a film of comparable thickness aged longer and exposed to similar CO_2 conditions would show a decrease in the initial permeability of the film, the same maximum permeability as the previous film, and increased time until reaching a maximum absolute permeability. The expected behavior did occur, and in fact the maximum permeability of each film differed by 2%. The relative change from time zero to maximum permeability was 42%.

Paralleling the evidence in Section 4.2, these data suggest that thin films respond relatively more quickly and intensely to plasticizing gases, such as CO_2, than thick films. The data shown in Figure 4.7Figure for thick and thin films, both aged 200 hr at 35°C, are consistent with these observations. After 5 hr of CO_2 exposure at 32 atm, the CO_2 permeability of the thin film increased by 17%, passed through a maximum, and then sharply declined with further exposure time at constant pressure. In contrast, the permeability of the thick film increased by only 8% over 1000 hr of CO_2 exposure at 32 atm. Though it is possible that the thick film could go through a maximum in permeability at a longer time or at significantly higher pressures, such as the supercritical CO_2 conditions tested by Kratochvil et al. [4,5], no maximum was distinctly observed within the bounds of this experiment.

The behavior in Figure 4.6 resembles the volumetric “memory effect” observed by Kovacs et al. [6] for temperature jumps about the glass transition of poly(vinyl acetate). Figure 4.8 attempts to generalize the Kovacs experiment by schematically showing the volume relaxation of a glassy polymer at a fixed temperature, T_f, below the glass transition temperature, T_g, versus time at that temperature for various thermal histories. Curve 1 shows the case where the polymer is simply down-quenched from T_1,

above T_g, to T_f. In all the other curves, the polymer was down-quenched from T_1 to T_i, held there for a certain time, and then up-quenched from T_i to T_f. These curves show the response of the volume versus time after arriving at T_f. Curve 1 shows a simple monotonic volume relaxation as expected, whereas curves 2 to 4 show a maximum. For the latter, the polymer responds to the up-quench with an initial increase in volume, but then goes through a maximum as it begins to relax, eventually following the course of curve 1. Kovacs termed this a "memory" effect. McKenna and coworkers showed similar behavior induced by concentration jumps in either relative humidity or CO_2 [7–11]. In the glassy state, the polymer cannot respond immediately to the change in temperature, leading to the non-monotonic volumetric response in the case of opposing changes in temperature. The permeability vs. time plots in Figure 4.6 represent a somewhat analogous situation as the concentration of plasticizing penetrant within the polymer changes, resulting in competition between two effects. First, the temperature quench to below T_g causes aging, manifesting itself by a tendency to decrease the permeability. Second, exposure to CO_2 tends to dilate the polymer, manifesting itself by a tendency to increase the permeability. Neither stimulus causes an immediate response, owing to the slow dynamics of the glassy state. However, it appears that the tendency for physical aging dominates at long times. There is no doubt the presence of CO_2 affects the subsequent physical aging kinetics.

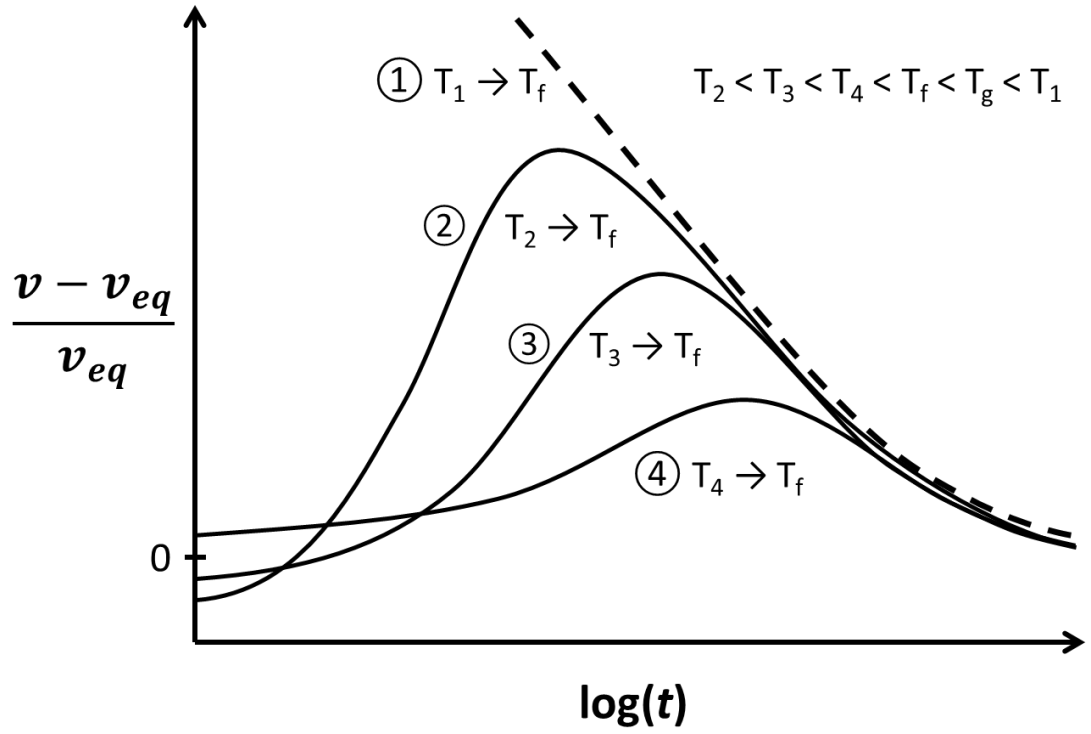

Figure 4.8: Generalization of the Kovacs temperature jump experiment for glassy polymers. The response shows the deviation of sample volume (v) from its equilibrium volume (v_{eq}) at temperature T_f versus the time the sample has been at T_f following the various thermal histories explained in the text.

4.4 CONCLUSIONS

Thickness plays a critical role in the CO_2 plasticization and conditioning processes of glassy polymer films. Thin films are more sensitive to changes in CO_2 pressure, and the response becomes more intense at greater pressures. Permeability changes occur even at short time scales for thin films, as opposed to thick films which take nearly the same amount of time merely to reach steady state. The difference in relaxation time distribution between thick and thin films plays a significant role in the time dependence of CO_2 response. At moderate timescales, thin glassy polymer films undergo more rapid plasticization by CO_2, in contrast with thick films. This behavior is analogous to more rapid physical aging of thin films. Moreover, the conventionally defined "plasticization pressure" is not adequate to determine when plasticization begins. Plasticization in thin films is strongly dependent on aging time of a film, whereas thick films show little change with aging time. Permeability data for O_2, N_2, and CH_4 following CO_2 exposure indicates that thinner films experience greater changes in gas permeability in response to prior sorption of CO_2, i.e., "conditioning" effects, than do thick films, but the effect on selectivity is unclear. Thus, CO_2 transport data from thick films cannot fully predict thin film behavior. The CO_2 response of thin films is dependent on thickness, aging time, CO_2 pressure, exposure time, and prior history.

At longer CO_2 exposure times, thin films behave much differently than thick films. Initially, thin films exhibit a large increase in CO_2 permeability, but the trend eventually reverses and the films decrease in permeability to a significant extent. This is attributed to competition between the CO_2 plasticization effect and physical aging, and the behavior resembles the volume recovery "memory effect" observed by Kovacs. Thick films do not seem to reach a well-defined maximum within the experimental timescale.

This behavior has yet to be fully explained, and other investigations are needed to determine its cause.

4.5 REFERENCES

[1] A. C. Puleo, N. Muruganandam, and D. R. Paul, "Gas sorption and transport in substituted polystyrenes," *Journal of Polymer Science, Part B: Polymer Physics*, vol. 27, no. 11, pp. 2385-2406, 1989.

[2] A. C. Puleo, D. R. Paul, and S. S. Kelley, "The effect of degree of acetylation on gas sorption and transport behavior in cellulose acetate," *Journal of Membrane Science*, vol. 47, no. 3, pp. 301-332, 1989.

[3] S. Jordan, W. J. Koros, and G. Fleming, "The effects of CO_2 exposure on pure and mixed gas permeation behavior: comparison of glassy polycarbonate and silicone rubber," *Journal of Membrane Science*, vol. 30, no. 2, pp. 191–212, 1987.

[4] A. M. Kratochvil and W. J. Koros, "Effects of Supercritical CO_2 Conditioning on Cross-Linked Polyimide Membranes," *Macromolecules*, vol. 43, no. 10, pp. 4679-4687, 2010.

[5] A. M. Kratochvil, S. Damle-Mogri, and W. J. Koros, "Effects of Supercritical CO_2 Conditioning on Un-Cross-Linked Polyimide Membranes for Natural Gas Purification," *Macromolecules*, vol. 42, no. 15, pp. 5670-5675, 2009.

[6] A. J. Kovacs, J. M. Hutchinson, and J. J. Aklonis, "Isobaric volume and enthalpy recovery in glasses. (I) A critical survey of recent phenomenological approaches.," in *The Structure of Non-Crystalline Materials*, 1977, no. 1977, pp. 153-163.

[7] M. Alcoutlabi, L. Banda, and G. B. McKenna, "A comparison of concentration-glasses and temperature-hyperquenched glasses: CO_2-formed glass versus temperature-formed glass," *Polymer*, vol. 45, pp. 5629-5634, 2004.

[8] Y. Zheng and G. B. McKenna, "Structural Recovery in a Model Epoxy: Comparison of Responses after Temperature and Relative Humidity Jumps," *Macromolecules*, vol. 36, no. 7, pp. 2387-2396, 2003.

[9] Y. Zheng, R. D. Priestley, and G. B. McKenna, "Physical aging of an epoxy subsequent to relative humidity jumps through the glass concentration," *Journal of Polymer Science, Part B: Polymer Physics*, vol. 42, no. 11, pp. 2107-2121, 2004.

[10] G. B. McKenna, "Glassy states: Concentration glasses and temperature glasses compared," *Journal of Non-Crystalline Solids*, vol. 353, no. 41-43, pp. 3820-3828, 2007.

[11] M. Alcoutlabi, F. Briatico-Vangosa, and G. B. McKenna, "Effect of chemical activity jumps on the viscoelastic behavior of an epoxy resin: Physical aging response in carbon dioxide pressure jumps," *Journal of Polymer Science, Part B: Polymer Physics*, vol. 40, no. 18, pp. 2050-2064, 2002.

Chapter 5: Carbon Dioxide Plasticization of Thin Glassy Polymer Films Monitored by Gas Permeability

---

This chapter has been adapted with permission from an article published in Polymer, 2011, 52, (24), 5587-5594.

5.1 SUMMARY

Chapter 4 demonstrated that thin glassy polymer films exhibit complex responses to highly-sorbing penetrants, such as CO_2, relative to their thick film counterparts. In this chapter, similar experiments have been applied to two new polymers, including a polysulfone made from bisphenol A (PSF) and poly(2,6-dimethyl-1,4-phenylene oxide) (PPO). Their responses are compared to Matrimid® to understand better CO_2 plasticization behavior of these materials when in thin film form. As expected, the extent of plasticization response tracks with CO_2 solubility; CO_2 diffusivity may also be an important factor at shorter exposure times. Experiments at longer CO_2 exposure times revealed that each polymer experiences the permeability maximum observed in the previous chapter as well. However, polymers that are not as highly-sorbing to CO_2, like polysulfone, may not at some conditions exhibit a distinct permeability maximum but will still decrease in permeability after a long period of CO_2 exposure owing to physical aging.

5.2 RESULTS AND DISCUSSION

5.2.1 CO_2 Plasticization Pressure Curves

CO_2 plasticization is frequently depicted in the literature in terms of plots of CO_2 permeability as a function of upstream gas pressure. Many gases, such as O_2, N_2, and CH_4, permeate through a glassy polymer without changing the polymer's properties owing to their rather low solubility in the polymer. As pressure is increased, a slight decrease in permeability is observed as expected from the dual sorption – dual mobility model [1]. In contrast, highly sorbing gases such as CO_2 cause the polymer matrix to swell and plasticize, leading to an upward inflection of the gas permeability curve with increasing pressure. The minimum in this curve is often called the "plasticization pressure." This term is somewhat misleading since it is well-known that plasticization occurs well below this pressure [2] and is especially evident in thin films [3].

Figure 5.1 displays the plasticization pressure curves for the Matrimid®, PPO, and PSF. Relative permeability data for CO_2 in corresponding thick films have been included for comparison [3,4], although the conditions of measurement are not fully comparable in some cases. The thin films all were of similar thickness (180-200 nm) and were aged for 100 hr at 35°C before testing with CO_2. In each experiment, the films were first exposed to 2 atm of CO_2 at the upstream side of the membrane. Pressure was incremented by 2 atm until reaching 20 atm, and then incremented by 4 atm until reaching 40 atm. Since thin films reach diffusional steady state in a short amount of time, the films were held at each pressure for 3 min, and permeability was measured during the final 60 s. The pressure was then immediately increased to the next set point.

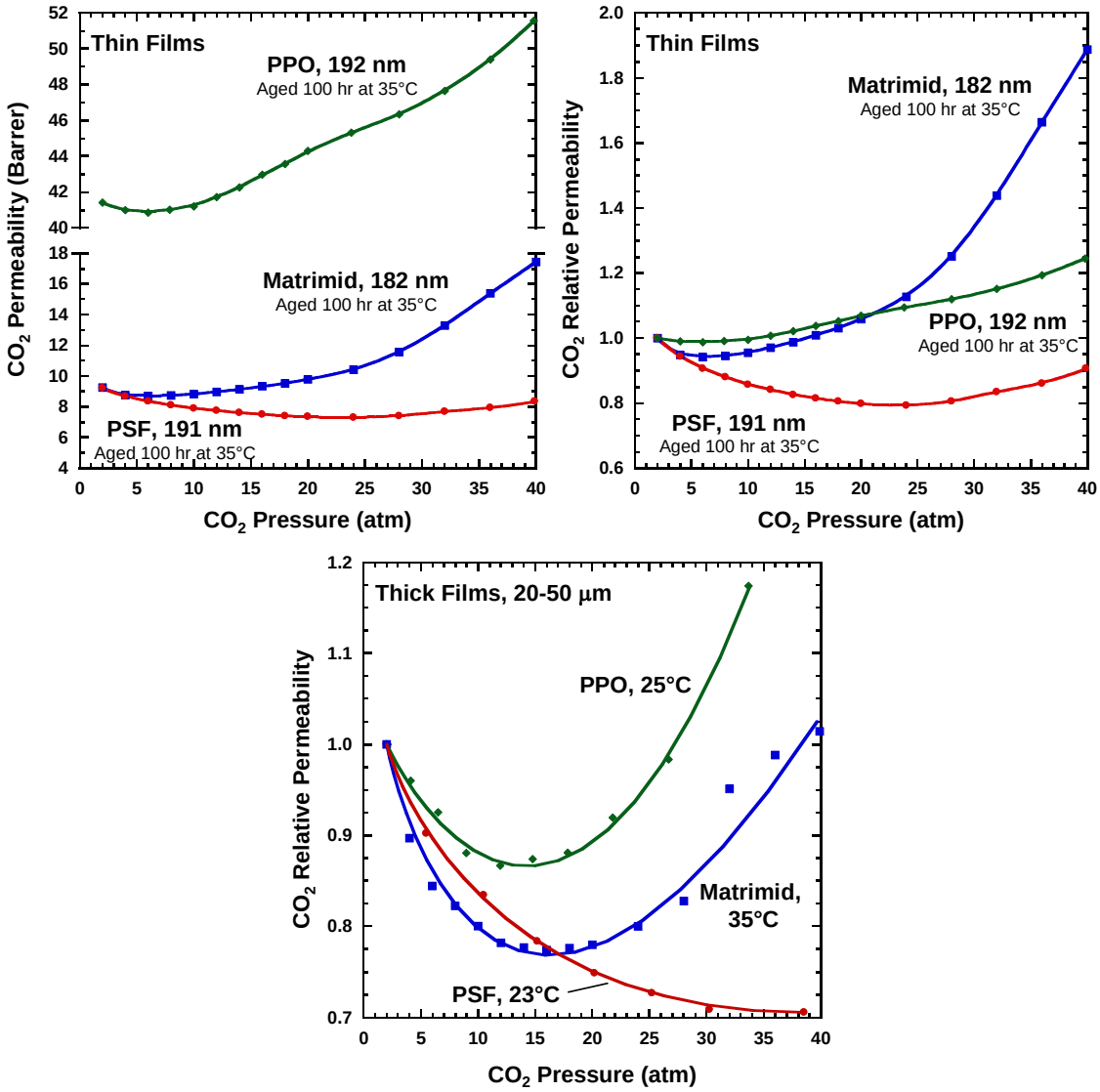

Figure 5.1: CO_2 plasticization pressure curves for thin films of similar thickness with similar thermal history. The films spent 3 min at each intermediate pressure. Relative permeability data of CO_2 in thick films [3,4] have been included for comparison.

The most obvious difference in the thin film curves in Figure 5.1 is the absolute permeability of PPO relative to Matrimid® and PSF. Despite PPO having a lower CO_2 solubility than Matrimid® as shown in Figure 3.1, the CO_2 diffusivity coefficient of PPO is nearly an order of magnitude greater than that of Matrimid®, and, thus, the permeability of PPO is substantially greater. Nevertheless, the Matrimid® thin film still undergoes the greatest relative change in permeability over the course of the procedure. This behavior contrasts with the thick film data which shows PPO having the greatest relative change with CO_2 pressure. Such discrepancies may be attributed to differences in thickness, temperature, or experimental procedure, and further attests to the importance of thickness in plasticization phenomena. The thin film behavior is more consistent with the understanding that solubility is the most important factor for changes due to plasticization. The more soluble CO_2 is in the polymer matrix, the greater changes one would generally expect to observe.

PSF exhibits a much different response than Matrimid® and PPO. The thick film data shows no minimum over the pressure range tested, but the thin film has a more distinct shaped curve that is typically seen in the literature for glassy polymers. This can be mainly attributed to PSF's lower sorption of CO_2 plus it's relatively more compact backbone and, thus, lower free volume, which suggest that it will respond to CO_2 more sluggishly than the other polymers studied. These general observations of how solubility affects CO_2 permeation behavior as a function of pressure can inform interpretation of further experimental results.

5.2.2 CO_2 Permeability Hysteresis

Plasticization pressure curves provide incomplete information regarding a polymer's response to CO_2 for longer times. A modified plasticization pressure curve method was used to examine the effect of CO_2 exposure history upon permeation behavior. This procedure was also used in our previous study and follows a similar method from Puleo et al. [5]. The films proceed through four steps:

1. Pressurization from 2 atm to 32 atm CO_2, spending 10 min at each intermediate pressure;

2. Hold at 32 atm CO_2 for 4 hr;

3. Depressurization from 32 atm to 4 atm CO_2, spending 10 min at each intermediate pressure;

4. Hold at 4 atm CO_2 for 12 hr.

This procedure was applied identically to each film of interest. The films were aged for 100 hr at 35°C and were between 160 and 230 nm thick. Permeability was measured during the pressurization stage at 2, 5, and 9 min and the depressurization stage at 5 and 9 min. More frequent measurements at intermediate pressures make more evident the effects of CO_2 at shorter exposure times.

Figures 5.2 and 5.3 shows the results for the procedure outlined above. The films generally follow their respective plasticization pressure curves from Figure 5.1, but the different procedure results in slightly different permeability values at each pressure. At 20 atm CO_2 in the pressurization step, the CO_2 permeability of Matrimid® began to

increase measurably within 10 min of exposure time. CO_2 permeability decreased during the depressurization step, owing to Matrimid® having rather short relaxation times. Permeability continued to decrease significantly throughout the 12 hr hold step at 4 atm CO_2 but did not return to the regressed curve for the pressurization step. PPO behaves similar to Matrimid®, but continues to show greater relative changes for shorter exposure times than Matrimid®. However, Matrimid® still experiences a greater reduction of permeability during the depressurization and hold step.

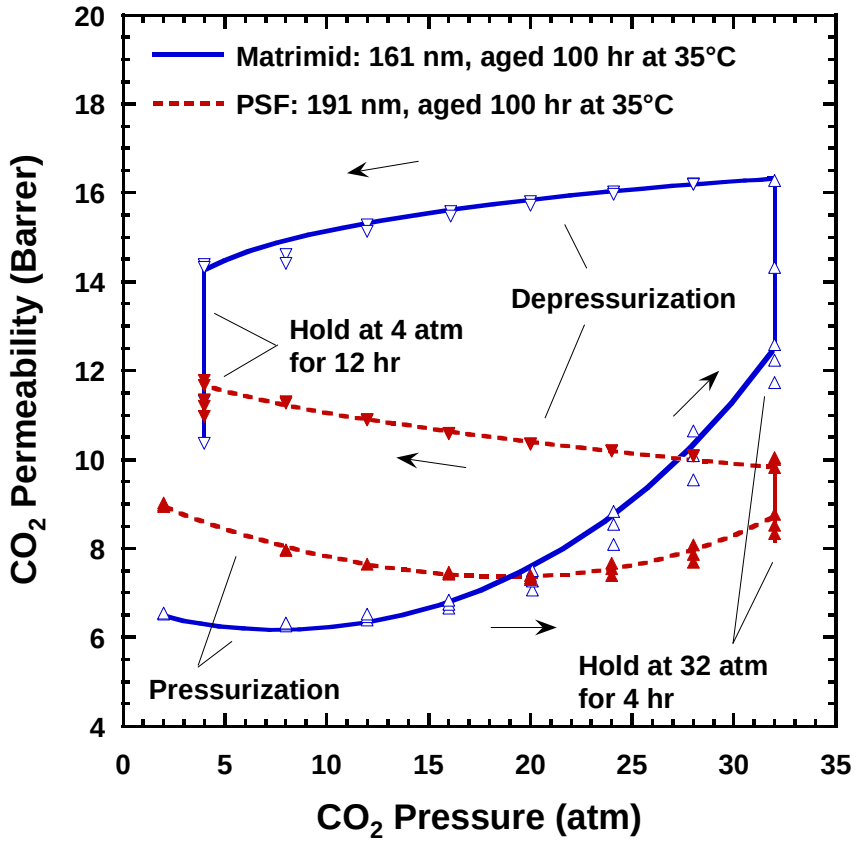

Figure 5.2: CO_2 permeability hysteresis for Matrimid® and PSF thin films with similar prior thermal history.

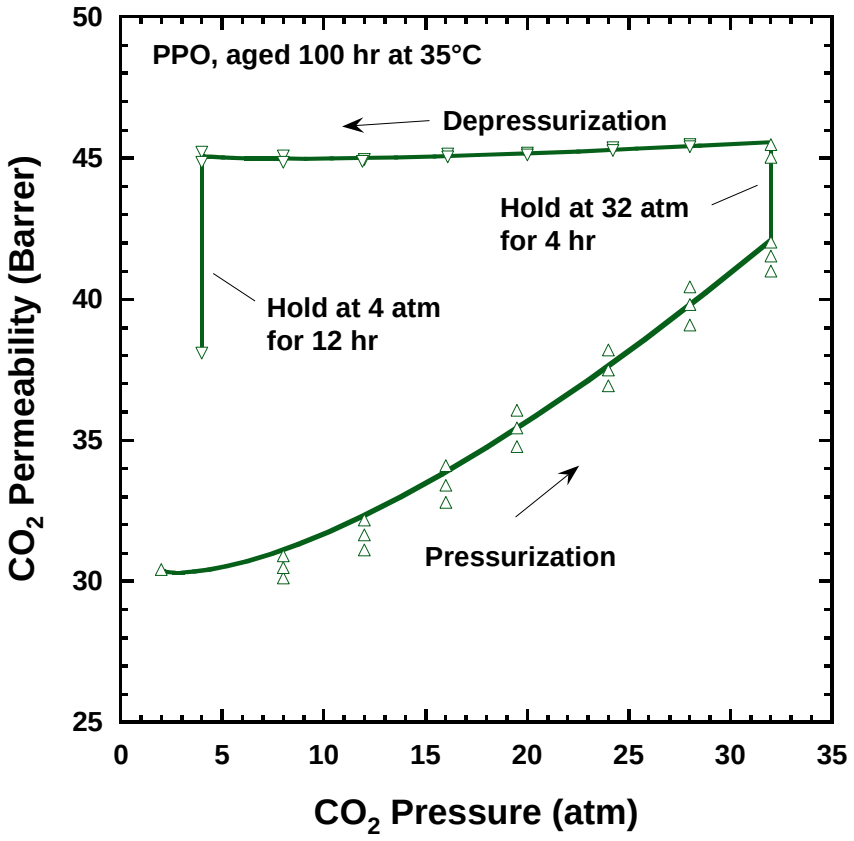

Figure 5.3: CO_2 permeability hysteresis for a PPO thin film. The prior thermal history was similar to the Matrimid® and PSF thin films in Figure 5.2.

The response of the PSF thin film to the procedure is notably different from that of Matrimid®, and seems to behave in some respects more like a thick film than a thin film. During the pressurization step, a minimum in the permeability vs. pressure curve can be distinctly observed, and is slightly less than observed in Figure 5.1. The permeability continued to increase during the depressurization step, a phenomenon typically observed in thick films rather than thin films [3,5–7]. In thick films, the increase is typically attributed to the polymer chain relaxation times being greater in thick films than in thin films [8]. As the pressure is decreased, the polymer relaxes toward its original state, but does not have sufficient time for significant relaxation and the dilated structure allows for greater gas flux. During the 12 hr hold step at 4 atm, the permeability decreased as expected, but as in other steps the PSF film did not show as substantial changes as seen for Matrimid®.

5.2.3 Short Time CO_2 Permeation Experiments

Sections 5.2.1 and 5.2.2 describe how thin films respond to CO_2 under varying conditions of exposure time and CO_2 pressure. Alternatively, relatively fewer pressures for somewhat longer periods of time could be used instead. In this section, CO_2 permeability is tracked for three 200 nm thin films, each aged for 100 hr at 35°C, as they were exposed to a sequence of four CO_2 pressures: 8 atm, 16 atm, 24 atm, and 32 atm. In Chapter 4, this sequence was chosen so that pressures both above and below the plasticization pressure of Matrimid® were included to strengthen further the observation that plasticization occurs well-below the "plasticization pressure" in thin films. Given that each film is relatively thin, the effect of differing plasticization pressures is insignificant and the respective CO_2 responses of the films can be compared more directly.

Figure 5.4 displays the results of these experiments. PSF and Matrimid® begin at 8 atm with close to the same absolute permeability. One can see from the relative permeability graph, though, that Matrimid® begins increasing in permeability immediately upon exposure to CO_2 at 8 atm, whereas PSF appears to decrease slightly over time. Moreover, the CO_2 permeability of PSF decreases upon each change in pressure, although it is difficult to discern any statistically significant decrease in CO_2 permeability over time at 16 atm and 24 atm. At 32 atm, the permeability begins to increase as anticipated. The substantial difference in CO_2 permeation behavior of PSF, relative to Matrimid®, could be attributed to PSF having relatively longer relaxation times (as evidenced in Figures 5.2 and 5.3) and a lower solubility than Matrimid®. The lack of a permeability minimum with increasing pressure for PSF, unlike Figure 5.1 or 5.2, is

somewhat puzzling, and attests to the complicated response of materials to plasticizing gases.

The explanation of PSF's behavior above, appealing to low solubility and a relatively short relaxation time distribution, seems inconsistent with the observation of permeability changes in PPO. As noted in each figure so far, PPO appears to change even more rapidly than Matrimid® at lower pressures, even though Matrimid® still has the greatest relative change by the end of the entire experimental procedure. Apparently, the properties of PPO that result in a substantially higher diffusivity coefficient than Matrimid® mitigate the effect of the lower solubility of CO_2 in PPO, insofar as lower solubility implies less sensitivity to longer exposure times. This might suggest that relaxation times are relatively more related to diffusivity of gases than to solubility. However, Figure 5.3 seems to imply that PPO has a relatively longer relaxation time distribution than Matrimid®. More information is clearly needed to understand the intricacies of the dynamics of plasticization in thin films.

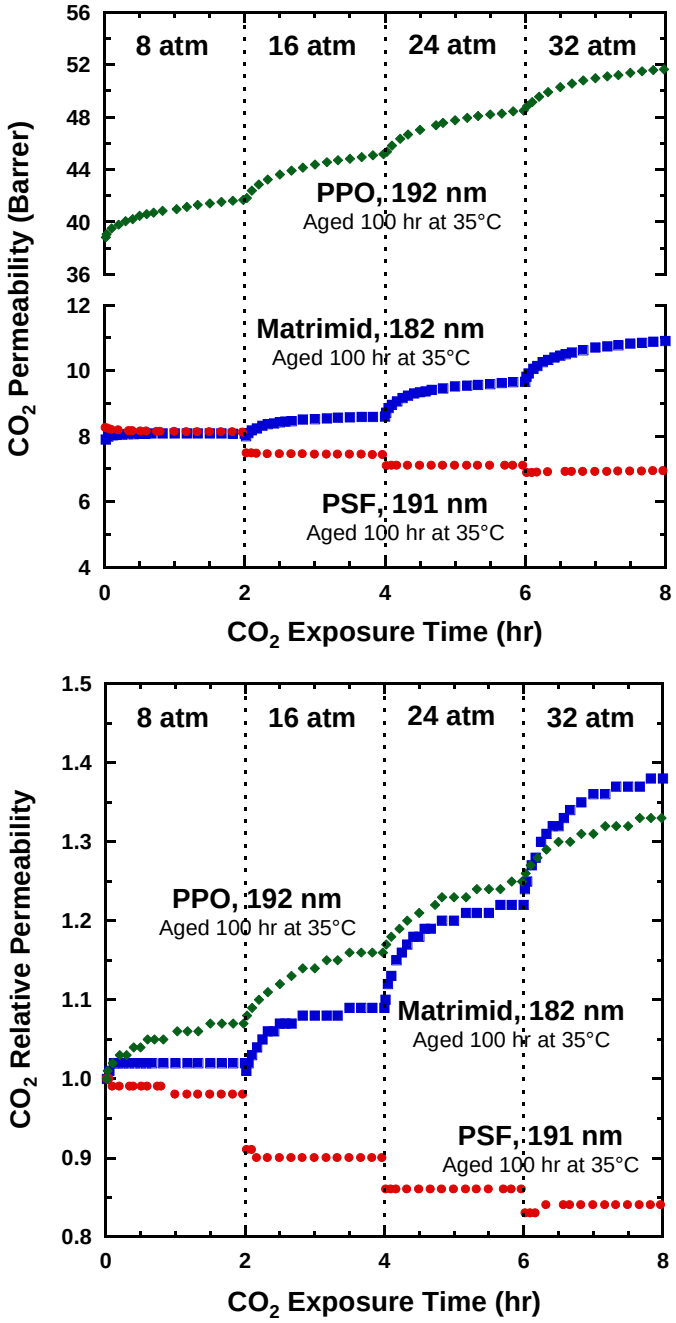

Figure 5.4: Short time CO_2 exposure experiments for thin films with similar prior thermal history.

5.2.4 CO_2 Permeation Behavior for Long Exposure Times

Our previous studies of Matrimid® thin films exposed to a constant pressure of CO_2 for long periods of time revealed that thin films tend to increase in CO_2 permeability until reaching a maximum, followed by a significant decrease in permeability over the remainder of the experiment. Similar experiments were performed at 32 atm and 8 atm CO_2 for at least 500 hr on thin films for each polymer, and permeability was tracked during the exposure period. The films had thicknesses ranging from 190 to 220 nm, and the films were aged for 200 hr at 35°C. The results are presented in Figures 5.5 and 5.6, respectively. In each CO_2 relative permeability graph, the original data has been normalized by the CO_2 permeability measured at 0.1 hr.

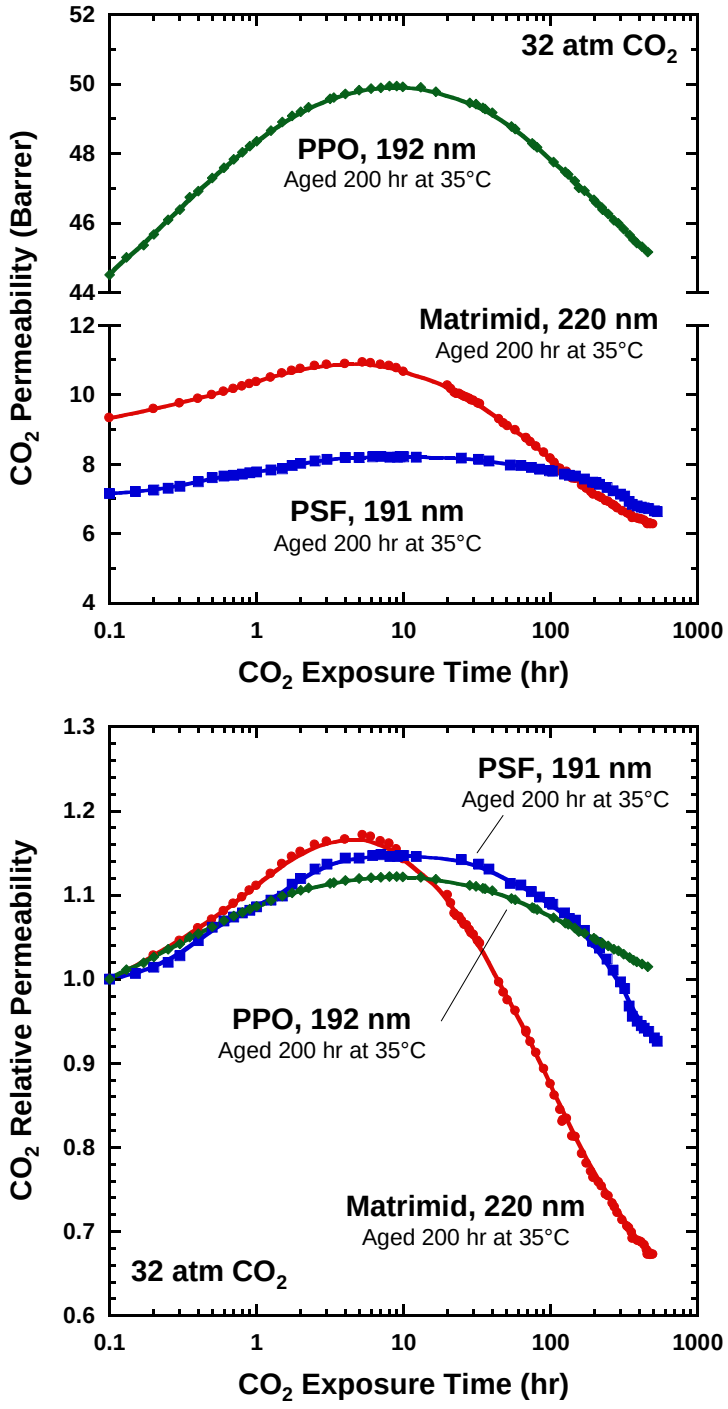

Figure 5.5: Effect of long time CO_2 exposure at 32 atm constant pressure for thin films at similar thickness and similar prior thermal history.

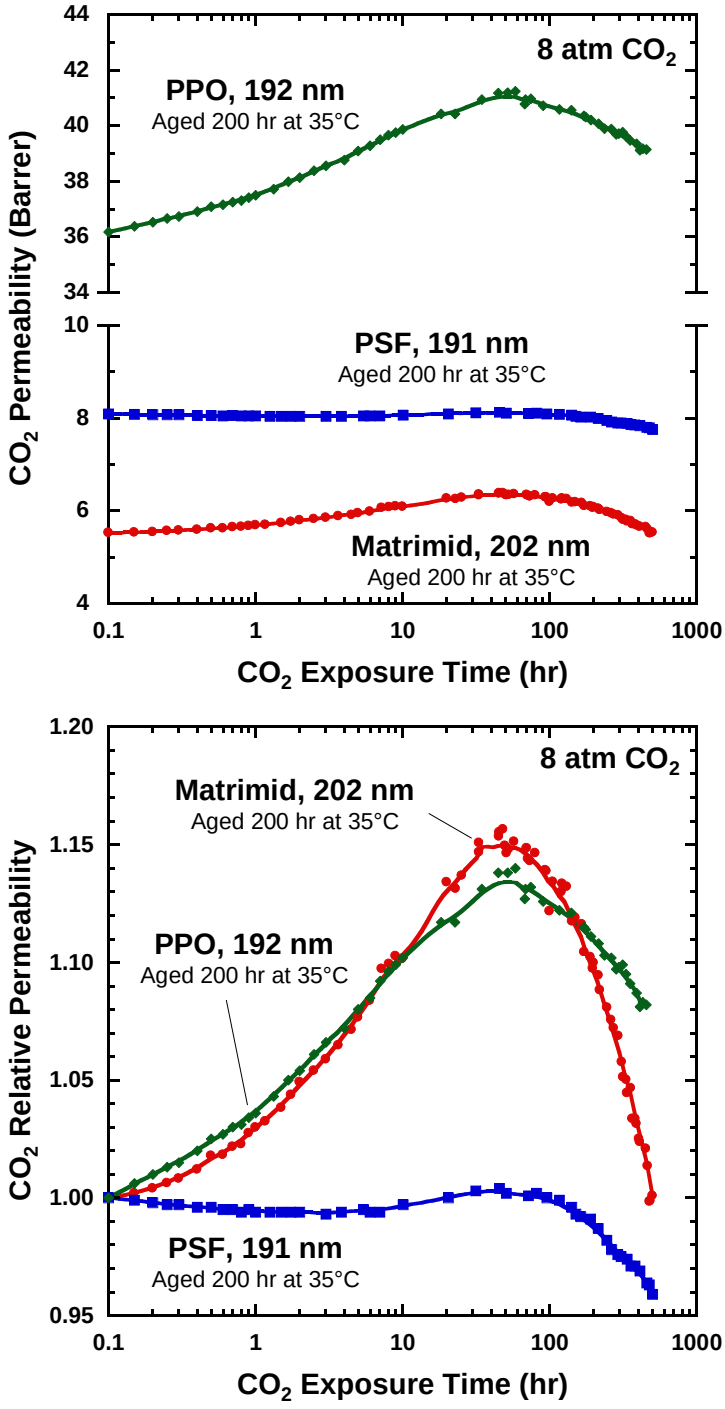

Figure 5.6: Effect of long time CO_2 exposure at 8 atm constant pressure for thin films at similar thickness and similar prior thermal history.

The films exposed to 32 atm CO_2 (Figure 5.5) behaved as expected, with each polymer increasing in permeability to a maximum then reversing the trend and decreasing indefinitely. The permeability turnover is particularly broad for PSF, while PPO and Matrimid® have a more clearly defined maximum. Matrimid® experiences the greatest relative change over the course of the experiment, both in the maximum permeability achieved and in the loss of permeability following the maximum. This behavior is attributed to Matrimid's greater CO_2 solubility than PSF or PPO. Interestingly, PSF appears to be next in the order of increasing relative changes, reaching a greater relative maximum and relative permeability loss than PPO. This result was not expected given the lower solubility of CO_2 in PSF, although it could be an artifact of our arbitrarily chosen time for normalization of the data. Visual inspection seems to indicate, though, that the exposure time required to reach the maximum permeability is shortest for Matrimid® (5 hr), followed by PPO (8 hr) then PSF (10-11 hr). This result is consistent with the order of CO_2 solubility from greatest to least.

Matrimid® and PPO also behave as expected when exposed to 8 atm CO_2 (Figure 5.6), with a reasonably defined maximum permeability between roughly 40-45 hr and 50-55 hr, respectively. Again, Matrimid® experiences the greatest relative maximum and permeability loss due to its greater CO_2 solubility, followed by PPO. However, PSF behaves somewhat differently. Instead of increasing to a permeability maximum, PSF's CO_2 permeability stays nearly constant for about 65 hours then begins to decrease for the remainder of the experiment. This suggests that plasticization and physical aging, which constantly are in competition, are in balance for the initial exposure period at 8 atm CO_2.

Aging still dominates at longer exposure times, though, and causes the permeability decline as observed in Matrimid® and PPO.

In Chapter 4, the long time CO_2 permeation behavior at high pressure was noted to resemble the "memory effect" that Kovacs observed for volume recovery [9]. Expanding upon this idea, one could further interpret this data by considering how the rate of physical aging changes as temperature approaches T_g. Figure 5.7 depicts a general schematic of how the physical aging rate depends on temperature. Beginning at a temperature deep within the glassy state, an initial increase in temperature causes an increase in the aging rate [10]. However, since aging must cease when T_g is reached, the trend must reverse and trend toward zero [11,12]. Isothermal plasticization can emulate this behavior because T_g for glassy polymers is known to decrease under plasticization conditions [13–16]. Since T_g decreases as the polymer is plasticized, the difference between the experimental temperature and T_g also decreases resulting in the physical aging rate increasing. Eventually, the aging rate outpaces any additional plasticization and a maximum in permeability is observed, followed by decreasing permeability for the duration of the experiment.

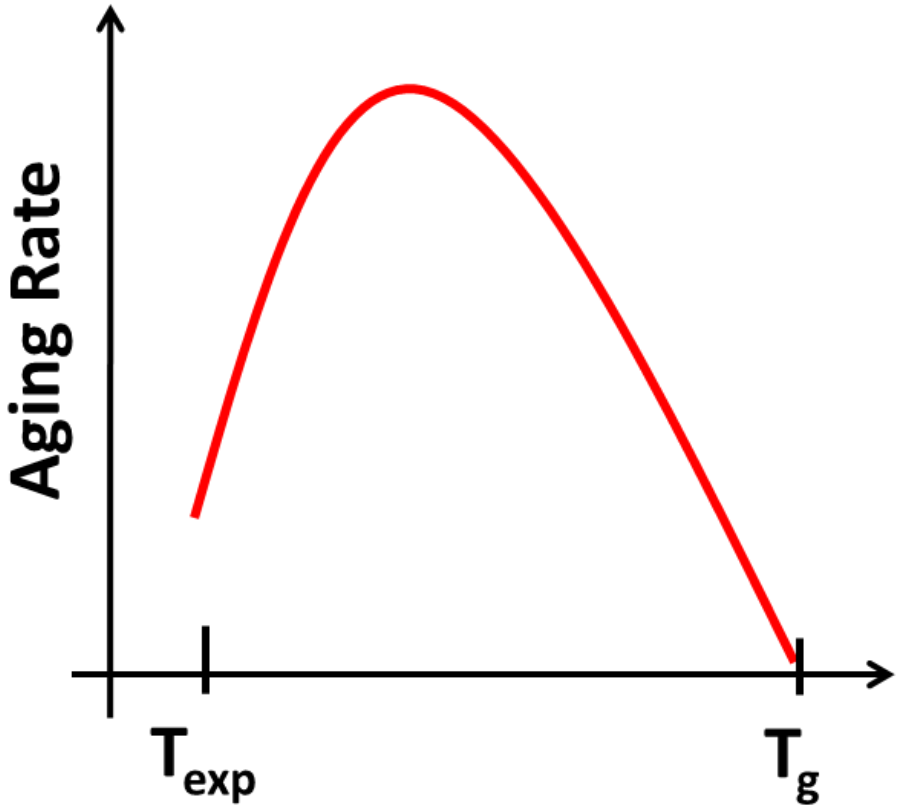

Figure 5.7: Schematic of aging rate of a glassy polymer versus temperature, from an arbitrary experimental temperature deep within the glassy state to T_g.

5.3 CONCLUSIONS

In summary, this chapter has put forward a more nuanced understanding of CO_2 plasticization in a series of fundamentally different thin glassy polymer films. Degree of plasticization response can be expected to follow CO_2 solubility in the polymer. For the polymers tested, Matrimid® had the greatest relative response, followed by PPO and PSF. Despite Matrimid's greater response, PPO appears to respond relatively more quickly to CO_2 plasticization at shorter times. This may be indicative of diffusion/kinetic concerns playing a more prominent role at short exposure times, while at longer exposure times thermodynamic concerns always dominate. PPO's high state of free volume may be responsible for this effect. Permeability maximums were observed in each polymer for long CO_2 exposure times, suggesting that this trend is likely universal for glassy polymers. However, under some conditions no obvious permeability maximum may be observed despite seeing the permeability decrease at long CO_2 exposure times. This behavior suggests that the competing effects of plasticization and aging are balanced. The lower solubility of CO_2 in PSF, plus this polymer's relatively more compact backbone and lower free volume, probably accounts for its more sluggish response to CO_2 plasticization, and such behavior was most evident in the long term exposure experiment at 8 atm CO_2 and the hysteresis experiment. The Kovacs "memory effect" analogy describes the slow dynamics of the polymer response, and observing how the physical aging rate depends on temperature helps explain what takes place within a thin glassy polymer film during plasticization.

Finally, these findings emphasize that long-term property changes are of critical importance to industrial membrane applications using glassy polymers. Knowledge of how membranes behave under plasticizing conditions should help in understanding how

commercial modules behave in practice and is a necessary step towards developing materials and fabrication procedures that minimize the deleterious effects of plasticization. A major point in this work has been to demonstrate that observing such responses on thick films may not be an adequate way to simulate what occurs with high flux commercial membranes.

5.4 REFERENCES

[1] W. J. Koros, D. R. Paul, and A. A. Rocha, "Carbon dioxide sorption and transport in polycarbonate," *Journal of Polymer Science, Part B: Polymer Physics*, vol. 14, no. 4, pp. 687–702, 1976.

[2] C. A. Scholes, G. Q. Chen, G. W. Stevens, and S. E. Kentish, "Plasticization of ultra-thin polysulfone membranes by carbon dioxide," *Journal of Membrane Science*, vol. 346, no. 1, pp. 208-214, 2010.

[3] N. R. Horn and D. R. Paul, "Carbon dioxide plasticization and conditioning effects in thick vs. thin glassy polymer films," *Polymer*, vol. 52, no. 7, pp. 1619-1627, 2011.

[4] A. Bos, I. G. M. Pünt, M. Wessling, and H. Strathmann, "CO_2-induced plasticization phenomena in glassy polymers," *Journal of Membrane Science*, vol. 155, no. 1, pp. 67-78, 1999.

[5] A. C. Puleo, N. Muruganandam, and D. R. Paul, "Gas sorption and transport in substituted polystyrenes," *Journal of Polymer Science, Part B: Polymer Physics*, vol. 27, no. 11, pp. 2385-2406, 1989.

[6] A. C. Puleo, D. R. Paul, and S. S. Kelley, "The effect of degree of acetylation on gas sorption and transport behavior in cellulose acetate," *Journal of Membrane Science*, vol. 47, no. 3, pp. 301-332, 1989.

[7] S. Jordan, W. J. Koros, and G. Fleming, "The effects of CO_2 exposure on pure and mixed gas permeation behavior: comparison of glassy polycarbonate and silicone rubber," *Journal of Membrane Science*, vol. 30, no. 2, pp. 191–212, 1987.

[8] B. W. Rowe, B. D. Freeman, and D. R. Paul, "Physical aging of ultrathin glassy polymer films tracked by gas permeability," *Polymer*, vol. 50, no. 23, pp. 5565-5575, 2009.

[9] A. J. Kovacs, J. M. Hutchinson, and J. J. Aklonis, "Isobaric volume and enthalpy recovery in glasses. (I) A critical survey of recent phenomenological approaches.," in *The Structure of Non-Crystalline Materials*, 1977, no. 1977, pp. 153-163.

[10] Y. Huang and D. R. Paul, "Effect of Temperature on Physical Aging of Thin Glassy Polymer Films," *Macromolecules*, vol. 38, no. 24, pp. 10148-10154, 2005.

[11] E. A. Baker, P. Rittigstein, J. M. Torkelson, and C. B. Roth, "Streamlined ellipsometry procedure for characterizing physical aging rates of thin polymer films," *Journal of Polymer Science, Part B: Polymer Physics*, vol. 47, no. 24, pp. 2509-2519, 2009.

[12] J. E. Pye, K. A. Rohald, E. A. Baker, and C. B. Roth, "Physical Aging in Ultrathin Polystyrene Films: Evidence of a Gradient in Dynamics at the Free Surface and Its Connection to the Glass Transition Temperature Reductions," *Macromolecules*, vol. 43, no. 19, pp. 8296-8303, 2010.

[13] J. S. Chiou and D. R. Paul, "Sorption and transport of CO_2 in PVF2/PMMA Blends," *Journal of Applied Polymer Science*, vol. 32, no. 1, pp. 2897-2918, 1986.

[14] J. S. Chiou, Y. Maeda, and D. R. Paul, "Gas and vapor sorption in polymers just below Tg," *Journal of Applied Polymer Science*, vol. 30, no. 10, pp. 4019-4029, 1985.

[15] J. S. Chiou, J. W. Barlow, and D. R. Paul, "Plasticization of Glassy Polymers by Co2," *Journal of Applied Polymer Science*, vol. 30, no. 6, pp. 2633-2642, 1985.

[16] Y. Mi, S. Zhou, and S. A. Stern, "Representation of gas solubility in glassy polymers by a concentration-temperature superposition principle," *Macromolecules*, vol. 24, no. 9, pp. 2361-2367, 1991.

Chapter 6: Carbon Dioxide Sorption and Plasticization of Thin Glassy Polymer Films Tracked by Optical Methods

---

This chapter has been adapted from an article published in Macromolecules, *submitted*.

6.1 SUMMARY

Chapters 4 and 5 demonstrated that thin glassy polymer films respond to highly-sorbing penetrants, such as CO_2, quite differently than thick films. These studies focused on CO_2 permeation behavior, and revealed that, for thin films, CO_2 permeability at constant CO_2 pressure goes through a maximum followed by a continual decrease in permeability owing to physical aging. So far, thick and thin glassy polymer films have been compared in the context of permeability, but lack of substantial means of obtaining thin film sorption data has prevented adequate comparison of thick and thin films in the context of gas solubility. In this chapter, spectroscopic ellipsometry is used to obtain simultaneously the film thickness and CO_2 sorption capacity for thin glassy polymer films. This allows a more comprehensive look at CO_2 permeability, sorption, and diffusivity as a function of both CO_2 pressure and exposure time. The evidence reported here suggests that thin film sorption behavior is substantially different than that of thick film counterparts. Partial molar volume is determined from sorption-induced swelling data. Fractional free volume and diffusivity are calculated as a function of CO_2 pressure. Dual sorption model parameters are presented for Matrimid® thin films for different aging times. Dynamic ellipsometry experiments show that refractive index minima, fractional free volume maxima, and CO_2 diffusivity maxima correlate well with observed CO_2 permeability maxima observed for thin Matrimid® films. The results support the claim that plasticization and physical aging are competing processes but that aging dominates over long time scales. The CO_2 diffusivity behavior over time is most affected by the competing effects of plasticization and aging, and the evolution of CO_2 diffusivity is shown to be the main contributing factor to changes in CO_2 permeability at constant pressure.

6.2 RESULTS FROM SORPTION ISOTHERM EXPERIMENTS

An example of the data produced by the sorption isotherm procedure described in Chapter 3.5 is presented in Figure 6.1, and includes the Ψ and Δ ellipsometric angles, sorption-induced swelling, and concentration of CO_2 for a 312 nm Matrimid® film aged 1 day at 35°C. As pressure is increased the features of the ellipsometric angle curves shift to the right toward greater wavelengths, which frequently indicates a change in thickness. Similar shifts to the right are observed for prolonged CO_2 exposure times during constant pressure experiments as well. Though the shifts in the features appear small, they represent significant changes induced by plasticization. For instance, this film swells over 4% over the pressure range tested, sorbing up to 44 cm^3(STP) of CO_2 per cm^3 of polymer.

Sorption isotherms are frequently presented in the literature with pressurization and depressurization steps, typically demonstrating hysteresis owing to the long relaxation times of the glassy state. In Figure 6.1, a small amount of hysteresis was observed during the depressurization step. The film thickness and CO_2 concentration decreased as pressure was decreased, but these measurements were still greater than those measured during the pressurization step. This behavior reflects the shorter relaxation times of thin films relative to thick films and the importance of exposure time to CO_2 plasticization. We observed similar hysteresis in other thin film sorption isotherm experiments, but here we do not present any further depressurization curves to preserve figure clarity.

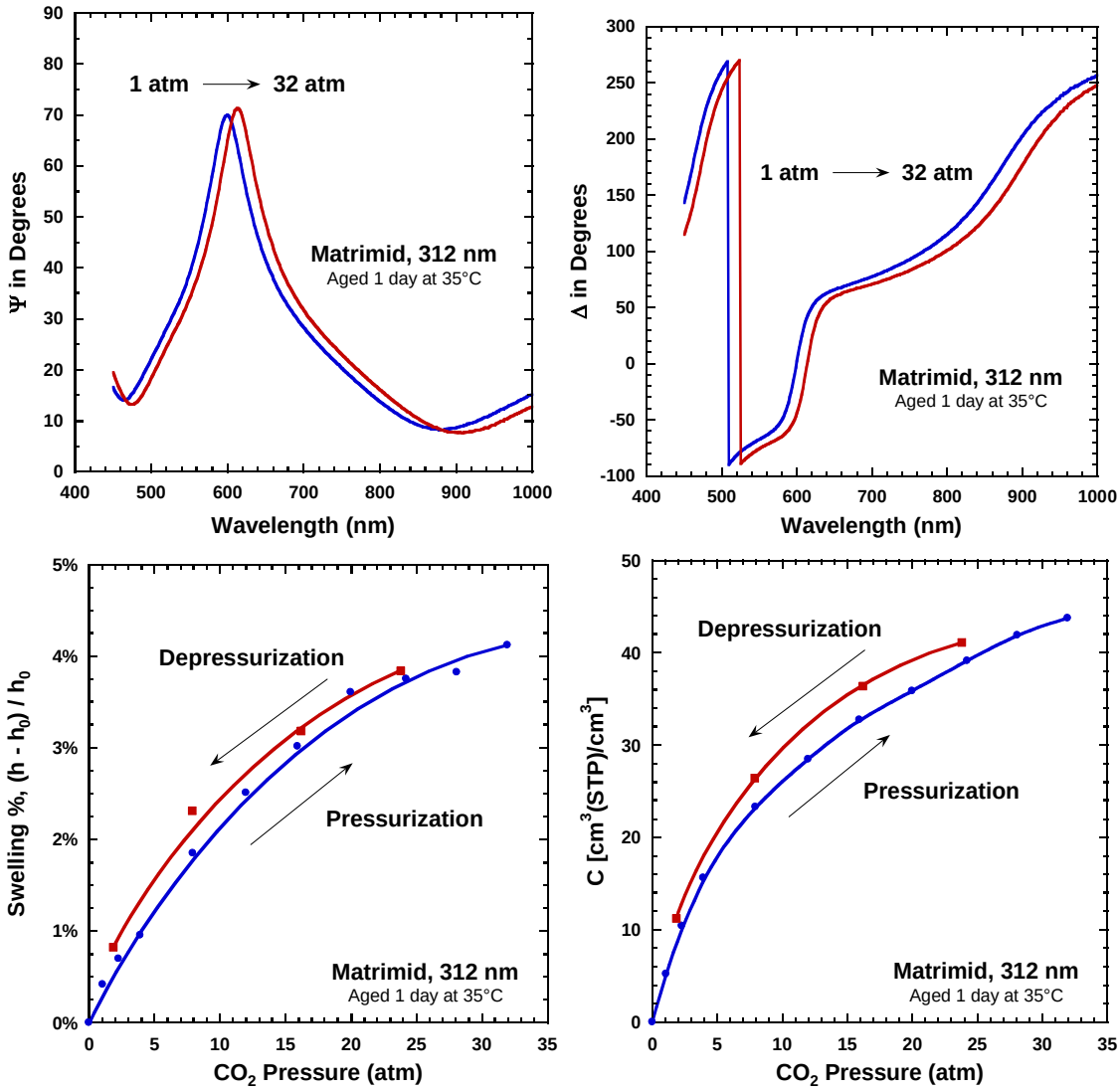

Figure 6.1: Example data for psi, delta, swelling, and concentration for a CO_2 sorption isotherm at 35°C obtained via ellipsometry (312 nm Matrimid® film, aged 1 day at 35°C).

6.2.1 Effect of thickness on CO_2 sorption

Figure 6.2 shows literature data for CO_2 sorption in Matrimid® using a variety of methods. In most cases, the thickness of the sample used to generate the data was not given. In Figure 6.3, select data from Figure 6.2 where thicknesses were known, are presented alongside thin film CO_2 sorption isotherms measured via ellipsometry. Thick film (~50 μm) data in this work were obtained with pressure decay instruments to check against the literature. It should be noted that Simons et al. measured sorption of a 2 μm Matrimid® with an ellipsometer, but used a different instrument than in our work. J.A. Woolam Co. generally recommends that only polymer samples with thicknesses <1.5 μm be tested with the M-2000 ellipsometer to ensure accuracy; however, the results of Simons et al. are somewhat similar to those measured here.

The difference between thin and thick films is apparent; as thickness is decreased, the CO_2 sorption capacity tends to decrease as well. For example, CO_2 sorption at 20 atm decreases by over a factor of 2 as thickness is reduced to less than 100 nm. Below 2 μm, the changes appear to become less pronounced.

Figure 6.4 presents CO_2 sorption isotherms of multiple polymers in both the bulk state and thin film form. Bulk data was obtained from the literature [1–4], and butyl rubber is included for comparison to a rubbery material [5,6]. Thin film data were obtained via ellipsometry with the procedure explained above; each film was aged 1 day at 35°C before testing. In both plots, CO_2 sorption proceeds in the order of increasing T_g, i.e., Polystyrene < PSF < PPO < Matrimid®. Thickness apparently does not change the relationship between T_g and sorption capacity. However, each thin film exhibited significantly less CO_2 sorption than its bulk film counterpart, supporting the growing

body of evidence suggesting that thick and thin films respond differently to gas sorption and permeation, especially when plasticization is significant. The greatest effect of thickness was observed with Matrimid®; the bulk and thin films differed by 30%. The thin polystyrene film, however, showed the least departure from the bulk isotherm. This could be related to the relatively low T_g of polystyrene. It is possible that thickness effects upon sorption are not as pronounced when the difference between the experimental temperature and T_g is small, but not enough data are available to be conclusive.

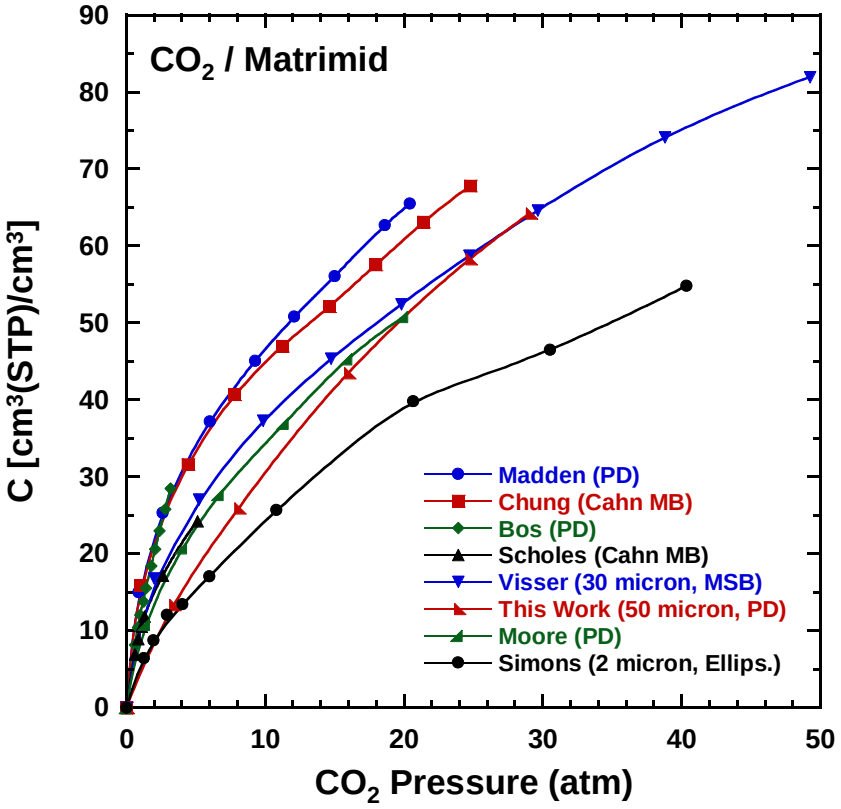

Figure 6.2: Literature data for Matrimid® CO_2 sorption Isotherms obtained from various methods and thicknesses. PD = Pressure Decay, MSB = Magnetic Suspension Balance, MB = Microbalance. [1,7–12]

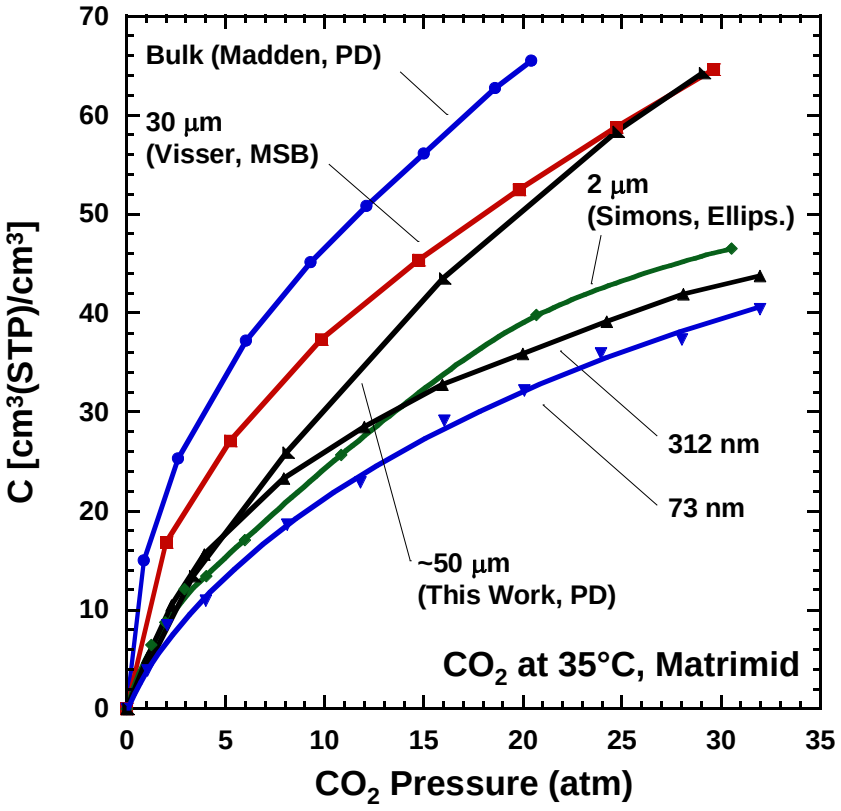

Figure 6.3: Effect of thickness on CO_2 sorption in Matrimid®.

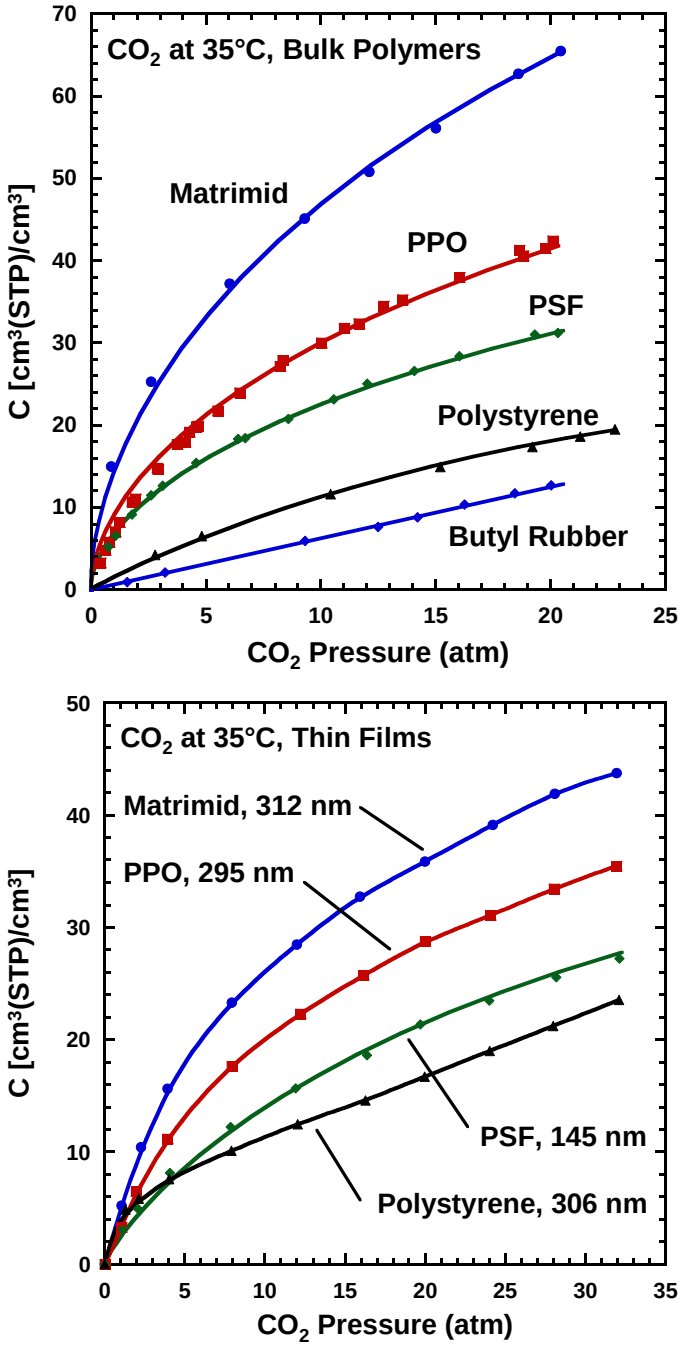

Figure 6.4: Sorption isotherms for various polymers. Bulk polymer data taken from the literature [1–6]. All thin films were aged for 1 day at 35°C.

6.2.2 Effect of aging time on thin film CO_2 sorption

Our previous work has demonstrated that aging time plays a significant role in CO_2 permeation behavior [13], thus it seems reasonable that CO_2 sorption would be affected by aging time as well. Figure 6.5 depicts sorption isotherms at multiple aging times for the four polymers of interest. Polystyrene, PPO, and PSF include aging times at 1 day and 1 month at 35°C; these aging times were arbitrarily selected and have no particular significance other than to show this effect. For Matrimid®, though, aging times of 1 h, 100 h, and 500 h at 35°C were chosen deliberately to coincide with aging times from our previous work with Matrimid®.

The polymers generally behaved as expected, with Matrimid®, PSF, and polystyrene exhibiting decreased CO_2 sorption at longer aging times. It is notable that the thin film aged for only 1 h still exhibited considerably less sorption than any thick films shown in Figure 6.4. These data, along with other thin film data collected at different aging times, suggest that the thickness effect upon sorption cannot be attributed merely to the accelerated aging characteristic of thin glassy polymer films. Interestingly, although Matrimid was most affected by a change in thickness, it was relatively less affected by aging time than PSF and polystyrene. Admittedly, the Matrimid® film was aged only for ~500 h (~21 days) whereas the PSF and polystyrene films were aged for 1 month. Polystyrene changed the most due to aging; at 32 atm CO_2 the film aged for 1 month sorbed nearly 20% less CO_2 than the film aged for 1 day. PPO, however, showed very little effect of aging time on sorption. Chapter 5 suggested that the unusual response of PPO to CO_2 may be related to kinetic concerns that our experiments cannot fully

ascertain [14]. Nonetheless, the data reported here indicate generally that aging time does affect CO_2 sorption significantly, but not as dramatically as thickness.

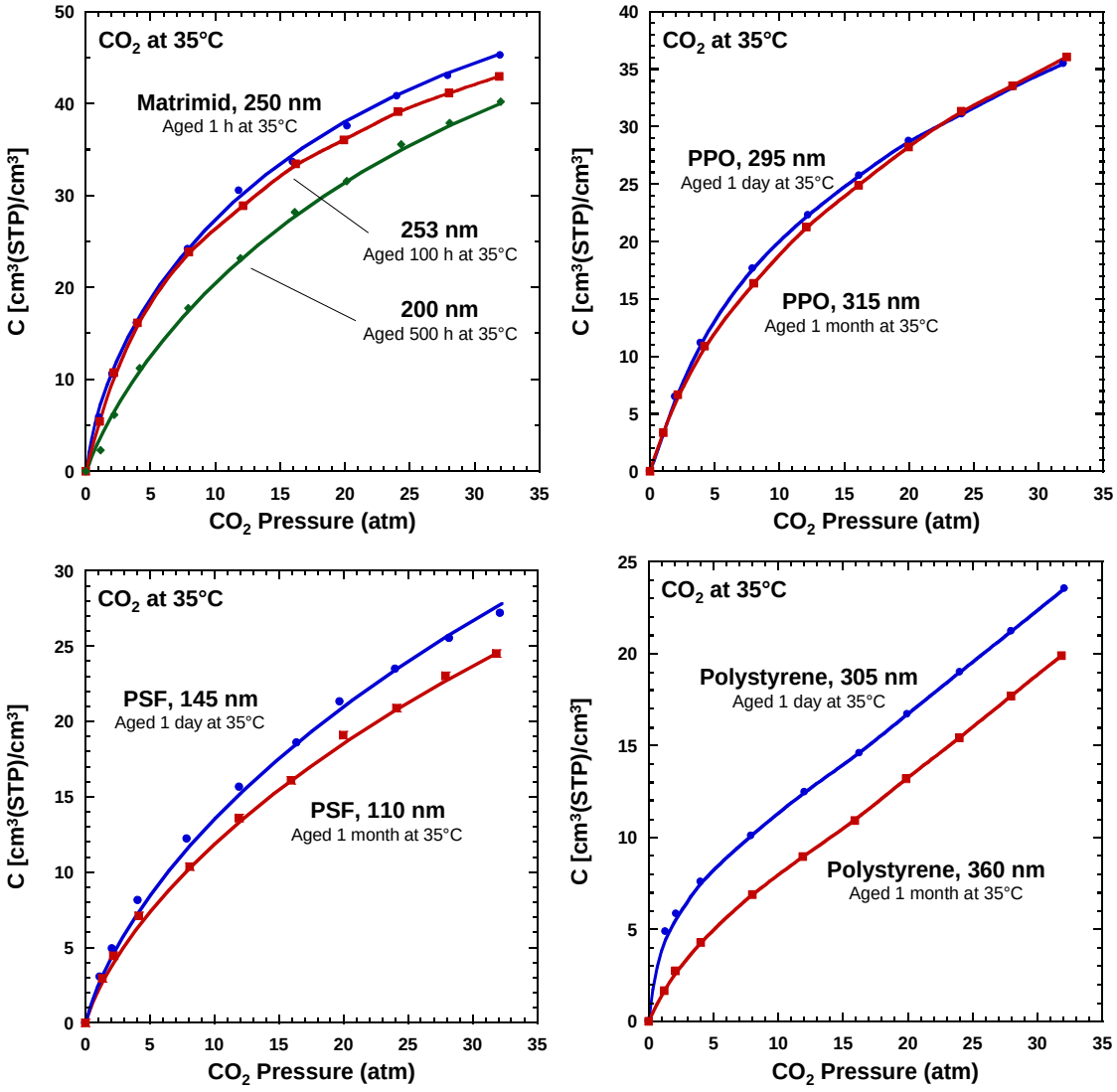

Figure 6.5: Effect of aging time on CO_2 sorption in thin films.

6.2.3 Partial molar volume

Plots of swelling as a function of CO_2 concentration are presented in Figure 6.6 for the films aged for 1 day. The slopes for each data set represent the partial molar volume of CO_2 in the polymer. The data generally fit well to a linear relationship, suggesting that molar volume of CO_2 in the polymer is independent of concentration, with a small offset in the low pressure range. Simons et al. noticed a similar offset in their work as well [7], attributing it to an artifact of their ellipsometer technique. The similarity of these offsets suggests that this may be more than an artifact; it could be that at low partial pressures CO_2 swells the polymer very little. Although they did not report partial molar volumes for each polymer separately, they reported an average value of 25.3 cm^3/mol. The partial molar volumes calculated in this work are listed in Figure 6.6 and have an average value of 23.0 cm^3/mol. Like Simons et al., no distinct correlation between partial molar volume and the polymer glass transition temperature was found.

Additionally, the partial molar volumes calculated in this work and in Simons et al. are lower than those found by Wind et al., who proposed that the onset of plasticization occurred at a threshold CO_2 partial molar volume of 29 cm^3/mol. Bos et al. previously suggested in a similar manner that a critical CO_2 concentration of 37 ± 7 cm^3STP/cm^3 indicated the onset of plasticization [15]. However, our results (and those of Simons et al.) indicate that neither of these conditions holds for thin films, which show significant plasticization at significantly different values of partial molar volume and pressure (or concentration). However, these data are for rather short exposure times (< 1 h), and both CO_2 concentration and sorption-induced swelling would be expected to increase over longer exposure times. Although both quantities may tend to increase in

tandem, such changes could potentially result in different partial molar volume calculations.

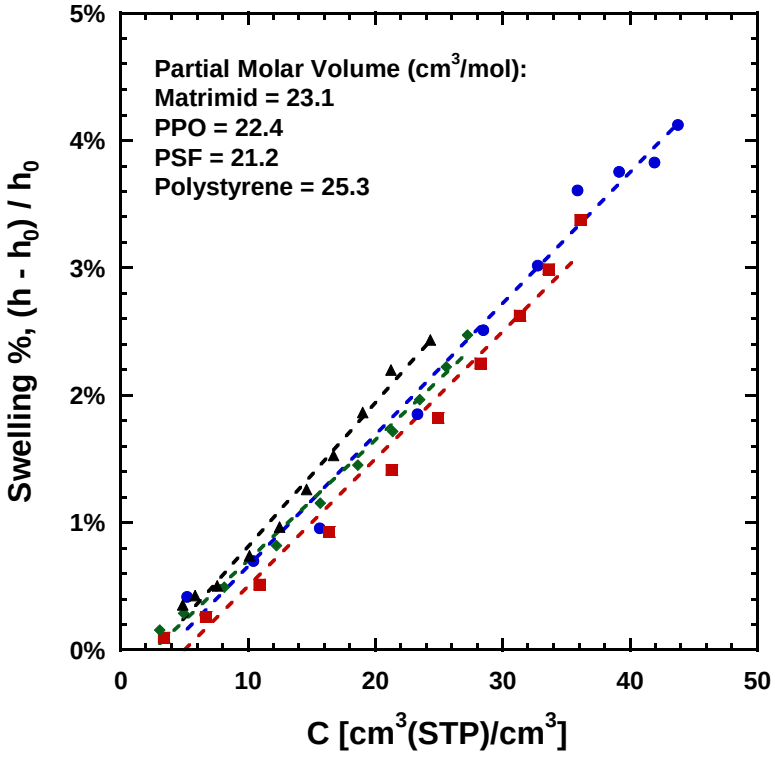

Figure 6.6: Swelling of thin films as a function of the CO_2 concentration at 35°C. Each film was aged for 1 day at 35°C prior to CO_2 exposure. Slopes of the lines represent CO_2 partial molar volume for (●) Matrimid®, (■) PPO, (◆) PSF, and (▲) polystyrene, and the values are listed in cm^3/mol.

6.2.4 Fractional free volume as a function of pressure

When a polymer is plasticized, the polymer's permeability to gases increases for a time, which implies that the fractional free volume increases as well. One would expect that fractional free volume would generally increase as a function of CO_2 pressure, because plasticization tends to increase as CO_2 is sorbed by the polymer. Hong et al. [16] and Chen et al. [17] observed such behavior via positron annihilation lifetime spectroscopy (PALS) for 1 mm thick samples of polycarbonate and polystyrene, respectively, plasticized by CO_2. Results from this work differed from those of prior researchers, but some further background is required to explain how these results were obtained.

Calculating the fractional free volume of a polymer typically requires knowing the density and occupied volume of the polymer alone. However, a mixed system requires accounting for the occupied volume of sorbed gas using a simple mixing rule (refer to Equation 2.14). Determining the van der Waals volume of a sorbed species such as CO_2, though, is a non-trivial task and the value chosen affects the calculations to a great extent. An upper bound for the occupied volume of CO_2 can be set by considering that the density of a CO_2 crystal at -78.5°C is 1.562 gm/cm^3, and thus the specific volume is 0.64 cm^3/gm. Since any sorbed CO_2 would by necessity include more space between molecules than the crystal, one can reasonably say that any value for the occupied volume of CO_2 in a polymer system will be less than 0.64 cm^3/gm. The "occupied volume" obtained from the van der Waals equation of state, 0.9739 cm^3/gm [18], can then be ruled out immediately. Theoretically determined values for the van der Waals

volume of CO_2 vary in the literature. Bondi [19], Ronova et al. [20], and Wong [21] report values of 0.448, 0.422, and 0.311 cm^3/gm, respectively.

In Figure 6.7, Wong's suggested value for the van der Waals volume, 0.311 cm^3/gm, was used to calculate the fractional free volume as a function of pressure for each thin film from Figure 6.4. Upon inspection, one can see that the polymers do not behave exactly as expected. Instead of fractional free volume increasing as a function of pressure, it decreases from the initial value for each polymer before CO_2 exposure. This decrease is followed by a minimum and a slight recovery as CO_2 pressure is increased. The bowl-shaped curves are somewhat similar to plots of CO_2 permeability versus pressure for glassy polymers, and suggest a similar interpretation. The decrease in fractional free volume with CO_2 pressure can be interpreted as "hole-filling" within the polymer, similar to the initial decrease in CO_2 permeability at low pressures. As pressure is increased and the holes become fully filled, the continued swelling is responsible for the slight increase in free volume. The order of the polymers in the top plot of Figure 6.7 is notable as well. Instead of following in order of increasing CO_2 solubility, the polymers generally follow in order of increasing CO_2 permeability. This appears consistent with the general understanding that permeability is closely related to free volume.

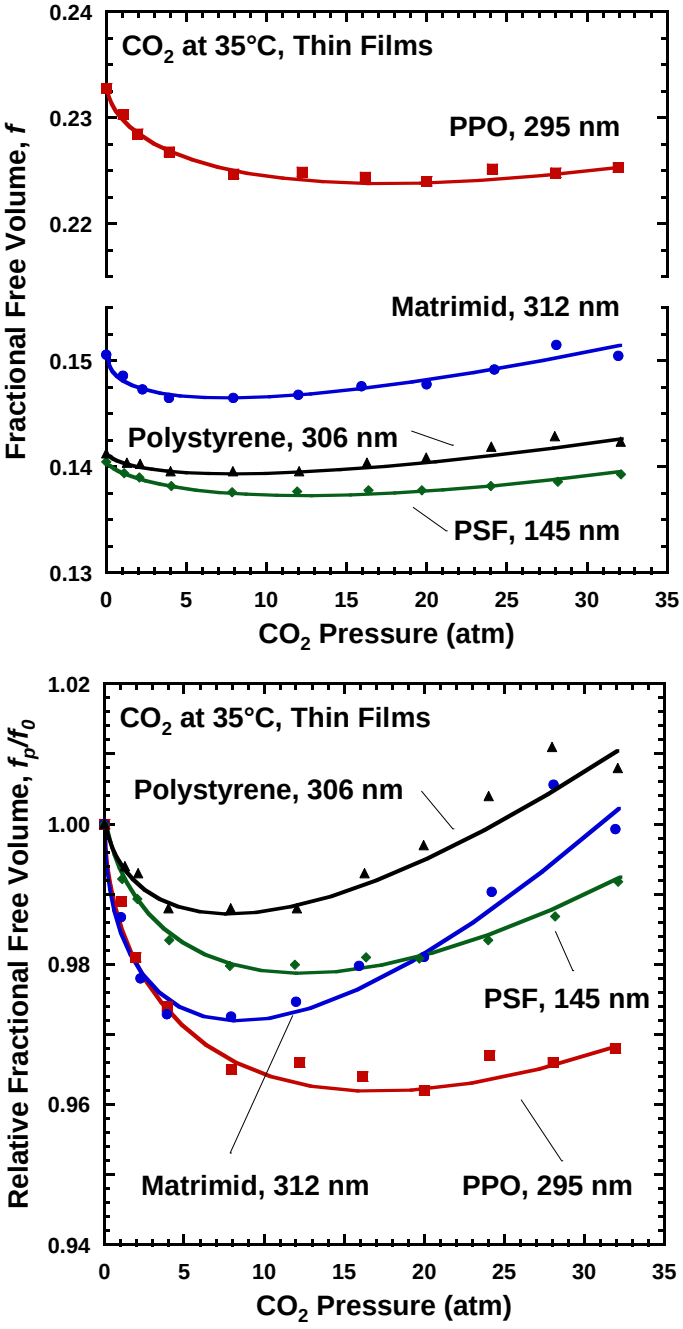

Figure 6.7: Fractional free volume of thin films as a function of CO_2 pressure, calculated from equation 9. Data at zero pressure indicate fractional free volume calculated before CO_2 exposure.

Again, these results are largely dependent upon the value of $V_{vdw,CO2}$ chosen for the calculations. For this set of data, a value of the van der Waals volume of CO_2 significantly greater than ~0.3 cm^3/gm will cause the fractional free volume to decrease continuously as a function of pressure. To check this observation, we considered again the results of Rowe et al. [22], using their data to calculate the fractional free volume of Matrimid® and polysulfone as a function of the activity of water, also known to plasticize polymers. Two values of the van der Waals volume of water, ~0.385 and ~0.535 cm^3/gm, were obtained from the literature [23,24]. Similar to the CO_2 experiments reported here, fractional free volume decreased with increased water uptake as shown in Figure 6.8.

One must keep in mind that there are multiple time scales at work during plasticization experiments, and the choices made during the execution of this work were rather arbitrary. The time scale for gas sorption to achieve a pseudo-steady state in a thin film is quite short, on the order of seconds, and holding pressure constant for a few minutes is sufficient to obtain useful ellipsometric measurements. Plasticization, though, occurs over a period of time much longer than the total time scale of these particular experiments (~1 h). Leaving the film at each pressure for a significantly longer time would have certainly resulted in higher fractional free volumes due to continued plasticization. As will be seen in Section 6.3.1, fractional free volume increases as a function of CO_2 exposure time at constant CO_2 pressure. Indeed, even during the depressurization steps free volume clearly increased from the earlier measurements at the same pressures. The "hole-filling" process is dependent upon time, and thus understanding the effect of one's experimental methodology is critical to interpreting properly.

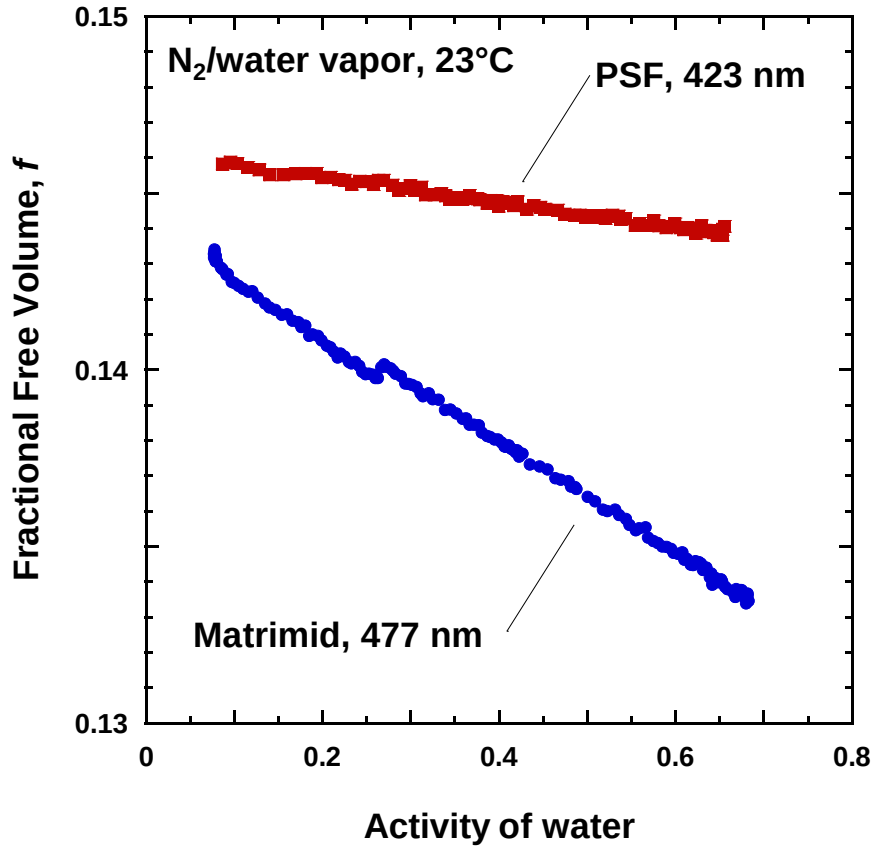

Figure 6.8: Fractional free volume of PSF and Matrimid® thin films as a function of the activity of water in an N_2 / water vapor environment. Calculated from reference [22], using a van der Waals volume of water of 0.535 cm^3/gm.

6.2.5 Estimating dual sorption model parameters and CO_2 diffusivity as a function of pressure for thin Matrimid® films

As mentioned previously, if accurate values of gas sorption and permeability are obtained under similar conditions then diffusivity can be calculated from $D = P / S$. In Figure 6.9, CO_2 diffusion coefficients as a function of pressure for Matrimid® thin films have been estimated using sorption data from this study (Figure 6.5) and permeability data from Figure 4.4. Although we have attempted to conduct comparable experiments with the different techniques by matching as many conditions as possible, some differences still exist between the two data sets and should be noted. First, the film thicknesses are not exactly the same in the two studies. The films in Figure 6.9 are ~250 nm, whereas those from the previous study (Figure 4.4) are ~180 nm. Second, the CO_2 pressures and exposure times are somewhat different in the procedures of the two studies. Since the sorption experiments were performed with films attached to substrates, the aging history may also make a difference. The error due to these differences is not expected to be significant.

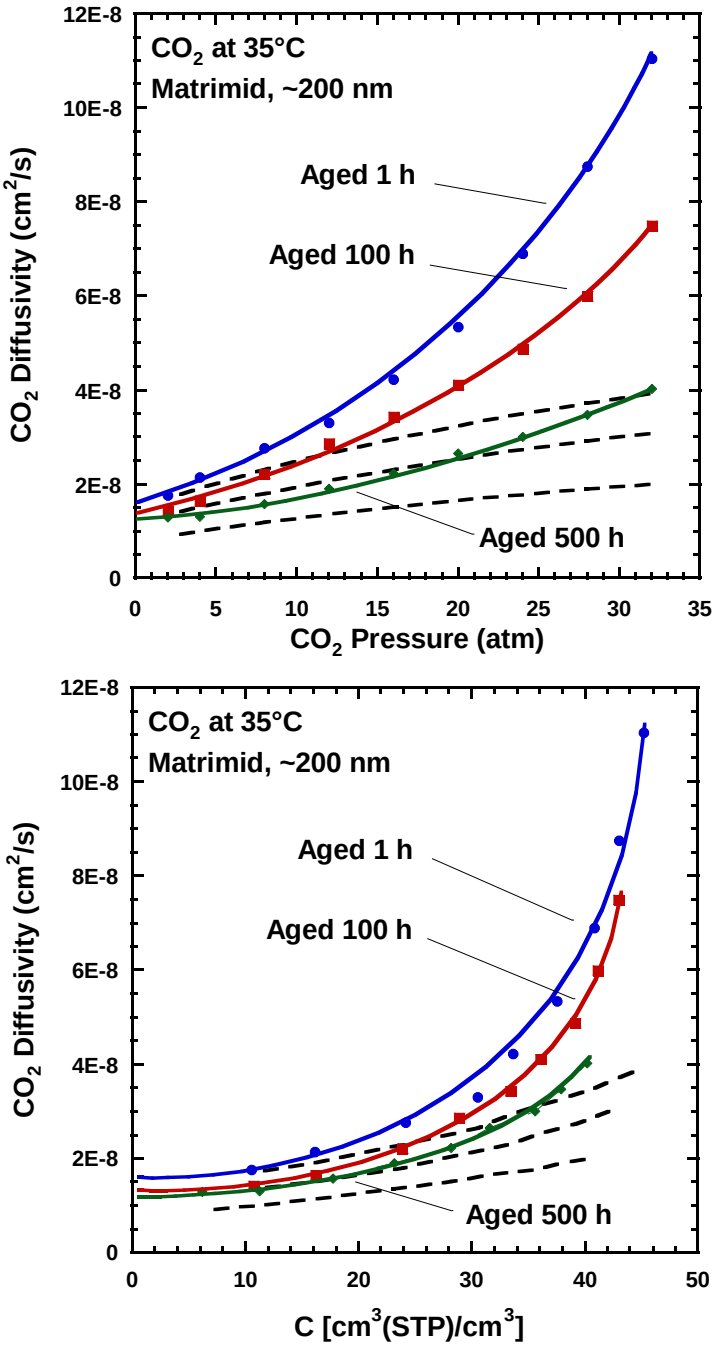

Figure 6.9: Apparent CO_2 diffusivity for Matrimid® at different aging times plotted as a function of CO_2 pressure and CO_2 concentration. Values were calculated from permeability measurements made previously [13] and sorption data obtained via ellipsometry. Dashed lines represent predictions from the dual-sorption model.

The dashed lines in Figure 6.9 represent the apparent CO_2 diffusivity predicted from the dual sorption, dual mobility model that do not take plasticization into account:

$$S = C/p = k_d + \frac{C_H' \cdot b}{1 + b \cdot p} \tag{6.1}$$

$$P = \left(k_d + \frac{F \cdot C_H' \cdot b}{1 + b \cdot p}\right) D_D \tag{6.2}$$

The model parameters k_d, C_H', and b for the thin films were obtained via nonlinear least-squares regression analysis of the sorption data in Figure 6.5. The partial immobilization factor F was taken to be 0.1, following the suggestion of Aitken et al. [25]. Next, the diffusion coefficient D_D was calculated from the experimentally determined permeability at 2 atm CO_2. The predicted apparent CO_2 diffusivity at each pressure was then calculated from the theoretically determined permeability and solubility. The regressed parameters are presented in Table 1 alongside literature values for comparison. Similar to Simons et al., the C_H' values for thin films differed significantly from bulk films, but values for k_d and b also exhibited thickness dependence. All model parameters show some dependence on aging time as well.

	$k_d \left(\frac{cm^3 STP}{cm^3 \cdot atm}\right)$	$C_H' \left(\frac{cm^3 STP}{cm^3}\right)$	$b\ (1/atm)$	$D_D\ (cm^2/s)$
Moore/Koros [10]	1.44	25.5	.367	
Chung *et al*. [9]	1.416	35.0	.702	
Thin Films (~200 nm)				
Aged 1 h	0.554	32.5	.204	13.9 x 10^{-8}
Aged 100 h	0.490	32.4	.202	11.9 x 10^{-8}
Aged 500 h	0.489	27.3	.174	6.52 x 10^{-8}

Table 6.1: Dual-sorption model parameters for Matrimid®.

At low pressures, the estimated diffusivity of the thin films generally agrees with prior observations. The diffusivity of CO_2 in thick Matrimid® films at 2 atm and 35°C is ~1.8 x 10^{-8} cm^2/s [14], and the estimated diffusivity of the thin film aged for 1 h was 1.76 x 10^{-8} cm^2/s. We believe this affirms the usefulness of our approach. The CO_2 diffusivity increases with CO_2 pressure (or concentration) as predicted by the dual sorption model [26,27], but the values obtained from measurement of *P* and *S* depart from the model predictions as pressure increases. This effect upon diffusivity, which is over and beyond the dependence on concentration expected from the dual sorption model, is understood to be the result of plasticization. Also, CO_2 diffusivity is significantly greater for shorter aging times at all pressures, reflecting that free volume is greater at shorter aging times. At 2 atm, CO_2 diffusivity differs 30% between the films aged 1 h and 500 h. At 32 atm, the difference is greater than 50%. Since plots of CO_2 diffusivity versus concentration do not collapse into a single curve, we can conclude that diffusion of plasticizing gases in glassy polymers is dependent on more variables than the gas concentration in the film alone. Aging and other effects of prior history must also play a role.

6.3 RESULTS FROM CONSTANT PRESSURE EXPERIMENTS

6.3.1 General observations

Figures 6.10 to 6.12 show results from three separate constant pressure experiments with Matrimid® thin films. Each film was 200-220 nm thick and had been aged for ~200 h at 35°C. Constant CO_2 pressure was maintained for ~100 h at 35°C. The thicknesses, aging time, and CO_2 pressures (8, 16, and 32 atm) correspond with previous long-time CO_2 exposure studies with the same material (Chapters 4 and 5). These conditions were originally selected to study the effect of pressure on CO_2 permeation behavior over exposure periods ranging from 500-1000 h, and included pressures both above and below the so-called "plasticization pressure" of Matrimid® (12-14 atm CO_2). There was significant scatter in the data at 8 atm, and moving averages of refractive index and fractional free volume were plotted instead of the raw data. The scatter was likely due to the instrument being more sensitive to instrument fluctuations at lower pressures than at higher pressures, but the trends are still reasonably sound.

The films swelled noticeably even within one minute of CO_2 exposure, and the initial swelling is directly related to the CO_2 pressure. Evidently, the greatest change in thickness occurs over a very short time period as the film responds to the sudden exposure to high-pressure gas. The films continued to swell over the course of 100 h and showed no signs of approaching a plateau within the time scale of this procedure. Correspondingly, the CO_2 concentration within the films followed a similar path. The initial sorption of CO_2 within the first minute of exposure was nominally greater than the additional sorption for the remainder of the experiment, and the initial sorption agrees with the sorption isotherms reasonably well. The film exposed to 32 atm CO_2 showed the

greatest increase in CO_2 concentration over 100 h, as expected. Like the swelling plots, there is no sign of approaching a plateau.

Plasticization is thought to increase free volume and decrease the density of the gas-polymer mixture. Since the refractive index is directly related to the density (see Equation 2.2), continued exposure to CO_2 should cause the refractive index to decrease with time. However, plasticization and physical aging are simultaneous, competitive processes, and physical aging tends to increase density. Previous observations have shown that CO_2 permeability goes through a maximum during constant exposure to CO_2 over long time periods, suggesting that physical aging eventually dominates any further plasticization over time [13,14]. The high-pressure ellipsometry results mirror these CO_2 permeation studies. In each experiment, the refractive index initially decreased, then passed through a minimum and proceeded to increase for the duration of the experiment. This indicates an initial decrease in density due to plasticization, but a trend toward densification for longer exposure times. The refractive index minima (1 h at 32 atm, 10-20 h at 16 atm, and 50-60 h at 8 atm) show remarkable agreement with the CO_2 permeability maxima from our previous work [13]. This clearly supports the interpretation that physical aging dominates plasticization for long exposure times and that CO_2 pressure governs the dynamics of the behavior. This behavior is particularly interesting given that the polymers evidently show continued swelling and CO_2 uptake long after the refractive index minima.

In Section 6.2.4, fractional free volume initially decreased with CO_2 pressure then, following a minimum, exhibited a slight increase. Fractional free volume at constant CO_2 pressure as a function of time behaved somewhat differently. (Note that the same value of $V_{vdw,CO2}$ was used for these calculations as before.) Comparing the

fractional free volume plots in Figures 6.10 to 6.12, one can ascertain that fractional free volume exhibits a different dependence on pressure than seen in Figure 6.7. Instead of remaining relatively flat, fractional free volume increases with pressure and the trend is maintained throughout the experiment. This dependence upon pressure appears consistent with the work of Hong, Chen, and their coworkers mentioned previously [16,17], who also performed their experiments under constant pressure conditions for long periods of time. More importantly, the evolution of fractional free volume over time mirrors the evolution of CO_2 permeability from our prior work. Like the refractive index minima, the fractional free volume maxima agree quite well with the CO_2 permeability maxima.

The nature of the time dependent data only permits the calculation of apparent molar volume instead of partial molar volume; these data are presented in Figure 6.13. Because of the large amount of scatter for these calculations, moving averages of 10 values were plotted at each time instead of nominal values to emphasize the long-term trend. As a result, our comments here will be limited to a few qualitative assessments. First, the initial values increase with pressure, but the quantitative change in the apparent molar volume seems unrelated to pressure at all. Second, the local maxima appear to correspond broadly with the permeability maxima and refractive index minima, although it appears that the 8 atm CO_2 experiment has shifted to the left somewhat. Finally, the convergence of the curves for 8 atm and 16 atm leads one to ask if the 32 atm curve will also converge under continued CO_2 exposure.

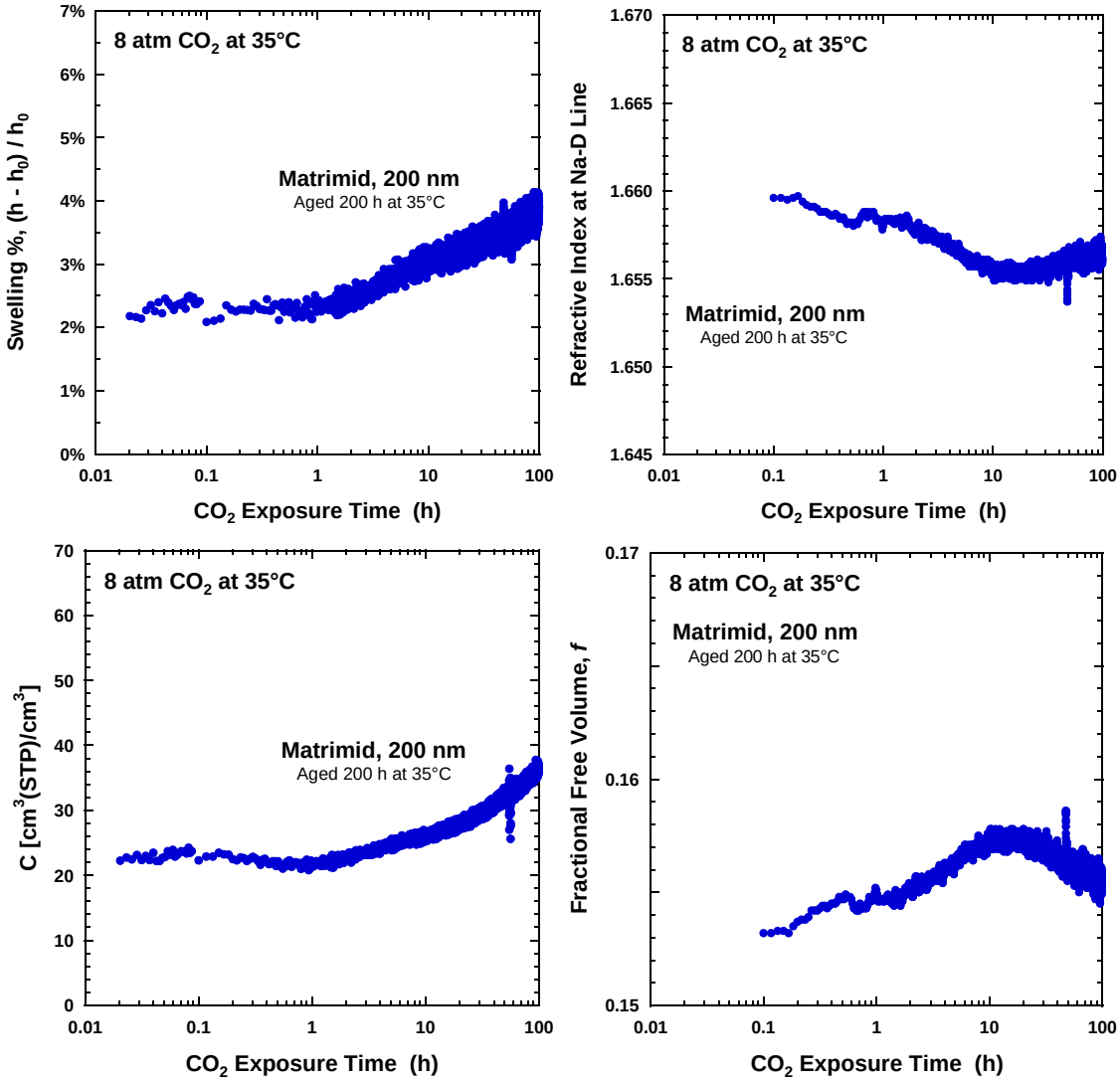

Figure 6.10: Results for a constant pressure experiment for a 200 nm Matrimid® film, aged for 200 h at 35°C, exposed to 8 atm CO_2 at 35°C for 100 h.

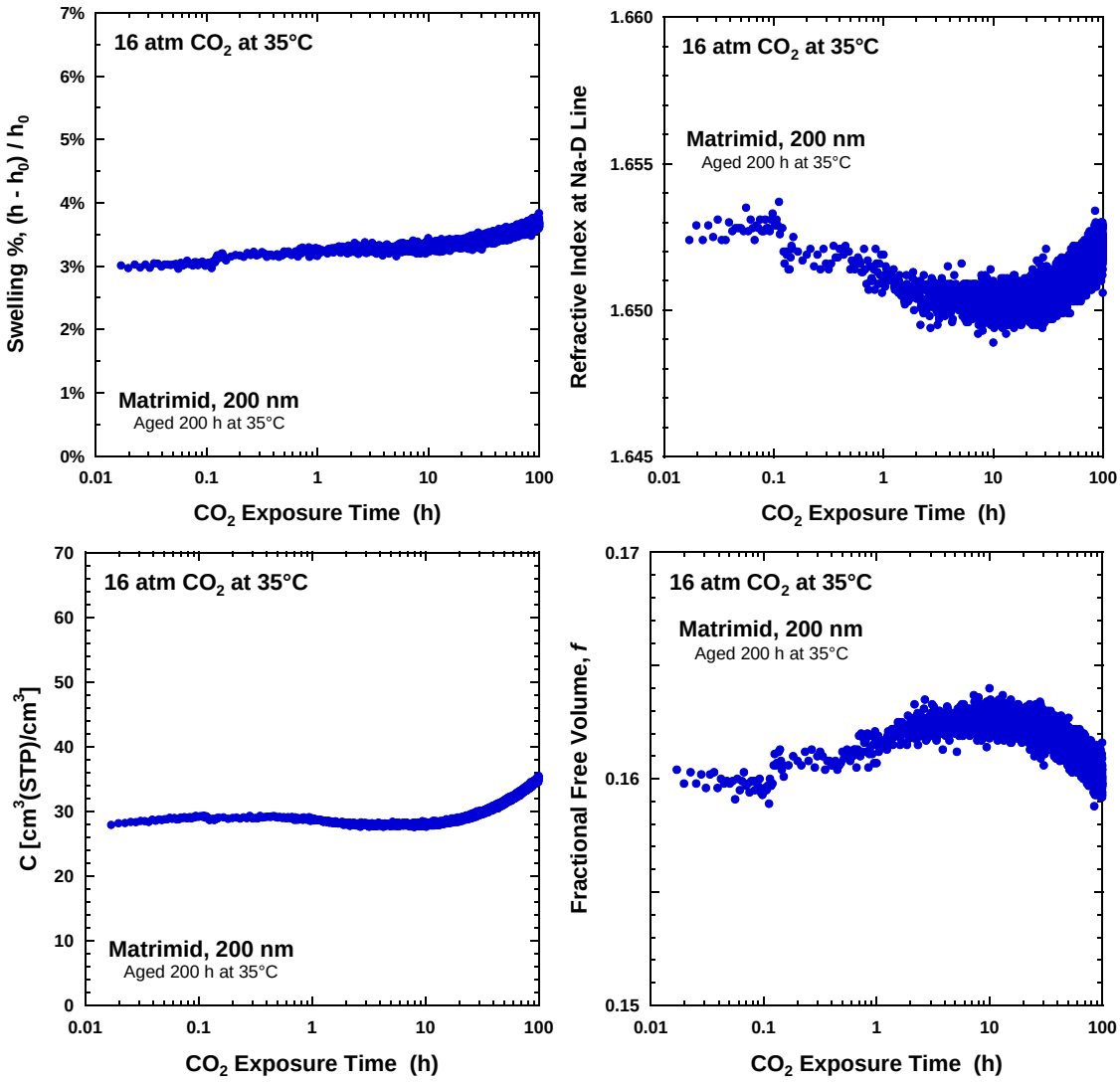

Figure 6.11: Results for a constant pressure experiment for a 200 nm Matrimid® film, aged for 200 h at 35°C, exposed to 16 atm CO_2 at 35°C for 100 h.

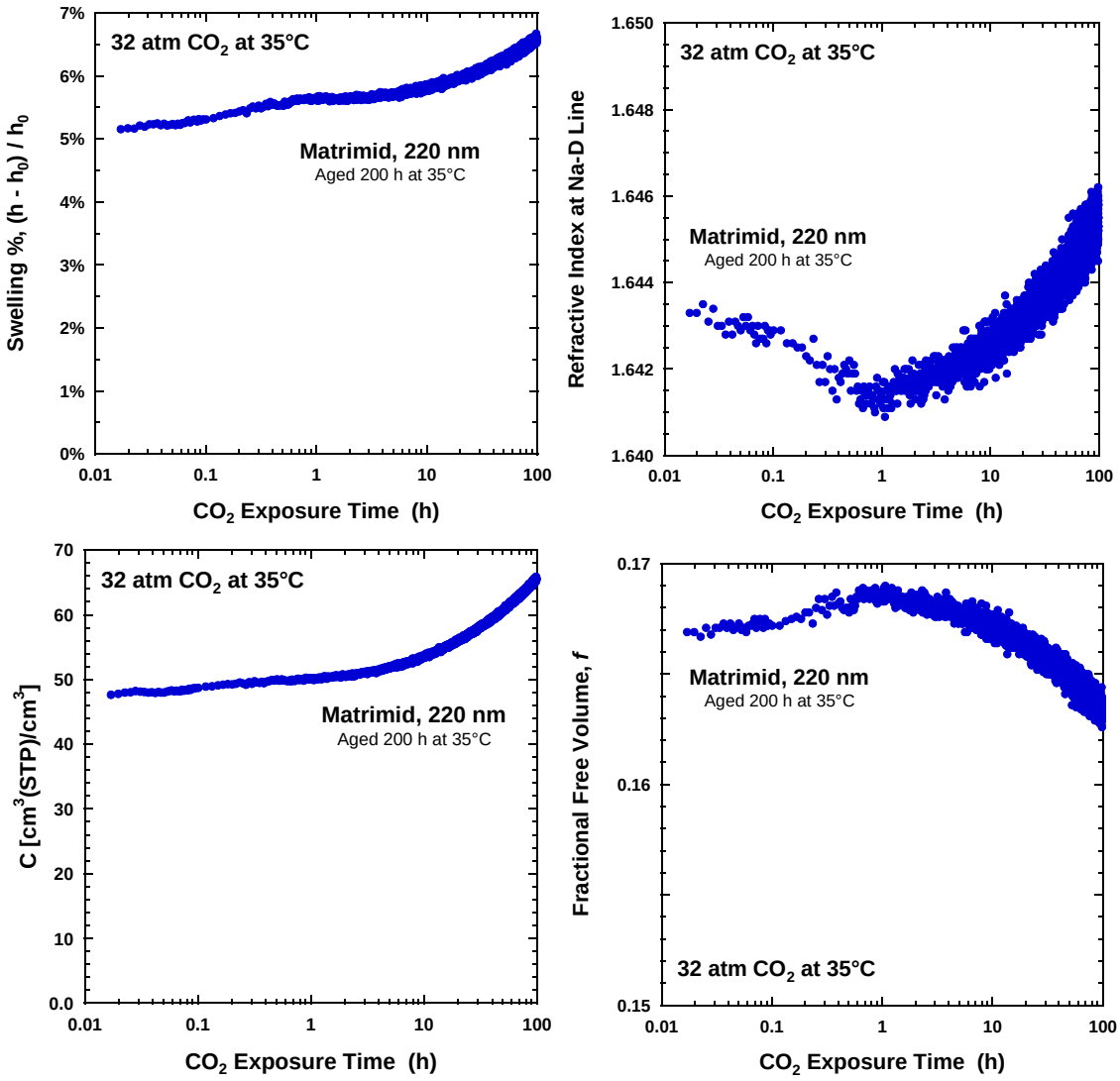

Figure 6.12: Results for a constant pressure experiment for a 220 nm Matrimid® film, aged for 200 h at 35°C, exposed to 32 atm CO_2 at 35°C for 100 h.

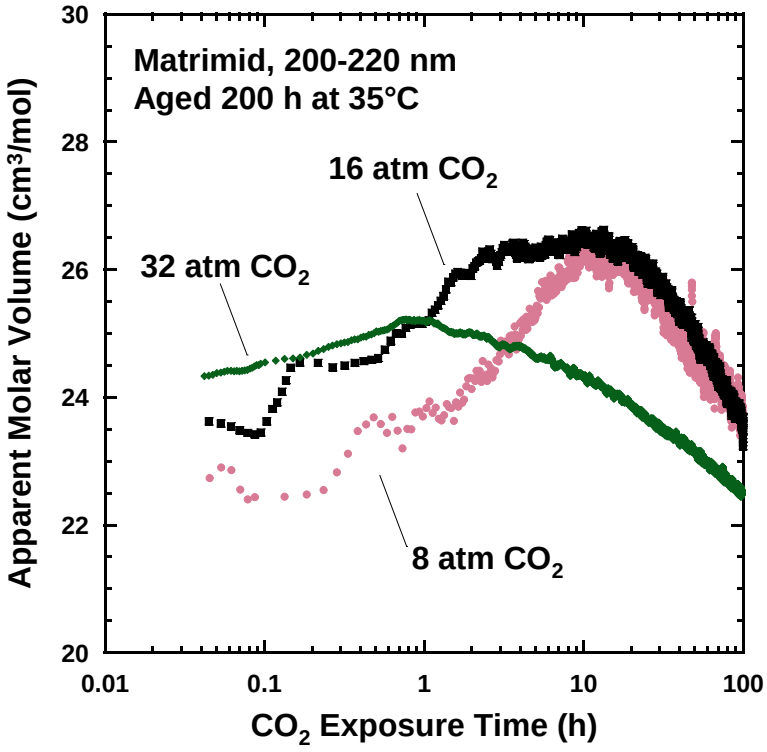

Figure 6.13: Apparent molar volume of CO_2 in Matrimid® for constant pressure experiments at 35°C.

6.3.2 Estimating CO_2 diffusivity as a function of time for thin Matrimid® films

The CO_2 sorption data versus time at constant pressure can be correlated with permeability from our previous work to estimate diffusivity as a function of time. Selected exposure times from the concentration data were matched to the exposure times from the permeability data. Before calculating diffusivity, the concentration at each of those times was averaged over 10 min to smooth out variation in the data. The differences in the experimental conditions, namely freestanding versus mounted films, probably affect the quantitative results to some extent, but the results presented in Figure 6.14 are still instructive. As expected, a maximum in diffusivity occurs in the 32 atm and 16 atm CO_2 data, generally correlating with the permeability maximum and refractive index minimum. However, the CO_2 diffusivity at 8 atm changes little for much of the first 100 h of CO_2 exposure, although it eventually shows a significant decrease at later times.

These trends further emphasize the complexity of combined plasticization and physical aging phenomena. Clearly, CO_2 diffusivity changes with continued CO_2 exposure. However, the effect is more pronounced at greater pressures. Figure 6.14 suggests that permeability changes at lower pressures are initially driven by the change in solubility, i.e., the continued uptake of CO_2. The change in diffusivity is slower, and it is also affected by the progress of physical aging. Eventually, aging causes the diffusivity to decline at a relatively faster rate than that of the increasing CO_2 solubility, resulting in decreasing permeability with continued CO_2 exposure. At higher pressures, diffusivity changes more rapidly. Although continued CO_2 sorption does affect the permeability, the change in diffusivity with time plays a significantly greater role throughout the experiment. Besides illustrating again the importance of physical aging to diffusivity (as

in Figure 6.9), the long-term trends strengthen our claim in Section 6.2.2 that although physical aging does affect CO_2 sorption the results are not quite as dramatic as other factors.

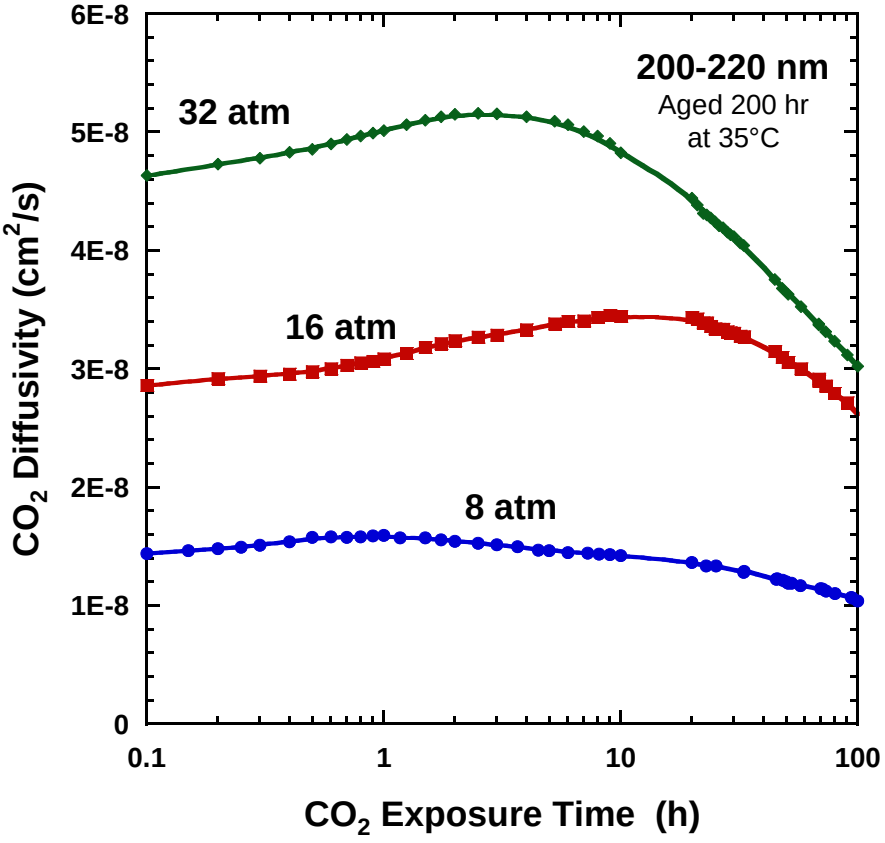

Figure 6.14: Apparent CO_2 diffusivity for Matrimid® as a function of time, calculated from permeability measurements made previously [13] and sorption data obtained via ellipsometry.

6.4 CONCLUSIONS

Ellipsometry has been used to characterize CO_2 sorption in a series of thin glassy polymer films, providing further evidence that the consequences of plasticization are dependent on film thickness for glassy polymers. In general, thin films sorb significantly less CO_2 than most bulk films, and the magnitude of this difference may be connected to the glass transition temperature. Physical aging affects sorption behavior as well, but not as dramatically as thickness. The partial molar volume of CO_2 in thin films showed no obvious relationship with the polymer type or T_g, and the data suggest that previous claims regarding critical values of partial molar volume or concentration to induce plasticization may be oversimplifications. Fractional free volume as a function of CO_2 pressure showed an analogous behavior to CO_2 permeability as a function of pressure. While this result was somewhat surprising, it is relatively dependent on the particular methodology used in the experiments. Changing the time spent at a given pressure will generally change one's results to some extent. Diffusivity as a function of pressure was estimated for Matrimid® from previously obtained permeability data at different aging times, and the results showed that aging and CO_2 sorption affect diffusivity strongly.

Dynamic ellipsometry experiments at constant CO_2 pressure demonstrated analogous behavior to previous permeability measurements as a function of time at constant pressure. The polymers exhibited continual sorption-induced swelling and CO_2 uptake throughout the experiment, and no approach toward a plateau could be determined within the experimental time scale. The times to reach refractive index minima and fractional free volume maxima corresponded well with previously observed times to reach permeability maxima, further demonstrating that physical aging dominates CO_2 plasticization for long exposure times. Fractional free volume did seem to exhibit a

dependence upon CO_2 pressure when comparing the trends of the different constant pressure experiments.

Similar to the sorption isotherm experiments, CO_2 diffusivity was estimated by matching sorption measurements with permeability data at corresponding experimental times. The results show that CO_2 solubility is the driving factor of changes in CO_2 permeability at lower pressures due to diffusivity changing relatively slower. At higher pressures, changes in diffusivity, driven by physical aging, clearly have the greatest effect on CO_2 permeability even at short exposure times. In both cases, diffusivity is the primary component affected by physical aging that leads to the reduction in permeability seen in previous experiments.

An important part of this research and our previous work [13,14] has been to emphasize the complex behavior of physical aging and CO_2 plasticization in competition, and to show how thin glassy polymer films differ from bulk films. Previously, knowledge of gas sorption behavior in thin films has been rather limited by the lack of adequate equipment able to measure film thickness and sorption capacity simultaneously, but ellipsometry overcomes these limitations and can be used to enhance our knowledge of gas transport behavior for both plasticizing and non-plasticizing gases. Understanding long-term property changes due to plasticization and physical aging is crucial toward the development of robust membrane separation modules, and this study provides a clearer picture of the dynamic relationship between CO_2 permeability, sorption, and diffusivity during plasticization over long time periods.

6.5 ACKNOWLEDGEMENTS

This chapter requires some special acknowledgement of a few people who were very helpful during the course of this work: Stephen Sirard for his helpful comments, Prof. Keith Johnston for providing the high-pressure ellipsometry cell, Zachary Smith for his help obtaining thick film sorption data, Katrina Czenkusch for her assistance with Matlab, Brandon Rowe for the use of his data from previous work, the University of Texas at Austin Center for Nano- and Molecular Technology for the use of their facilities, and the J.A. Woolam Company (especially Ping He) for advice regarding dynamic data analysis.

6.6 REFERENCES

[1] W. C. Madden, D. Punsalan, and W. J. Koros, "Age dependent CO_2 sorption in Matrimid® asymmetric hollow fiber membranes," *Polymer*, vol. 46, no. 15, pp. 5433-5436, 2005.

[2] Y. Maeda, *Ph.D. Dissertation, University of Texas at Austin*, 1985.

[3] Y. Maeda and D. R. Paul, "Effect of antiplasticization on gas sorption and transport. II. Poly(phenylene oxide)," *Journal of Polymer Science, Part B: Polymer Physics*, vol. 25, no. 5, pp. 981-1003, 1987.

[4] G. Morel and D. R. Paul, "CO_2 sorption and transport in miscible poly(phenylene oxide)/polystyrene blends," *Journal of Membrane Science*, vol. 10, no. 2-3, pp. 273-282, 1982.

[5] D. R. Paul, in *Comprehensive Membrane Science and Technology, Volume 1*, E. Drioli and L. Giorno, Eds. Oxford: Academic Press, 2010, pp. 75-90.

[6] W. J. Koros, "Personal communication," *Personal communication*, 1978.

[7] K. Simons et al., "CO_2 sorption and transport behavior of ODPA-based polyetherimide polymer films," *Polymer*, vol. 51, no. 17, pp. 3907-3917, 2010.

[8] A. Bos, I. Pünt, H. Strathmann, and M. Wessling, "Suppression of gas separation membrane plasticization by homogeneous polymer blending," *AIChE Journal*, vol. 47, no. 5, pp. 1088-1093, 2001.

[9] T.-S. Chung, S. S. Chan, R. Wang, Z. Lu, and C. He, "Characterization of permeability and sorption in Matrimid/C60 mixed matrix membranes," *Journal of Membrane Science*, vol. 211, no. 1, pp. 91-99, 2003.

[10] T. T. Moore and W. J. Koros, "Gas sorption in polymers, molecular sieves, and mixed matrix membranes," *Journal of Applied Polymer Science*, vol. 104, no. 6, pp. 4053–4059, 2007.

[11] C. A. Scholes, W. X. Tao, G. W. Stevens, and S. E. Kentish, "Sorption of methane, nitrogen, carbon dioxide, and water in Matrimid 5218," *Journal of Applied Polymer Science*, vol. 117, no. 2, pp. 2284-2289, 2010.

[12] T. Visser and M. Wessling, "When Do Sorption-Induced Relaxations in Glassy Polymers Set In?," *Macromolecules*, vol. 40, no. 14, pp. 4992-5000, 2007.

[13] N. R. Horn and D. R. Paul, "Carbon dioxide plasticization and conditioning effects in thick vs. thin glassy polymer films," *Polymer*, vol. 52, no. 7, pp. 1619-1627, 2011.

[14] N. R. Horn and D. R. Paul, "Carbon dioxide plasticization of thin glassy polymer films," *Polymer*, vol. 52, no. 24, pp. 5587-5594, 2011.

[15] A. Bos, I. G. M. Pünt, M. Wessling, and H. Strathmann, "CO_2-induced plasticization phenomena in glassy polymers," *Journal of Membrane Science*, vol. 155, no. 1, pp. 67-78, 1999.

[16] X. Hong, Y. Jean, H. Yang, S. Jordan, and W. J. Koros, "Free-volume hole properties of gas-exposed polycarbonate studied by positron annihilation lifetime spectroscopy," *Macromolecules*, vol. 29, no. 24, pp. 7859–7864, 1996.

[17] H. Chen, M. L. Cheng, Y. Jean, L. J. Lee, and J. Yang, "Effect of CO_2 exposure on free volumes in polystyrene studied by positron annihilation spectroscopy," *Journal of Polymer Science, Part B: Polymer Physics*, vol. 46, no. 4, pp. 388–405, 2008.

[18] D. R. Lide, *CRC Handbook of Chemistry and Physics*, 78th ed. New York: CRC Press, 1997.

[19] A. Bondi, "Van der Waals Volumes and Radii," *Journal of Physical Chemistry*, vol. 68, no. 3, pp. 441-451, 1964.

[20] I. a. Ronova, E. M. Rozhkov, A. Y. Alentiev, and Y. P. Yampolskii, "Occupied and Accessible Volumes in Glassy Polymers and Their Relationship with Gas Permeation Parameters," *Macromolecular Theory and Simulations*, vol. 12, no. 6, pp. 425-439, 2003.

[21] J. M. Wong, *Ph.D. Dissertation, University of Texas at Austin*. 1986.

[22] B. W. Rowe, B. D. Freeman, and D. R. Paul, "Effect of Sorbed Water and Temperature on the Optical Properties and Density of Thin Glassy Polymer Films on a Silicon Substrate," *Macromolecules*, vol. 40, no. 8, pp. 2806-2813, 2007.

[23] M. T. Stone, P. J. In 'T Veld, Y. Lu, and I. C. Sanchez, "Hydrophobic/hydrophilic solvation: inferences from Monte Carlo simulations and experiments," *Molecular Physics*, vol. 100, no. 17, pp. 2773-2792, 2002.

[24] J. R. Scherer, “The partial molar volume of water in biological membranes.,” *Proceedings of the National Academy of Sciences of the United States of America*, vol. 84, no. 22, pp. 7938-42, 1987.

[25] C. L. Aitken, W. J. Koros, and D. R. Paul, “Gas transport properties of biphenol polysulfones,” *Macromolecules*, vol. 25, no. 14, pp. 3651-58, 1992.

[26] S. A. Stern and V. Saxena, “Concentration-dependent transport of gases and vapors in glassy polymers,” *Journal of Membrane Science*, vol. 7, pp. 47-59, 1980.

[27] W. J. Koros, D. R. Paul, and A. A. Rocha, “Carbon dioxide sorption and transport in polycarbonate,” *Journal of Polymer Science, Part B: Polymer Physics*, vol. 14, no. 4, pp. 687–702, 1976.

Chapter 7: Conclusions and Recommendations

Carbon dioxide plasticization of thick and thin glassy polymer films has been investigated using gas permeability measurements and gas sorption measurements. Below is a brief summary of the conclusions from Chapters 4 through 6, followed by recommendations for future research and mentions of current research already influenced by this work.

7.1. CONCLUSIONS

Chapter 4 presented a new study of the critical role of thickness in the CO_2 plasticization and conditioning processes of glassy polymer films. Thin films are more sensitive to changes in CO_2 pressure, and the response becomes more intense at greater pressures. Permeability changes occur even at short time scales for thin films, as opposed to thick films which take nearly the same amount of time merely to reach steady state. The difference in relaxation time distribution between thick and thin films plays a significant role in the time dependence of CO_2 response. At moderate timescales, thin glassy polymer films undergo more rapid plasticization by CO_2, in contrast with thick films. This behavior is analogous to more rapid physical aging of thin films. Moreover, the conventionally defined "plasticization pressure" is not adequate to determine when plasticization begins. Plasticization in thin films is strongly dependent on aging time of a film, whereas thick films show little change with aging time. Permeability data for O_2, N_2, and CH_4 following CO_2 exposure indicates that thinner films experience greater "conditioning" effects than do thick films, but the effect on selectivity is unclear. Thus, CO_2 transport data from thick films cannot fully predict thin film behavior. The CO_2

response of thin films is dependent on thickness, aging time, CO_2 pressure, exposure time, and prior history.

At longer CO_2 exposure times, thin films behave much differently than thick films as well. Initially, thin films exhibit a large increase in CO_2 permeability, but the trend eventually reverses and the films decrease in permeability to a significant extent. This is attributed to competition between the CO_2 plasticization effect and physical aging, and the behavior resembles the volume recovery "memory effect" observed by Kovacs. Thick films do not seem to reach a well-defined maximum within the experimental timescale. This behavior has yet to be fully explained, and other investigations are needed to determine its cause.

Chapter 5 put forward a more nuanced understanding of CO_2 plasticization in the context of three different polymer types. Degree of plasticization response can be expected to follow CO_2 solubility in the polymer. For the polymers tested, Matrimid® had the greatest relative response, followed by PPO and PSF. Despite Matrimid's greater response, PPO appears to respond relatively more quickly to CO_2 plasticization at shorter times. This may indicate that kinetic concerns play a more prominent role at short exposure times, while at longer exposure times thermodynamic concerns always dominate. The high state of free volume of PPO may be responsible for this effect. Permeability maximums were observed in each polymer for long CO_2 exposure times, suggesting that this trend is likely universal for glassy polymers. However, under some conditions no obvious permeability maximum may be observed despite seeing the permeability decrease at long CO_2 exposure times. This behavior observed for PSF suggests that the competing effects of plasticization and aging are balanced. The lower solubility of CO_2 in PSF, plus this polymer's relatively more compact backbone and

lower free volume, probably accounts for its more sluggish response to CO_2 plasticization, and such behavior was most evident in the long term exposure experiment at 8 atm CO_2 and the hysteresis experiment. The Kovacs "memory effect" analogy describes the slow dynamics of the polymer response, and observing how the physical aging rate depends on temperature helps explain what takes place within a thin glassy polymer film during plasticization.

In Chapter 6, ellipsometry was shown to be a useful means of obtaining sorption data for thin polymer films. The characterization of CO_2 sorption in a series of thin glassy polymer films provided further evidence that plasticization of glassy polymers is heavily dependent on film thickness. In general, thin films sorb significantly less CO_2 than most bulk films, and the magnitude of this difference may be connected to the glass transition temperature (T_g). Physical aging affects sorption behavior as well, but not as dramatically as thickness. The partial molar volume of CO_2 in thin films showed no obvious relationship with the polymer type or T_g, and the data suggest that previous claims regarding critical values of partial molar volume or concentration to induce plasticization may be oversimplifications. Fractional free volume as a function of CO_2 pressure showed an analogous behavior to CO_2 permeability as a function of pressure. While this result was somewhat surprising, it is relatively dependent on the particular methodology used in the experiments. Changing the time spent at a given pressure will generally change one's results to some extent. Diffusivity as a function of pressure was estimated for Matrimid® from previously obtained permeability data at different aging times, and the results showed that aging and CO_2 sorption affect diffusivity strongly.

Dynamic ellipsometry experiments at constant CO_2 pressure demonstrated analogous behavior to previous permeability measurements as a function of time at

constant CO_2 pressure. The polymers exhibited continual sorption-induced swelling and CO_2 uptake throughout the experiments, and no approach toward a plateau could be determined within the experimental time scale. The times to reach refractive index minima and fractional free volume maxima corresponded well with previously observed times to reach permeability maxima, further demonstrating that physical aging dominates CO_2 plasticization for long exposure times. Fractional free volume did seem to exhibit a dependence upon CO_2 pressure when comparing the trends of the different constant pressure experiments.

Similar to the sorption isotherm experiments, CO_2 diffusivity was estimated by matching sorption measurements with permeability data at corresponding experimental times. The results show that CO_2 solubility is the driving factor of changes in CO_2 permeability at lower pressures due to diffusivity changing relatively slower. At higher pressures, changes in diffusivity, driven by physical aging, clearly have the greatest effect on CO_2 permeability even at short exposure times. In both cases, diffusivity is the primary component affected by physical aging that leads to the reduction in permeability seen in previous experiments.

An important part of this research has been to emphasize the complex behavior of physical aging and CO_2 plasticization in competition, and to show how thin glassy polymer films differ from bulk films. Previously, knowledge of gas sorption behavior in thin films has been rather limited by the lack of adequate equipment able to measure film thickness and sorption capacity simultaneously, but ellipsometry overcomes these limitations and can be used to enhance our understanding of gas transport behavior for both plasticizing and non-plasticizing gases. This study provides a clearer picture of the

dynamic relationship between CO_2 permeability, sorption, and diffusivity during plasticization over long time periods.

Finally, these findings emphasize that long-term property changes are of critical importance to industrial membrane applications using glassy polymers. Knowledge of how membranes behave under plasticizing conditions should help in understanding how commercial modules behave in practice and is a necessary step towards developing materials and fabrication procedures that minimize the deleterious effects of plasticization. A major point in this work has been to demonstrate that observing such responses for thick films may not be an adequate way to simulate what occurs with high flux commercial membranes.

7.2. RECOMMENDATIONS

The research presented here suggests a variety of experimental paths that can further our fundamental understanding of glassy polymers, CO_2 plasticization, and gas separation processes. The following recommendations can be categorized under two general headings. First, the carefully refined methodology in this research establishes a basis for new gas transport studies of thin glassy polymer films, especially with respect to plasticizing molecules such as CO_2. Second, this improved understanding of known materials allows for new inquiry into novel polymer membrane materials.

7.2.1. Expanded Gas Transport Studies of Thin Glassy Polymer Films

Influence of thermal history and temperature on CO_2 plasticization behavior

An industrial membrane module typically acquires a varied thermal history before installation. Such history has a measureable effect upon its performance. Thermal history is known to play an important role in physical aging [1] but the effect of history upon CO_2 plasticization behavior is not well-understood. Cui et al. suggested that polymers prepared without annealing above T_g would behave analogously to films that had been annealed above T_g, but the scope of their study did not allow a full comparison [2]. In Chapters 4 and 6, physical aging was shown to have a significant impact upon CO_2 plasticization and sorption, respectively. These data indicate that further investigation of thermal history would yield fruitful results. Some preliminary permeability studies of this behavior are underway in the Paul research group, which will examine the effect of different annealing temperatures and aging times upon CO_2 plasticization.

Additionally, investigating the effect of temperature upon CO_2 plasticization of thin films could be useful. Typical gas transport experiments are performed at 35°C, but realistic membranes must operate at a variety of temperatures. Temperature effects are well-known for bulk films, but thin films may respond differently. A combined study of the effects of thermal history and different operating temperatures would prove valuable.

CO_2 plasticization behavior during mixed gas transport of thin glassy polymer films

This work has enhanced the fundamental understanding of CO_2 plasticization of thin glassy polymer films in the context of pure gas feeds. Gas separations obviously involve more than one component and, thus, pure gas permeation measurements cannot

fully capture the complex behavior that would occur in a mixed gas feed. Mixed gas experiments, probably focusing on Matrimid® thin films, are the natural next step toward improving practical membrane separation systems in the future. A number of studies have addressed mixed gas permeability with feeds including CO_2 [3–12], but few have involved thin films and none have applied techniques such as those outlined in this work. In particular, Visser et al. observed suppressed CO_2 plasticization of hollow fiber membranes as a function of CO_2 exposure time for mixed gas feeds [6]. This behavior could be of significant interest in future studies.

One could envision an infinite number of experiments combining various partial pressures of CO_2 and a second non-plasticizing gas (such as CH_4 or N_2). Some criteria must be used to select a subset of these that is manageable and that has the greatest potential to provide new insight. Three reasonable series of experiments follow.

In the first series, the proportions of CO_2 and non-plasticizing gas remain the same. These experiments would readily compare to previous work in a reasonable manner. For example, the CO_2 permeability of Matrimid® could be measured as a function of total pressure (or CO_2 partial pressure) for an 80/20 mixture of CO_2 and CH_4, and then be compared to the results in Chapter 4.2.1. This would show how plasticization is affected in the presence of a small (or perhaps substantial) amount of a second gas species. The CH_4 permeability and CO_2/CH_4 selectivity can clearly be tracked as a function of pressure as well. Similarly, comparing the CO_2 permeability as a function of time at constant CO_2 pressure of an 80/20 feed mixture and pure CO_2 (from Chapter 4.3) could demonstrate how plasticization is suppressed over time for mixed gases.

In the second series, the partial pressure of non-plasticizing gas remains constant. One possible experiment would mimic the "short time CO_2 permeation experiment" from Chapter 4.2.3 and 5.2.3, during which a film is exposed to a sequence of four pressures for two hours at each pressure. However, instead of starting at a low pressure, this experiment could begin at a higher pressure. For instance, the sequence could begin with a feed containing a CO_2 partial pressure of 32 atm and a CH_4 partial pressure of 2 atm. Following two hours of exposure, the pressure could be reduced to 24 atm CO_2 and 2 atm CH_4, and so on. Such an experiment could simulate a feed that is dominated by a plasticizing gas but is slowly enriching the second species, and could be compared to prior work.

In the third series, the partial pressure of CO_2 remains constant. These experiments essentially reverse the procedure of the second series mentioned above. For example, the experiment could begin with a feed containing a CO_2 partial pressure of 4 atm and a CH_4 partial pressure of 8 atm. After two hours of exposure, the CH_4 partial pressure could be increased to 16 atm while the CO_2 partial pressure would remain the same. This could simulate conditions where a feed is dominated by a non-plasticizing gas, but the feed is also being affected by a small amount of plasticizing gas that is being removed over time.

Continued high-pressure ellipsometry experiments

An important conclusion of this work is that spectroscopic ellipsometry has been largely overlooked as a tool for measuring gas sorption of thin polymer films. Little is known of gas sorption in thin films, and CO_2 is one of many gases that could be studied.

Testing other gases would provide further confirmation of the differences between thick and thin films, and moreover would help further an understanding of free volume behavior of thin glassy polymer films while undergoing gas sorption. A plasticizing gas such as CO_2 shows a slight upward inflection in free volume following a minimum, which looks similar to a plot of permeability versus pressure. This makes physical sense considering that permeability and free volume are thought to be closely related. One could then expect that for non-plasticizing gases, such as O_2, N_2, or CH_4, free volume as a function of pressure likely exhibits a slight decrease then remains relatively constant with increasing pressure (see Figure 7.1). Additionally, the relative ease with which the temperature of a high-pressure ellipsometry cell can be controlled suggests that studying the effect of temperature on gas sorption of thin films would be useful.

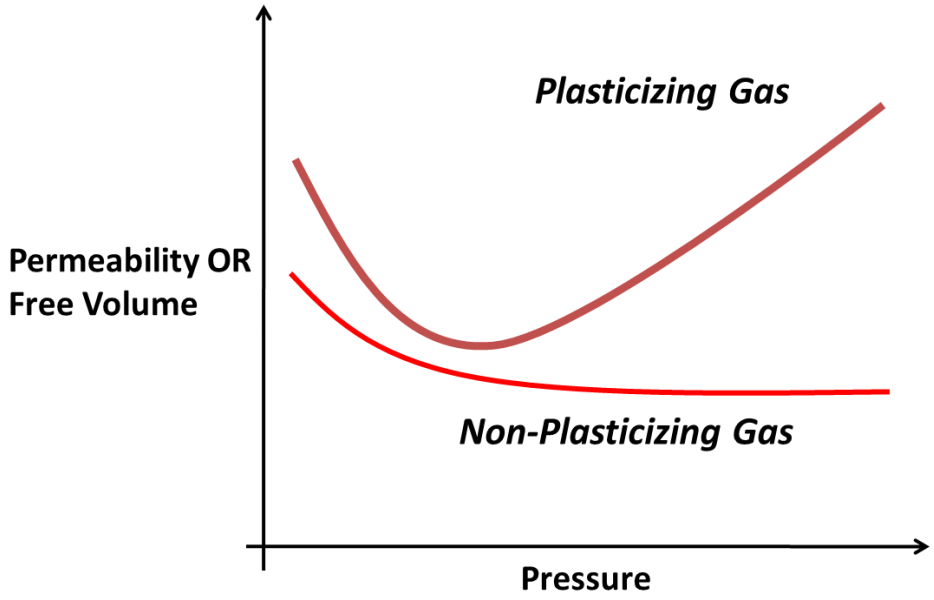

Figure 7.1: Schematic of how permeability or free volume changes generally as a function of pressure.

The results presented in Chapter 6 were noted to be dependent upon the sequence of CO_2 pressures the film experienced. Furthermore, the effect of CO_2 exposure time upon the film was clearly demonstrated in the constant pressure experiments. This cannot be avoided due to the shorter relaxation times of thin films relative to thick films. In particular, this phenomenon was reflected in the calculations of partial molar volume and fractional free volume. New procedures, perhaps analogous to those presented in Chapters 4 and 5, should be developed to explore these effects in more detail. For instance, a film could experience four different CO_2 pressures, spending two hours at each pressure, and optical data could be obtained once each minute. This data could be compared to the CO_2 permeability data from Chapter 4.2.3.

It should be mentioned that the work presented here was done with a relatively simple system for controlling temperature and pressure. The instrument setup could be improved in a number of ways to reduce potential error and give greater control over the experiment overall. The most important of these improvements is pressure automation and control. In this work, pressure was controlled by the regulator connected to the gas cylinder. Although it was sufficient for this work, it is not ideal. Including a PID controller and valve manifold would allow for more consistent control over the experiments, and would make easier programming more complicated pressure sequences. Using a vacuum pump instead of a house vacuum line would improve the instrument as well. Finally, stress-free quartz windows would reduce the in-plane and out-of-plane correction offsets significantly.

Influence of CO_2 plasticization upon glass transition temperature (T_g) of thin glassy polymer films

In Chapter 5, it was suggested that the observed maximum of CO_2 permeability as a function of pressure could be explained by considering how the aging rate changes as temperature approaches T_g. Since a glassy polymer's T_g is known to decrease upon CO_2 plasticization [13–17], the aging rate is expected to pass through a maximum during prolonged CO_2 exposure. While testing this particular hypothesis is quite difficult using a constant volume permeation apparatus, high-pressure ellipsometry has interesting potential to explore this possibility further.

Two experimental paths can be pursued. First, at higher pressures of CO_2 a sorption isotherm will eventually become linear. This was observed by Maeda for mixtures of polystyrene and either 3% mineral oil or 10% tricresyl phosphate [15,18,19]. A schematic depicting his observations is reproduced in Figure 7.2. The point where the isotherm begins increasing linearly with pressure indicates the CO_2 concentration necessary to reduce the T_g to the experimental temperature.

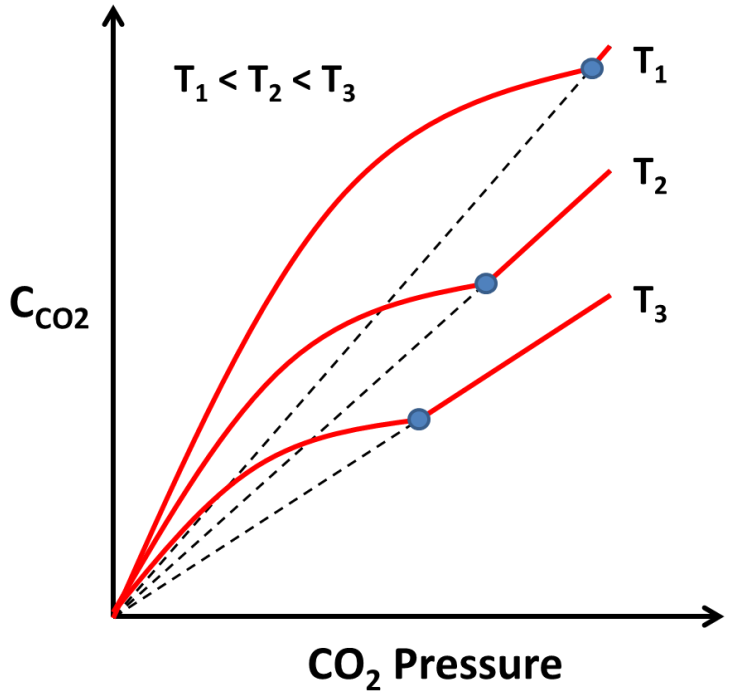

Figure 7.2: Schematic of CO_2 sorption isotherms. The dotted points indicate where CO_2 concentration increases to such an extent that the T_g has been reduced to the experimental temperature, and further sorption is linear with pressure.

Second, optical properties can be monitored over long exposure times at constant CO_2 pressure to determine T_g more directly. Ellipsometry has been used extensively to measure T_g [20–23] but has not been used to study depressed T_g in the presence of plasticizing gases. After a certain elapsed time, the temperature could be increased, and measurable shifts in the ellipsometric angles with temperature indicate the new range of T_g. One potential result could be that the necessary CO_2 concentration for a given T_g depression is the same at all CO_2 pressures. However, T_g is known to decrease somewhat for supported thin films [23,24], and such effects should be studied independently to provide for proper controls in experiments involving CO_2. For these experiments,

polystyrene may be the material of choice due to its relatively low T_g (~105°C) and numerous ellipsometry studies in the literature [21,23,25–28].

Effect of CO_2 exposure on free volume of thin glassy polymer films studied by positron annihilation lifetime spectroscopy (PALS)

Hong et al. [29] and Chen et al. [30] studied, via PALS, the effects of CO_2 exposure upon polycarbonate and polystyrene films approximately 1 mm thick. Both groups observed that free volume was dependent upon CO_2 pressure. Spectroscopic technology has improved significantly since their work, and much thinner samples can now be studied with PALS [31]. Considering the results presented in Chapter 6.2.4, it would be quite useful to perform a new PALS study of thin glassy polymer films in the presence of CO_2. This could help explain the free volume behavior observed in this work, as well as provide new insights into the distribution of free volume elements in thin films as a function of CO_2 pressure and exposure time.

7.2.2. Investigating CO_2 Plasticization of Novel Membrane Materials

Crosslinked Polymer Systems

Plasticization is thought to increase the freedom of movement of polymer chains, termed segmental mobility. Suppressing plasticization could be accomplished, then, by decreasing the ability of a polymer to move freely through crosslinking, and substantial effort has been expended to study such possibilities [5,32–43]. Recently, Cui et al. [2] used the methods developed in this work [44,45] to examine the CO_2 plasticization behavior over long exposure times of two 6FDA-based polyimide systems crosslinked

with DABA units. They observed substantially suppressed plasticization, attributed to crosslinking, with little loss of overall membrane flux. This suggests that crosslinking procedures for other membrane materials should be explored as well.

Two possible crosslinking methods have been explored preliminarily in this work, but with minimal success. The first method involved thermal crosslinking of Matrimid®, described previously by Bos et al. [40]. Thin films were annealed at 350°C for up to 20 minutes in the presence of air, and crosslinking was verified after selected samples failed to dissolve in cyclohexanone solvent. The films exhibited slightly suppressed aging over ~200 h. However, when these films were exposed to CO_2 using a the standard CO_2 plasticization pressure curve procedure described in Chapter 4.2.1, most films failed between before completing the experiment. This could indicate that the Matrimid® had decomposed somewhat in the presence of air and could not withstand even a moderate concentration of CO_2. Also, in all cases, the permeability of Matrimid® to penetrant gases (CO_2 or otherwise) was substantially reduced, usually by a factor 4-5. The inconsistency of the results dissuaded us from pursuing this path in detail, but this thermal crosslinking method might still be profitable in the future.

The second method involved crosslinking by exposure to ethylenediamine (EDA) vapor, described previously by Shao et al. [46]. Following the standard annealing procedure above the T_g, thin Matrimid® films were held above EDA vapor for up to 30 seconds, then immediately masked and put into a permeation cell to be held under vacuum before testing. The films had visibly turned off-white or cream colored and became nearly opaque, signifying that the chemical reaction had taken place. Select samples did not dissolve in solvent, verifying the crosslinks had formed. However, none of the thin films performed well in permeation cells. This could be due to the EDA vapor

causing pitting in the film, creating large defects that rendered selective permeation impossible. This methodology is still in its infancy, though, and thus it is recommended that this procedure be further tested and fine-tuned to remedy these undesirable results. It may be that simply reducing the time of EDA exposure or diluting the EDA could eliminate these problems.

Cellulose Acetate

Cellulose acetate (Figure 7.3) is a commonly used membrane material in natural gas separations due to its chemical resistance to aggressive feeds [47], but it is quite susceptible to plasticization [48]. Though cellulose acetate has been studied extensively in the literature as either dense films or hollow-fibers [7,47–55], there are few studies focusing on single-layer thin films. The lack of any substantial study of this kind presents an opportunity to apply methods developed in this work to a traditionally important membrane material in industrial separations.

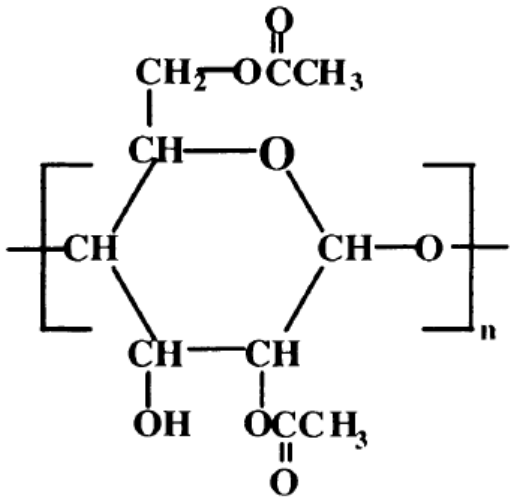

Figure 7.3: Structure of Cellulose Acetate

One difficulty encountered when studying cellulose acetate is the presence of crystalline regions in the polymer. Determining the percentage of crystalline regions in a cellulose acetate thin film would be required for computation of accurate permeabilities. Since crystallinity and optical properties are closely related, this difficulty can perhaps be overcome with spectroscopic ellipsometry. The J.A. Woollam Company suggests in their ellipsometer manual using an effective medium approximation (EMA) model for determining the percentage of crystalline content in partially crystalline materials [56]. However, it may be found that crystallization in very thin cellulose acetate films is negligible. Despotopoulou et al. showed that crystallization was hindered in films less than 300 nm thick, with greater effects observed as the thickness was decreased [57]. Considering their results, studying the effect of thickness upon crystalline content in the context of cellulose acetate could also be relevant for future research with other semi-crystalline polymers.

Thermally Rearranged (TR) Polymers

Recent advances in the ability to fine-tune cavity size in certain polymers present an interesting opportunity for future research. Certain aromatic polymers, such as hydroxyl-containing polyimides, can undergo a structural rearrangement (Figure 7.4) during high-temperature annealing, and the products are typically termed "thermally rearranged" polymers [58]. The exact structures of TR polymers are unknown, but mechanisms have been proposed that suggest that the products are either polybenzoxazoles or polybenzothiazoles (depending on the precursors). These polymers

have unusually high free volume, and in some cases perform above the Robeson upper bound [59,60].

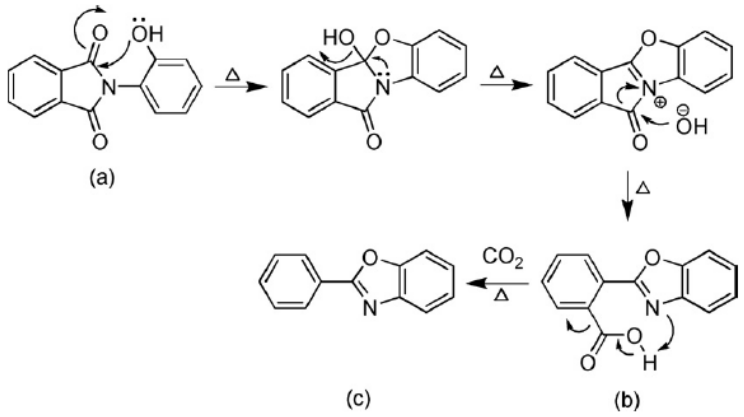

Figure 7.4: Proposed mechanism of thermal rearrangement from hydroxyl-containing polyimide to polybenzoxazole: (a) an imide ring with ortho-positioned hydroxyl group, (b) a carboxyl-benzoxazole ring, (c) a benzoxazole ring. Reproduced from Park et al. [61].

The superb gas transport properties of TR polymers have attracted much interest in recent years. Although much is known of the performance of dense TR polymer films, no one has of yet published a significant study of CO_2 plasticization of these materials. Applying the methods developed in this work to TR polymers would help determine whether these materials are stable over the long periods of time necessary for an industrial separation process.

Again, the structures of TR polymers have at this time not been determined. Thus, the van der Waals volume of the polymer is also unknown and the Bondi / Van Krevelen method of calculating fractional free volume for a polymer cannot be used. However, a frequently overlooked conclusion of the work of Sanchez and Cho (see Chapter 6) is that one does not necessarily need the structure of a polymer to calculate free volume [62]. They suggested that the specific volume at absolute zero was a better measure of the occupied volume than the van der Waals volume, and it can be obtained by extrapolating zero-pressure densities above the glass transition temperature to absolute zero. In many

cases, the glass transition temperatures of TR polymers (post-rearrangement) are near or above the decomposition temperature, and, thus, this method cannot be used. Nonetheless, this may be a pathway toward understanding the free volume properties of certain TR polymers with lower glass transition temperatures, or to determine the free volume of TR polymer precursors.

Polymers of Intrinsic Microporosity (PIM)

Introducing bulky groups into a polymer's repeat unit disrupts efficient chain packing and, in some cases, creates a polymer with very high internal free volume. The so-called polymers of intrinsic microporosity (PIM) were originally conceived with this approach [63–65], and frequently contain large, interconnected aromatic groups (for example, Figure 7.5). These polymers have large internal surface area, high free volume, and correspondingly high gas permeability [66–70].

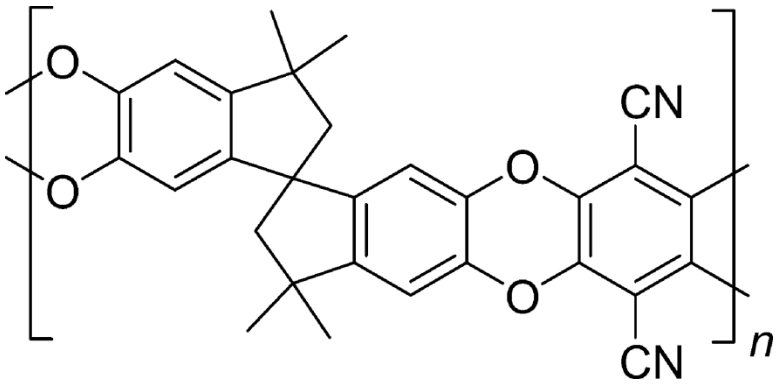

Figure 7.5: Molecular structure of PIM-1 [66].

Most studies of PIM materials have focused on thicker films, and it would be useful to begin examining the behavior of these polymers in thin film form. Some PIM materials have exhibited greatly varied gas permeability depending on the history of the film as well. For instance, Budd et al. [68] noticed that PIM-1 contacted with water had a relatively low O_2 permeability (~120 Barrer), but when contacted with methanol the O_2 permeability changed by an order of magnitude (~1600 Barrer). Such behavior is quite unusual for any polymer and suggests that the effect of CO_2 plasticization and thermal history ought to be studied as well, especially with respect to thin films.

7.3. REFERENCES

[1] B. W. Rowe, B. D. Freeman, and D. R. Paul, "Influence of previous history on physical aging in thin glassy polymer films as gas separation membranes," *Polymer*, vol. 51, no. 16, pp. 3784-3792, 2010.

[2] L. Cui, W. Qiu, D. R. Paul, and W. J. Koros, "Responses of 6FDA-based polyimide thin membranes to CO_2 exposure and physical aging as monitored by gas permeability," *Polymer*, vol. 52, no. 24, pp. 5528-5537, 2011.

[3] E. S. Sanders, W. J. Koros, H. B. Hopfenberg, and V. T. Stannett, "Pure and mixed gas sorption of carbon dioxide and ethylene in poly (methyl methacrylate)," *Journal of Membrane Science*, vol. 18, pp. 53–74, 1984.

[4] S. Jordan, W. J. Koros, and G. Fleming, "The effects of CO_2 exposure on pure and mixed gas permeation behavior: comparison of glassy polycarbonate and silicone rubber," *Journal of Membrane Science*, vol. 30, no. 2, pp. 191–212, 1987.

[5] J. D. Wind, D. R. Paul, and W. J. Koros, "Natural gas permeation in polyimide membranes," *Journal of Membrane Science*, vol. 228, no. 2, pp. 227-236, 2004.

[6] T. Visser, G. Koops, and M. Wessling, "On the subtle balance between competitive sorption and plasticization effects in asymmetric hollow fiber gas separation membranes," *Journal of Membrane Science*, vol. 252, no. 1-2, pp. 265-277, 2005.

[7] T. Visser, N. Masetto, and M. Wessling, "Materials dependence of mixed gas plasticization behavior in asymmetric membranes," *Journal of Membrane Science*, vol. 306, no. 1-2, pp. 16-28, 2007.

[8] L. A. El-Azzami and E. A. Grulke, "Dual mode model for mixed gas permeation of CO_2, H_2, and N_2 through a dry chitosan membrane," *Journal of Polymer Science, Part B: Polymer Physics*, vol. 45, no. 18, pp. 2620-2631, 2007.

[9] T. Visser and M. Wessling, "Auto and mutual plasticization in single and mixed gas C3 transport through Matrimid-based hollow fiber membranes," *Journal of Membrane Science*, vol. 312, no. 1-2, pp. 84-96, 2008.

[10] O. David, D. Gorri, I. Ortiz, and A. Urtiaga, "Dual-sorption model for H_2/CO_2 permeation in glassy polymeric Matrimid membrane," *Desalination and Water Treatment*, vol. 27, pp. 31–36, 2011.

[11] O. C. David, D. Gorri, A. Urtiaga, and I. Ortiz, "Mixed gas separation study for the hydrogen recovery from H_2/CO/N2/CO_2 post combustion mixtures using a Matrimid membrane," *Journal of Membrane Science*, vol. 378, no. 1-2, pp. 359-368, 2011.

[12] M. K. Barillas, R. M. Enick, M. O'Brien, R. Perry, D. R. Luebke, and B. D. Morreale, "The CO_2 permeability and mixed gas CO_2/H_2 selectivity of membranes composed of CO_2-philic polymers," *Journal of Membrane Science*, vol. 372, no. 1-2, pp. 29-39, 2011.

[13] J. S. Chiou, J. W. Barlow, and D. R. Paul, "Plasticization of Glassy Polymers by Co2," *Journal of Applied Polymer Science*, vol. 30, no. 6, pp. 2633-2642, 1985.

[14] J. S. Chiou and D. R. Paul, "Sorption and transport of CO_2 in PVF2/PMMA Blends," *Journal of Applied Polymer Science*, vol. 32, no. 1, pp. 2897-2918, 1986.

[15] J. S. Chiou, Y. Maeda, and D. R. Paul, "Gas and vapor sorption in polymers just below Tg," *Journal of Applied Polymer Science*, vol. 30, no. 10, pp. 4019-4029, 1985.

[16] Y. Mi, S. Zhou, and S. A. Stern, "Representation of gas solubility in glassy polymers by a concentration-temperature superposition principle," *Macromolecules*, vol. 24, no. 9, pp. 2361-2367, 1991.

[17] A. G. Wonders and D. R. Paul, "Effect of CO_2 exposure history on sorption and transport in polycarbonate," *Journal of Membrane Science*, vol. 5, pp. 63–75, 1979.

[18] Y. Maeda, *Ph.D. Dissertation, University of Texas at Austin*, 1985.

[19] Y. Maeda and D. R. Paul, "Effect of antiplasticization on gas sorption and transport. III. Free volume interpretation.," *Journal of Polymer Science, Part B: Polymer Physics*, vol. 25, no. 5, pp. 1005-1016, 1987.

[20] C. B. Roth and J. R. Dutcher, "Glass transition temperature of freely-standing films of atactic poly(methyl methacrylate).," *The European Physical Journal E, Soft Matter*, vol. 12, no. 1, pp. S103-7, 2003.

[21] S. Kim, S. a Hewlett, C. B. Roth, and J. M. Torkelson, "Confinement effects on glass transition temperature, transition breadth, and expansivity: comparison of ellipsometry and fluorescence measurements on polystyrene films.," *The European Physical Journal E, Soft Matter*, vol. 30, no. 1, pp. 83-92, 2009.

[22] J. L. Keddie, R. A. L. Jones, and R. A. Cory, "Interface and surface effects on the glass-transition temperature in thin polymer films," *Faraday Discussions*, vol. 98, p. 219, 1994.

[23] J. L. Keddie, R. A. L. Jones, and R. A. Cory, "Size-Dependent Depression of the Glass Transition Temperature in Polymer Films," *Europhysics Letters (EPL)*, vol. 27, no. 1, pp. 59-64, 1994.

[24] J. Forrest, K. Dalnoki-Veress, J. Stevens, and J. Dutcher, "Effect of Free Surfaces on the Glass Transition Temperature of Thin Polymer Films.," *Physical Review Letters*, vol. 77, no. 10, pp. 2002-2005, 1996.

[25] A. N. Raegen, M. V. Massa, J. A. Forrest, and K. Dalnoki-Veress, "Effect of atmosphere on reductions in the glass transition of thin polystyrene films.," *The European Physical Journal E, Soft Matter*, vol. 27, no. 4, pp. 375-377, 2008.

[26] E. A. Baker, P. Rittigstein, J. M. Torkelson, and C. B. Roth, "Streamlined ellipsometry procedure for characterizing physical aging rates of thin polymer films," *Journal of Polymer Science, Part B: Polymer Physics*, vol. 47, no. 24, pp. 2509-2519, 2009.

[27] J. E. Pye, K. A. Rohald, E. A. Baker, and C. B. Roth, "Physical Aging in Ultrathin Polystyrene Films: Evidence of a Gradient in Dynamics at the Free Surface and Its Connection to the Glass Transition Temperature Reductions," *Macromolecules*, vol. 43, no. 19, pp. 8296-8303, 2010.

[28] M. Y. Efremov, A. V. Kiyanova, and P. F. Nealey, "Temperature-Modulated Ellipsometry: A New Probe for Glass Transition in Thin Supported Polymer Films," *Macromolecules*, vol. 41, no. 16, pp. 5978-5980, 2008.

[29] X. Hong, Y. Jean, H. Yang, S. Jordan, and W. J. Koros, "Free-volume hole properties of gas-exposed polycarbonate studied by positron annihilation lifetime spectroscopy," *Macromolecules*, vol. 29, no. 24, pp. 7859–7864, 1996.

[30] H. Chen, M. L. Cheng, Y. Jean, L. J. Lee, and J. Yang, "Effect of CO_2 exposure on free volumes in polystyrene studied by positron annihilation spectroscopy," *Journal of Polymer Science, Part B: Polymer Physics*, vol. 46, no. 4, pp. 388–405, 2008.

[31] B. W. Rowe, S. J. Pas, A. J. Hill, R. Suzuki, B. D. Freeman, and D. R. Paul, "A variable energy positron annihilation lifetime spectroscopy study of physical aging in thin glassy polymer films," *Polymer*, vol. 50, no. 25, pp. 6149-6156, 2009.

[32] J. D. Wind, C. Staudt-Bickel, D. R. Paul, and W. J. Koros, "The Effects of Crosslinking Chemistry on CO_2 Plasticization of Polyimide Gas Separation Membranes," *Industrial and Engineering Chemistry Research*, vol. 41, no. 24, pp. 6139-6148, 2002.

[33] J. H. Kim, W. J. Koros, and D. R. Paul, "Effects of CO_2 exposure and physical aging on the gas permeability of thin 6FDA-based polyimide membranes. Part 2. with crosslinking," *Journal of Membrane Science*, vol. 282, no. 1-2, pp. 32-43, 2006.

[34] A. M. W. Hillock, S. J. Miller, and W. J. Koros, "Crosslinked mixed matrix membranes for the purification of natural gas: Effects of sieve surface modification," *Journal of Membrane Science*, vol. 314, no. 1-2, pp. 193-199, 2008.

[35] S. D. Kelman, S. Matteucci, C. W. Bielawski, and B. D. Freeman, "Crosslinking poly(1-trimethylsilyl-1-propyne) and its effect on solvent resistance and transport properties," *Polymer*, vol. 48, no. 23, pp. 6881-6892, 2007.

[36] J. Peter and K.-V. Peinemann, "Multilayer composite membranes for gas separation based on crosslinked PTMSP gutter layer and partially crosslinked Matrimid® 5218 selective layer," *Journal of Membrane Science*, vol. 340, no. 1-2, pp. 62-72, 2009.

[37] C.-C. Chen, W. Qiu, S. J. Miller, and W. J. Koros, "Plasticization-resistant hollow fiber membranes for CO_2/CH_4 separation based on a thermally crosslinkable polyimide," *Journal of Membrane Science*, vol. 382, no. 1-2, pp. 212-221, 2011.

[38] J. K. Ward and W. J. Koros, "Crosslinkable mixed matrix membranes with surface modified molecular sieves for natural gas purification: I. Preparation and experimental results," *Journal of Membrane Science*, vol. 377, no. 1-2, pp. 75-81, 2011.

[39] J. K. Ward and W. J. Koros, "Crosslinkable mixed matrix membranes with surface modified molecular sieves for natural gas purification: II. Performance characterization under contaminated feed conditions," *Journal of Membrane Science*, vol. 377, no. 1-2, pp. 82-88, 2011.

[40] A. Bos, I. G. M. Pünt, M. Wessling, and H. Strathmann, "Plasticization-resistant glassy polyimide membranes for CO_2/CH_4 separations," *Separation and Purification Technology*, vol. 14, no. 1-3, pp. 27-39, 1998.

[41] C. Zhou, T.-S. Chung, R. Wang, Y. Liu, and S. H. Goh, "The accelerated CO_2 plasticization of ultra-thin polyimide films and the effect of surface chemical cross-linking on plasticization and physical aging," *Journal of Membrane Science*, vol. 225, no. 1-2, pp. 125-134, 2003.

[42] P. S. Tin, T.-S. Chung, Y. Liu, R. Wang, S. L. Liu, and K. P. Pramoda, "Effects of cross-linking modification on gas separation performance of Matrimid membranes," *Journal of Membrane Science*, vol. 225, pp. 77-90, 2003.

[43] J. N. Barsema, S. D. Klijnstra, J. H. Balster, N. van der Vegt, G. Koops, and M. Wessling, "Intermediate polymer to carbon gas separation membranes based on Matrimid PI," *Journal of Membrane Science*, vol. 238, no. 1-2, pp. 93-102, 2004.

[44] N. R. Horn and D. R. Paul, "Carbon dioxide plasticization of thin glassy polymer films," *Polymer*, vol. 52, no. 24, pp. 5587-5594, 2011.

[45] N. R. Horn and D. R. Paul, "Carbon dioxide plasticization and conditioning effects in thick vs. thin glassy polymer films," *Polymer*, vol. 52, no. 7, pp. 1619-1627, 2011.

[46] L. Shao, T.-S. Chung, S. Goh, and K. Pramoda, "Polyimide modification by a linear aliphatic diamine to enhance transport performance and plasticization resistance," *Journal of Membrane Science*, vol. 256, pp. 46-56, 2005.

[47] R. W. Baker and K. Lokhandwala, "Natural Gas Processing with Membranes: An Overview," *Industrial and Engineering Chemistry Research*, vol. 47, no. 7, pp. 2109-2121, 2008.

[48] A. Y. Houde, B. Krishnakumar, S. G. Charati, and S. A. Stern, "Permeability of dense (homogeneous) cellulose acetate membranes to methane, carbon dioxide, and their mixtures at elevated pressures," *Journal of Applied Polymer Science*, vol. 62, no. 13, pp. 2181-2192, 1996.

[49] J. R. Scherer and G. Bailey, "Water in polymer membranes. Part I: Water sorption and refractive index of cellulose acetate," *Journal of Membrane Science*, vol. 13, no. 1, pp. 29–41, 1983.

[50] B. A. Bolton, S. Kint, G. F. Bailey, and J. R. Scherer, "Ethanol sorption and partial molar volume in cellulose acetate films," *The Journal of Physical Chemistry*, vol. 90, no. 6, pp. 1207-1211, 1986.

[51] A. C. Puleo, D. R. Paul, and S. S. Kelley, "The effect of degree of acetylation on gas sorption and transport behavior in cellulose acetate," *Journal of Membrane Science*, vol. 47, no. 3, pp. 301-332, 1989.

[52] R. T. Chern and C. N. Provan, "Gas-induced plasticization and the permselectivity of poly(tetrabromophenolphthalein terephthalate) to a mixture of carbon dioxide and methane," *Macromolecules*, vol. 24, no. 9, pp. 2203-2207, 1991.

[53] D. F. Stamatialis, M. Wessling, M. Sanopoulou, H. Strathmann, and J. H. Petropoulos, "Optical vs . direct sorption and swelling measurements for the study of stiff-chain polymer-penetrant interactions," *Journal of Membrane Science*, vol. 130, pp. 75-83, 1997.

[54] A. F. Ismail and W. Lorna, "Penetrant-induced plasticization phenomenon in glassy polymers for gas separation membrane," *Separation and Purification Technology*, vol. 27, no. 3, pp. 173-194, 2002.

[55] J. Guo and T. a. Barbari, "A dual mode interpretation of the kinetics of penetrant-induced swelling and deswelling in a glassy polymer," *Polymer*, vol. 51, no. 22, pp. 5145-5150, 2010.

[56] J.A. Woollam Company, "Ex Situ Data Analysis," in *Guide to Using WVASE32*, 2001.

[57] M. M. Despotopoulou, R. D. Miller, J. F. Rabolt, and C. W. Frank, "Polymer chain organization and orientation in ultrathin films: A spectroscopic investigation," *Journal of Polymer Science Part B: Polymer Physics*, vol. 34, no. 14, pp. 2335-2349, 1996.

[58] H. B. Park et al., "Polymers with cavities tuned for fast selective transport of small molecules and ions.," *Science*, vol. 318, no. 5848, pp. 254-8, 2007.

[59] J. H. Kim, J. Jang, and W.-C. Zin, "Thickness Dependence of the Melting Temperature of Thin Polymer Films," *Macromolecular Rapid Communications*, vol. 22, no. 6, pp. 386-389, 2001.

[60] L. M. Robeson, "The upper bound revisited," *Journal of Membrane Science*, vol. 320, no. 1-2, pp. 390-400, 2008.

[61] H. B. Park, S. H. Han, C. H. Jung, Y. M. Lee, and A. J. Hill, "Thermally rearranged (TR) polymer membranes for CO_2 separation," *Journal of Membrane Science*, vol. 359, no. 1-2, pp. 11-24, 2010.

[62] I. C. Sanchez and J. Cho, "A universal equation of state for polymer liquids," *Polymer*, vol. 36, no. 15, pp. 2929-2939, 1995.

[63] P. M. Budd, B. S. Ghanem, S. Makhseed, N. B. McKeown, K. J. Msayib, and C. E. Tattershall, "Polymers of intrinsic microporosity (PIMs): robust, solution-processable, organic nanoporous materials," *Chemical Communications*, no. 2, pp. 230-231, 2004.

[64] N. B. McKeown et al., "Polymers of Intrinsic Microporosity (PIMs): Bridging the Void between Microporous and Polymeric Materials," *Chemistry - A European Journal*, vol. 11, no. 9, pp. 2610-2620, 2005.

[65] P. M. Budd, N. B. McKeown, and D. Fritsch, "Free volume and intrinsic microporosity in polymers," *Journal of Materials Chemistry*, vol. 15, no. 20, pp. 1977-1986, 2005.

[66] R. Lima de Miranda et al., "Unusual temperature dependence of the positron lifetime in a polymer of intrinsic microporosity," *Physica Status Solidi (RRL) – Rapid Research Letters*, vol. 1, no. 5, pp. 190-192, 2007.

[67] J. Weber, Q. Su, M. Antonietti, and A. Thomas, "Exploring Polymers of Intrinsic Microporosity – Microporous, Soluble Polyamide and Polyimide," *Macromolecular Rapid Communications*, vol. 28, no. 18–19, pp. 1871-1876, 2007.

[68] P. Budd et al., "Gas permeation parameters and other physicochemical properties of a polymer of intrinsic microporosity: Polybenzodioxane PIM-1," *Journal of Membrane Science*, vol. 325, no. 2, pp. 851-860, 2008.

[69] B. S. Ghanem et al., "Synthesis, Characterization, and Gas Permeation Properties of a Novel Group of Polymers with Intrinsic Microporosity: PIM-Polyimides," *Macromolecules*, vol. 42, no. 20, pp. 7881-7888, 2009.

[70] T. Emmler et al., "Free Volume Investigation of Polymers of Intrinsic Microporosity (PIMs): PIM-1 and PIM1 Copolymers Incorporating Ethanoanthracene Units," *Macromolecules*, vol. 43, p. 6075-6085, 2010.

Appendix A: Literature Data for the Refractive Index of CO_2

Most refractive index data for gases in the literature are reported at temperatures ranging from 0°C to ~23°C and at ~1 atm. Such data is generally not useful outside of these general ranges, for it is well-known that the refractive index of a gas is somewhat dependent on temperature and pressure. In high-pressure ellipsometry experiments such as those outlined in this work, much more care must be taken to model the refractive index of the gas over the range of conditions to be explored. Fortunately, Michels and Hamers have recorded extensive measurements of the refractive index of CO_2 at various temperatures, pressures, and wavelengths [1]. To aid future researchers, a selection of relevant data is reproduced in Table A.1.

Even with this data available, one must make some assumptions to simplify the analysis. In this work, the refractive index of CO_2 was assumed to be constant over the wavelength range of interest (450 to 750 nm). From Table A.1, the data for the sodium-D line, 587.6 nm, were selected for further analysis. The data analysis software package within Microsoft Excel was used to regress these data for two pressure ranges: 0-320 psia, and 300-600 psia. The objective was to develop equations whereby simply inputting the temperature and pressure of CO_2 would give a reasonable measure of the refractive index. The following two equations were determined for each respective range:

$$n_{0\text{-}300} = 1.00014765 + (\text{-}3.52352E\text{-}06)\cdot T + (\text{-}1.32562E\text{-}07)\cdot T\cdot P + (3.08249E\text{-}05)\cdot P + (1.23334E\text{-}06)\cdot P^2 \quad \text{(A.1)}$$

$$n_{320\text{-}600} = 0.998887561 + (6.65427\text{E-}05)\cdot T + (\text{-}3.47168E\text{-}07)\cdot T\cdot P + (3.12367E\text{-}05)\cdot P + (2.28193E\text{-}08)\cdot P^2 \quad \text{(A.2)}$$

where *n* is the refractive index of CO_2, T is temperature in degrees Celsius, and P is pressure in psia.

Temperature	Pressure	Pressure	*n*, Refractive Index, at wavelengths (nm)					
(°C)	(psia)	(atm)	667.8	587.6	501.6	492.2	471.3	447.1
25.053	14.6	0.99	1.0004	1.0005	1.0004	1.0004	1.0004	1.0004
25.053	109.2	7.43	1.0031	1.0032	1.0032	1.0032	1.0032	1.0032
25.053	191.8	13.05	1.0058	1.0057	1.0058	1.0058	1.0058	1.0058
25.053	246.3	16.76	1.0075	1.0076	1.0076	1.0076	1.0076	1.0076
25.053	314.1	21.37	1.0098	1.01	1.0101	1.0101	1.0101	1.0101
25.053	315.4	21.46	1.0099	1.01	1.0101	1.0101	1.0101	1.0101
25.053	315.5	21.47	1.0098	1.0098	1.01	1.01	1.0099	1.01
25.053	383.7	26.11	1.0124	1.0124	1.0125	1.0126	1.0126	1.0126
25.053	384.2	26.14	1.0125	1.0126	1.0127	1.0127	1.0127	1.0127
25.053	452.8	30.81	1.0153	1.0154	1.0155	1.0155	1.0155	1.0156
25.053	521.9	35.51	1.0184	1.0185	1.0186	1.0187	1.0187	1.0188
25.053	590.5	40.18	1.0218	1.0219	1.0221	1.0221	1.0221	1.0222
25.053	658.4	44.80	1.0256	1.0257	1.0258	1.0259	1.026	1.026
25.053	659.0	44.84	1.0256	1.0258	1.0259	1.0259	1.026	1.0261
25.053	723.9	49.26	1.0297	1.0298	1.0301	1.0302	1.0302	1.0304
25.053	723.9	49.26	1.0297	1.0298	1.0301	1.0301	1.0302	1.0303
25.053	725.0	49.33	1.0299	1.03	1.0302	1.0302	1.0303	1.0305
25.053	825.6	56.18	1.0384	1.0386	1.0388	1.0389	1.039	1.0391
25.053	825.6	56.18	1.0383	1.0385	1.0388	1.0389	1.039	1.039
25.053	833.3	56.70	1.0391	1.0393	1.0396	1.0397	1.0397	1.0399
25.053	932.3	63.44	1.0551	1.0553	1.0557	1.0558	1.0559	1.0561
32.075	313.8	21.35	1.0094	1.0097	1.0097	1.0097	1.0097	1.0098
32.075	723.6	49.24	1.0276	1.0278	1.0279	1.028	1.028	1.0281
32.075	826.7	56.25	1.0344	1.0345	1.0347	1.0347	1.0348	1.0349
32.075	931.0	63.35	1.0435	1.0438	1.0441	1.0442	1.0443	1.0444
32.075	990.7	67.41	1.0509	1.0512	1.0517	1.0517	1.0517	1.0521
49.712	15.9	1.08	1.0003	1.0003	1.0003	1.0004	1.0004	1.0004
49.712	107.9	7.34	1.0028	1.0028	1.0029	1.0028	1.0029	1.0029
49.712	190.6	12.97	1.005	1.0051	1.0051	1.0051	1.0052	1.0052
49.712	245.1	16.68	1.0066	1.0066	1.0067	1.0068	1.0066	1.0068
49.712	314.4	21.39	1.0086	1.0087	1.0088	1.0088	1.0089	1.0089
49.712	315.2	21.45	1.0088	1.0089	1.0089	1.0089	1.0089	1.009
49.712	383.3	26.08	1.0109	1.0109	1.011	1.0111	1.011	1.0111
49.712	451.6	30.73	1.0132	1.0133	1.0133	1.0134	1.0134	1.0135
49.712	520.2	35.40	1.0156	1.0157	1.0158	1.0158	1.0159	1.0159
49.712	588.1	40.02	1.0182	1.0182	1.0183	1.0184	1.0184	1.0185
49.712	656.6	44.68	1.0209	1.021	1.0212	1.0212	1.0212	1.0212
49.712	721.0	49.06	1.0236	1.0237	1.0239	1.0239	1.024	1.0241
49.712	721.4	49.09	1.0237	1.0237	1.0239	1.0239	1.024	1.0241

Table A.1: Literature Data for the refractive Index of CO_2

REFERENCES

[1] A. Michels and J. Hamers, "The effect of pressure on the refractive index of CO_2: The Lorentz-Lorenz formula," *Physica*, vol. 4, no. 10, pp.995–1006, 1937.

Appendix B: On Occupied Volume

INTRODUCTION AND HISTORY

The space between polymer chains where no dissolved small molecules are present, termed "free volume," can have a significant effect on the properties of any polymer. In polymer membrane separations, for instance, penetrant permeability is thought to be well correlated with the free volume of a polymer. Free volume, however, is not easily accessible experimentally. The most direct route to determining free volume of a polymer is to use positron annihilation lifetime spectroscopy [1], which measures the lifetime of incident positrons in the polymer as they are annihilated as *ortho*-positronium. Several free volume models besides PALS have been proposed in the literature [2], but one that has gained wide acceptance is that of Lee [3]. Lee's general method involves experimentally measuring the density of the polymer, then subtracting the "occupied volume" of the polymer chains from the specific volume (the reciprocal of the density). The specific free volume and fractional free volume can be calculated respectively as:

$$SFV = V - V_0 \tag{B.1}$$

$$f = \frac{V - V_0}{V} = 1 - \rho V_0 \tag{B.2}$$

where $V = 1/\rho$ is the specific volume and V_0 is the occupied volume of the polymer (or mixed system). Lee said that this occupied volume is the zero point molar volume, and is closely related to the van der Waals volume (determined theoretically via the Bondi group contribution method) with the following equation:

$$V_0 = 1.3 \cdot V_{vdw} \tag{B.3}$$

Lee's method has been cited to such an extent since its original publication in 1980 that rarely are the assumptions of the model, especially the important "1.3" factor,

ever challenged. It is of considerable interest, then, to understand the developmental history of this method, how it became widely accepted in the polymer membrane community, and what adjustments can be made to improve its accuracy.

In 1972, Van Krevelen published the first edition of *Properties of Polymers* [4]. The book's primary purpose was to apply group contribution techniques to prediction of polymer properties where experimental data was unavailable. Chapter 4 addresses prediction of volumetric properties, which are important for numerous phenomena and processes. Van Krevelen expanded upon the contribution of Bondi [5,6] to compile group contributions of various structural groups to the van der Waals volume of a polymer. He states that the zero point molar volume, denoted as $V^0(0)$, is closely related to the van der Waals volume. "According to Bondi [6], a good approximation is given by the following expression":

$$\frac{V^0(0)}{V_{vdw}} = \frac{V_c(0)}{V_{vdw}} \approx 1.3 \qquad \text{(B.4)}$$

Other than crediting Bondi, Van Krevelen does not explain the origin or physical meaning of the "1.3" factor.

As previously mentioned, Lee was the first to suggest applying the relationship found in Van Krevelen to calculate free volume [3]. In his 1980 publication, Lee, like Van Krevelen, credits Bondi with introducing the "1.3" factor to relate the van der Waals and occupied volume without explaining its origin or physical meaning, even using the same language of Van Krevelen by calling it a "good approximation." Despite this novel merger of group contribution methods and free volume theory, it remained relatively obscure for some time. Between 1980 and 1984, Lee's paper was cited only once [7].

According to Don Paul [8], Paul's graduate student Yasushi Maeda read Lee's paper in 1984 and applied it to the study of gas permeability in pure polymers and polymer blends [9]. Later that year, Lee received his first journal citation in three years in a review article by Paul [10]. Paul did not discuss the "1.3" factor in the paper, but rather commented on the impressive correlation Lee's relationship had with experimental data. Maeda's dissertation in 1985 [9] and subsequent paper [11] reintroduced Lee's innovative idea once again to the literature. Like Lee and Van Krevelen, he does credit Bondi with the "1.3" factor but did not elaborate upon its origin and physical meaning in great detail. Interestingly, though Maeda essentially brought Lee's paper back from total obscurity, Maeda is less frequently credited with the rediscovery. As of January 2012, Lee's paper has accumulated over 250 citations, while Maeda's 1987 paper has been cited about 140 times. In short, the "1.3" factor has now been quoted enough that it is essentially accepted without question.

REVISING THE METHOD OF LEE, MAEDA, AND VAN KREVELEN

In all of the major sources for the development of this method of calculating free volume, Bondi is credited as the originator of the "1.3" factor. Generally, these sources cite Chapters 3 and 4 of Bondi's book, *Physical Properties of Molecular Crystals, Liquids, and Glasses* [6]. Bondi did not have great interest in free volume; his primary goal was to establish corresponding states relationships for property predictions of all kinds of molecules. Current researchers still cite the "1.3" factor as "following Bondi" in many papers. However, it is impossible to find this factor anywhere in Bondi's book. In fact, we find in Bondi a slightly different presentation of the terms: "An obvious fundamental property of a crystal is $\rho_0^* = V_{vdw}/V_0 = \rho^*$ at T = 0 K, the *packing density*

in the absence of thermal vibrations." The packing density is always less than unity and, thus, the "1.3" factor is actually the reciprocal of the packing density of a polymer crystal at 0 K.

Van Krevelen's fundamental assumption, then, is that all polymers have the same packing fraction, 1/1.3 = 0.77, at absolute zero. Perhaps what Van Krevelen found in Bondi was a packing density of ~0.77 for polymers. Still, we find no direct reference to such a universal packing density for polymers in the text. One cannot even average the packing densities of select polymers given in Table 4.3 or any small molecules from tables throughout Chapters 3 and 4 of Bondi's book [6] to obtain such a value. Incidentally, the greatest value from Bondi's Table 4.3 is 0.775 for polyvinylidene chloride, but it seems unlikely that Van Krevelen would take this single polymer as representative of all polymers.

However, a single sentence at the beginning of Chapter 3 of Bondi may point to the solution: "[The packing density] can vary in principle… from 0.785 to 0.903 for open- and close-packed arrays, respectively, of infinitely long cylinders." Polymer chains could possibly be approximated as "infinitely long cylinders," and many polymer crystals form open-packed arrays [12]. It could be that Van Krevelen took the value of 0.785 from this section to make his approximation: 1/0.785 = 1.273, and then rounded the result to obtain "1.3". Sanchez and Cho [13] have suggested that the "1.3" value perhaps originated from extrapolations of the packing fraction of polyethylene to absolute zero, but this seems unlikely considering that the packing fraction of polyethylene is given as 0.732 in Table 4.3 of Bondi.

When calculating the molar density at 0 K, or zero point molar volume, for a material with an unknown packing density ρ^*, Bondi suggests guessing a value by comparison with ρ^* data from materials believed to have a similar crystal structure to the material of interest. The occupied volume of the molecule then becomes:

$$V_0 = (1/\rho^*) \cdot V_{vdw} \tag{B.5}$$

This adjustment to Lee's method is particularly useful when calculating free volume of a mixed system of a polymer and a small molecule, such as demonstrated in Chapter 6 with polymer/CO_2 mixed systems. The packing density of many small molecules are well-known and presented in various tables in Bondi's book and elsewhere [5,6].

Sanchez and Cho [13] suggested that a more appropriate measure of V_0 was the specific volume at absolute zero, i.e., $V_0 = v_{0K} = 1/\rho_{0K}$. They noticed that the zero pressure density of many materials is linear with temperature, and that the characteristic mass density, ρ_{0K}, can be obtained by extrapolating zero pressure densities to absolute zero (this must be done with values obtained above the glass transition temperature). A particularly interesting result of their analysis is that fractional free volume is not only related to the reduced density but also to the reduced temperature:

$$f = 1 - \frac{\rho}{\rho_{0K}} = 1 - \tilde{\rho} = \frac{T}{T^*} = \tilde{T} \tag{B.6}$$

Consequently, one does not necessarily need to calculate the van der Waals volume in order to estimate free volume. In fact, no knowledge of the polymer structure is needed at all. This important, but frequently overlooked, conclusion of their work provides the synthetic chemist with an interesting tool for property estimation in the face

of little structural data. Moreover, it is often more feasible to measure zero pressure density or determine the characteristic temperature for a polymer than to obtain the packing density of a polymer crystal.

Sanchez and Cho tabulated zero pressure density data for 29 polymers and found that the average ratio of the van der Waals density to the characteristic density (which is the reciprocal of the packing fraction) was 1.288 with a standard deviation of 0.52, which is quite close to the "1.3" factor of Van Krevelen, and to the value calculated from the open-packed array of infinitely long cylinders, 1.273, as well. In the end, the "1.3" factor is not a bad approximation after all, provided no other data exists for the polymer. The contribution of Sanchez and Cho to this area cannot be underestimated.

Figure B.1 illustrates the relative sensitivity of free volume to variation in the packing density factor for polyphenylene oxide (PPO). This first set of data was presented in Chapter 6, Figure 6.7 (for $1/\rho^* = 1.21$). The other data are the results of using Van Krevelen's approximation ($1/\rho^* = 1.3$) for the free volume calculation. A nominal difference of ~6% for free volume may seem small, but it has a substantial effect upon expected permeability values.

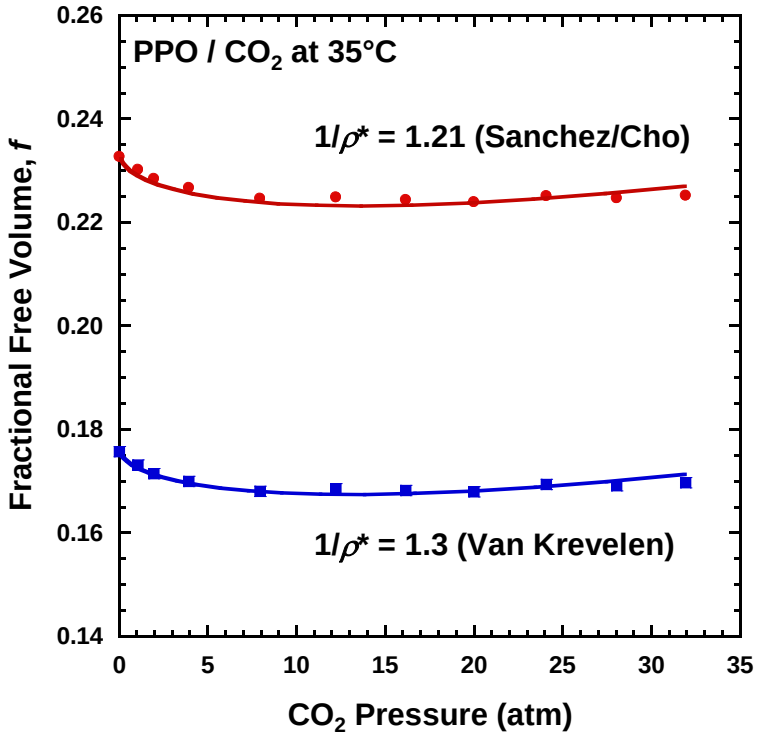

Figure B.1: Sensitivity of PPO free volume calculations to the packing density.

Park and Paul [14] attempted to correlate fractional free volume with gas permeability using a modified group contribution method to calculate the occupied volume. Instead of summing the van der Waals volumes of the groups and assuming the "1.3" factor, they proposed that each structural group should have a separate, empirically-derived front factor denoted as $\gamma_{n,i}$ (again, this is the reciprocal of the packing density) that depends upon the penetrant of interest. They deemed this notion reasonable because all gases should have a different effective fractional free volume within a polymer system. In other words, the size or structure of a gas molecule ought to influence the how it accesses free volume. The occupied volume of the polymer with sorbed gas n then becomes:

$$V_{0,n} = \sum_i \gamma_{n,i} V_{w,i} \qquad \text{(B.7)}$$

By analyzing gas permeability data for over 100 polymers, Park and Paul obtained $\gamma_{n,i}$ values for CH_4, N_2, O_2, CO_2, H_2, and He, for 41 structural groups. This library of data allowed them to correlate fractional free volume with gas permeability with the well-known expression:

$$P = A \exp(-B/FFV)$$

(B.8)

Park and Paul's approach resulted in a considerable improvement over previous correlations of fractional free volume with gas permeability, but there are still a few subtle issues that were not fully addressed. First, even though the authors attempted to account for the effective free volume of different gases, they did not use an equation for a mixed system of polymer and gas in the calculation of the occupied volume. Sorbed gas can account for up to 5-10 wt% of the system, and cannot be ignored without introducing some error into the calculations. Such data, however, is extremely rare in the literature. It is possible that this error was slightly mitigated by the gas- and structural group-dependent front factor. Second, Park and Paul's method is ultimately an empirical model. Even though the authors discussed some rationale for why their empirical factors could be dependent on the gas and structural group, it was still a fitted model and could very well be a fortunate occurrence rather than a theoretical certainty.

COMPARING FRACTIONAL FREE VOLUME CALCULATIONS AND GAS PERMEABILITY CORRELATIONS

Estimating the fractional free volume requires either density data (bulk and characteristic) or characteristic temperature data. Using data assembled from Park and

Paul [14], Sanchez and Cho [13], and polymer reference works, fractional free volume calculations based on reduced temperature and density were compared to the calculations of Park (Figure B.2). Only polymers included in all the works were plotted. The diagonal line signifies where the free volume prediction of Park would exactly match the calculation based on the reduced parameter.

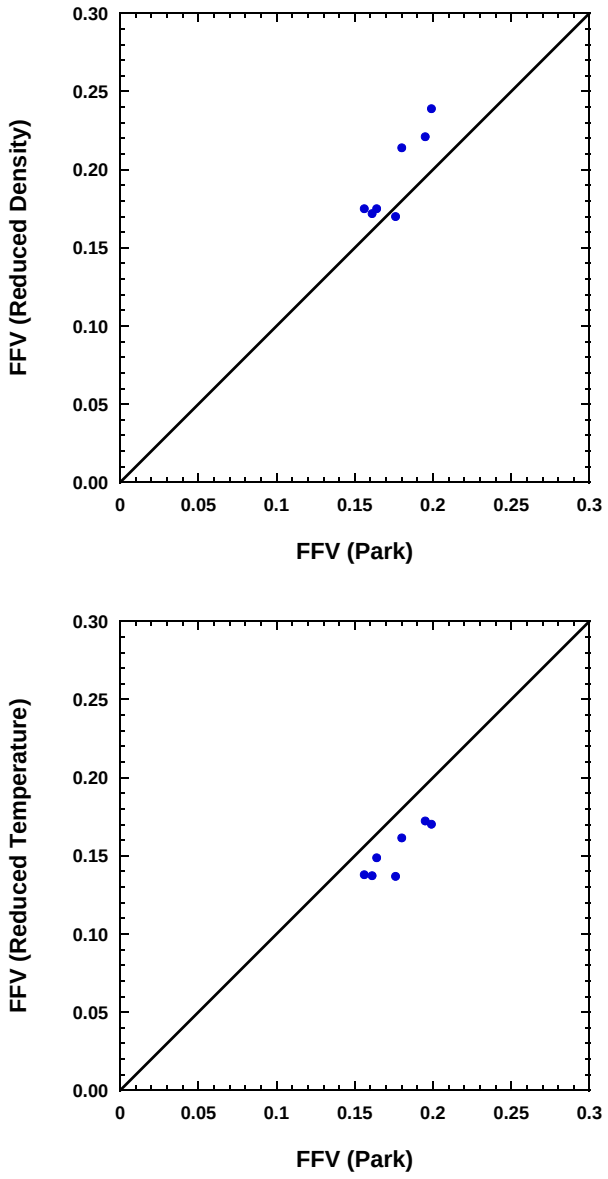

Figure B.2: Comparison of fractional free volume estimations based on different calculation methods.

The reduced density method appears to over-predict free volume relative to Park's method, whereas the reduced temperature method under-predicts. However, neither plot contains a large number of data points, so these trends may not be representative. The calculations suggest that the reduced density method will likely predict higher values for free volume than the reduced temperature method. Figure B.3 displays this comparison; the plot contains many more points than Figure B.2 because all of the data comes from Sanchez and Cho's full list of polymers as opposed to matching the data to Park.

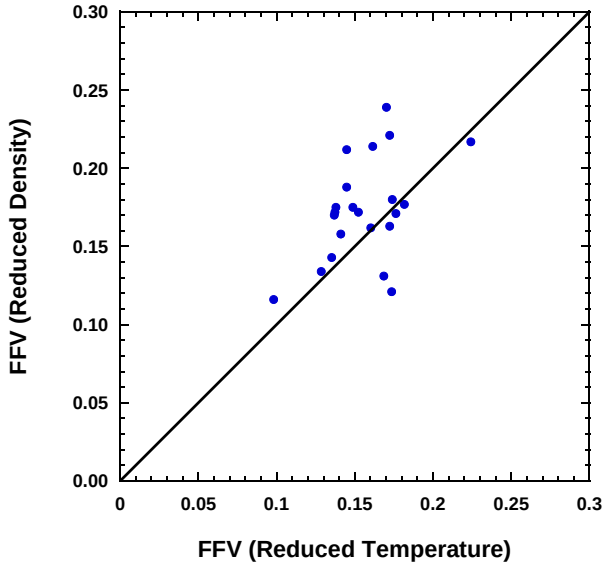

Figure B.3: Comparison of fractional free volume estimations based on reduced parameters.

If reduced parameters are better measures of fractional free volume for polymers, then perhaps correlations of permeability and free volume can be improved as well. Polymers from the previous analysis that have well-established gas permeability values from the literature [15,16] were plotted along with equation B.8, using Park's regressed *A*

and *B* parameters, to examine if these different free volume estimations result in better permeability correlations. Figure B.4 plots the permeability of six gases versus reciprocal free volume based on reduced density. Figure B.5 displays similar plots, but the free volume is based on the reduced temperature.

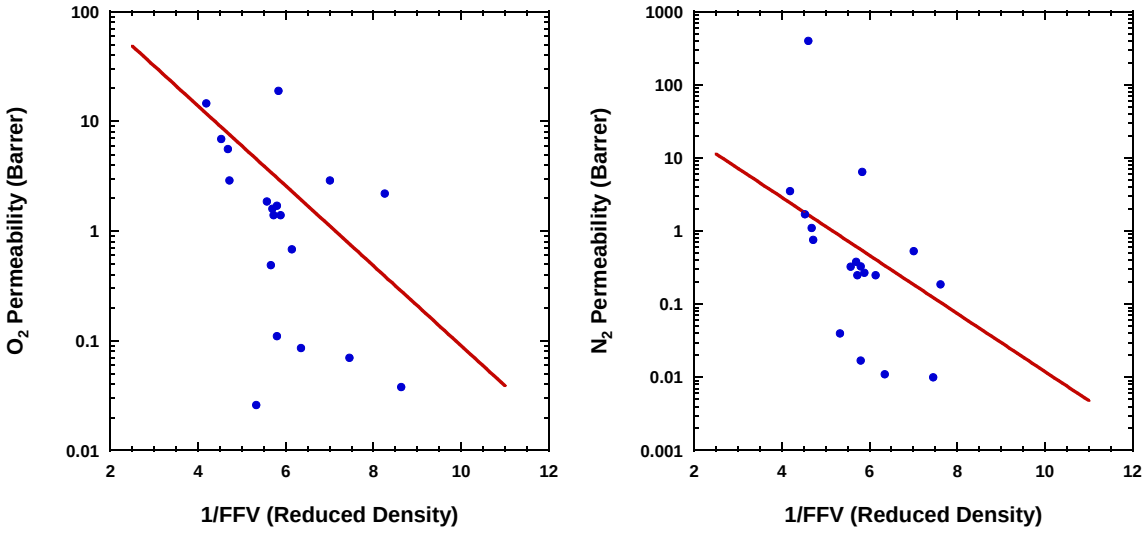

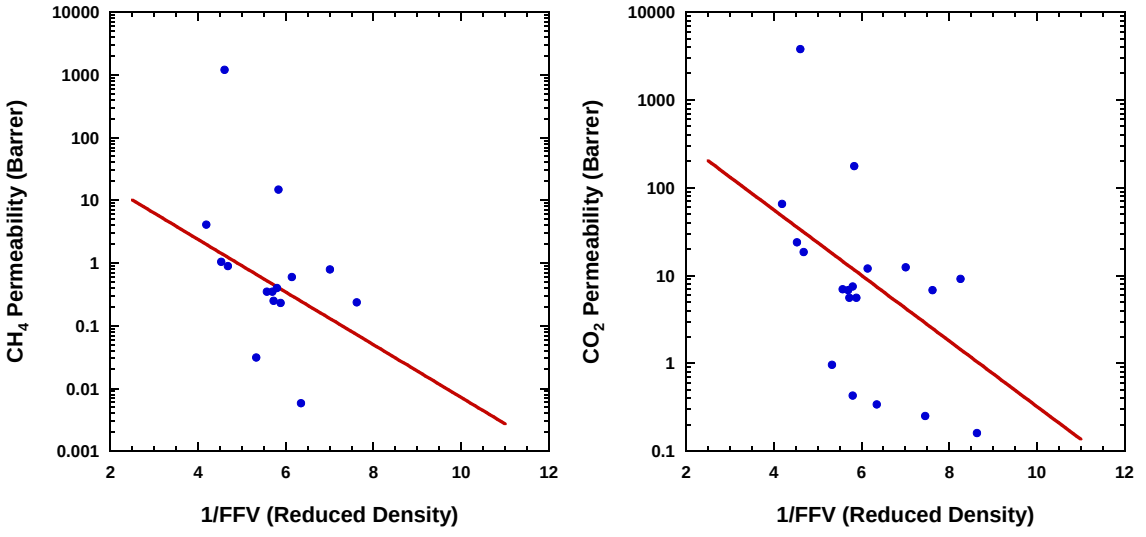

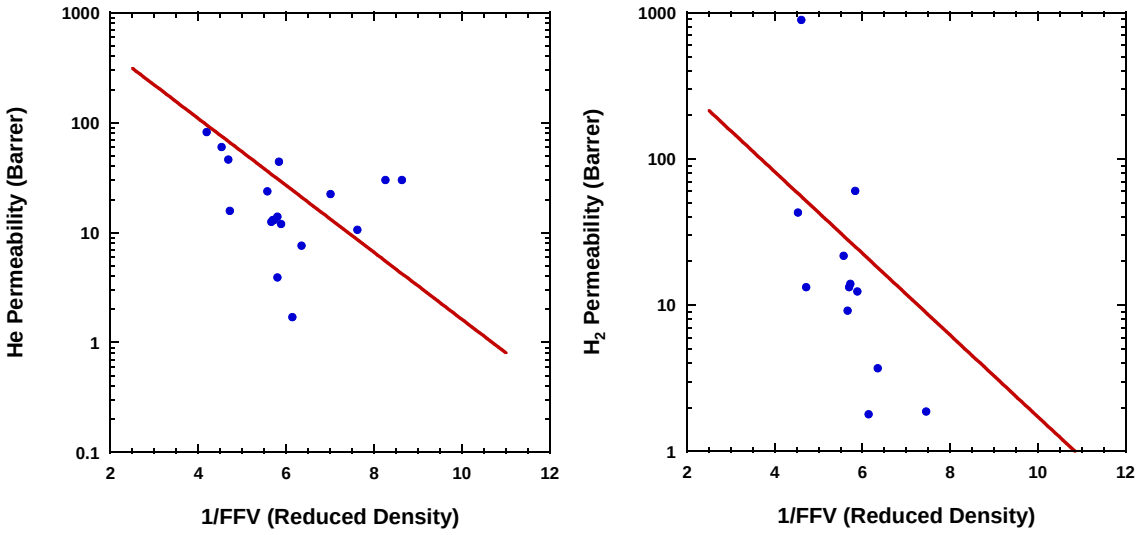

Figure B.4: Gas permeability for various polymers plotted against 1/FFV. Fractional free volume was estimated using the reduced density. Solid lines represent Equation B.8 where the *A* and *B* parameters were taken from Park and Paul [14].

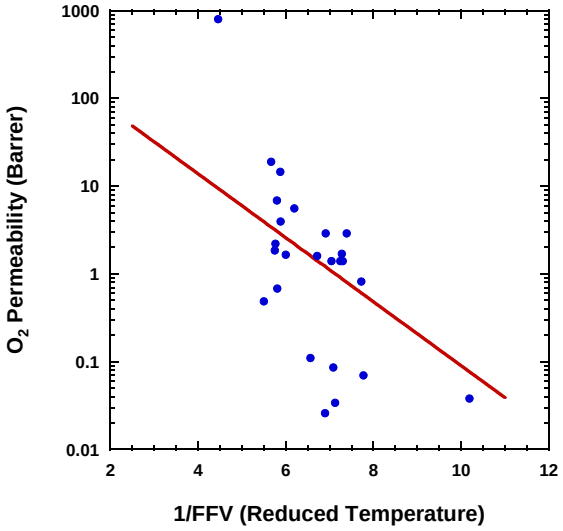
1000
100
10
1
0.1
0.01
2
4
6
8
10
12
O2 Permeability (Barrer)
1/FFV (Reduced Temperature)

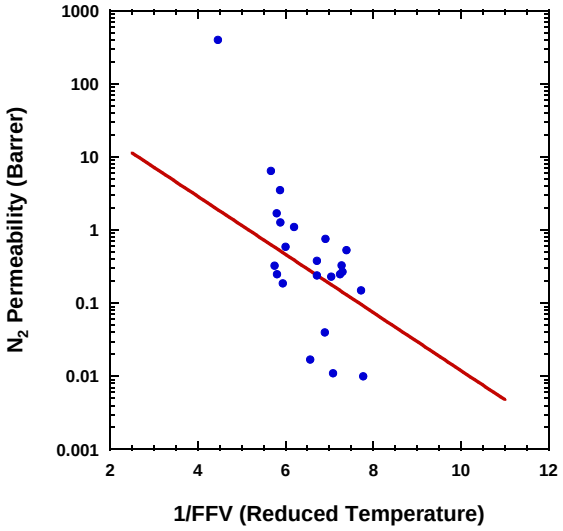
1000
100
10
1
0.1
0.01
0.001
2
4
6
8
10
12
N2 Permeability (Barrer)
1/FFV (Reduced Temperature)

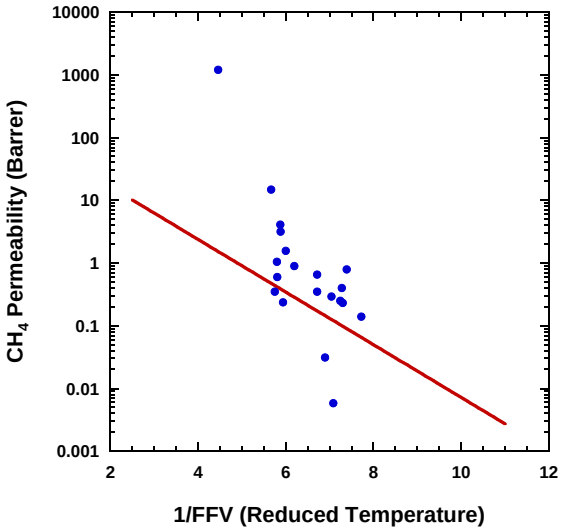
10000
1000
100
10
1
0.1
0.01
0.001
2
4
6
8
10
12
CH4 Permeability (Barrer)
1/FFV (Reduced Temperature)

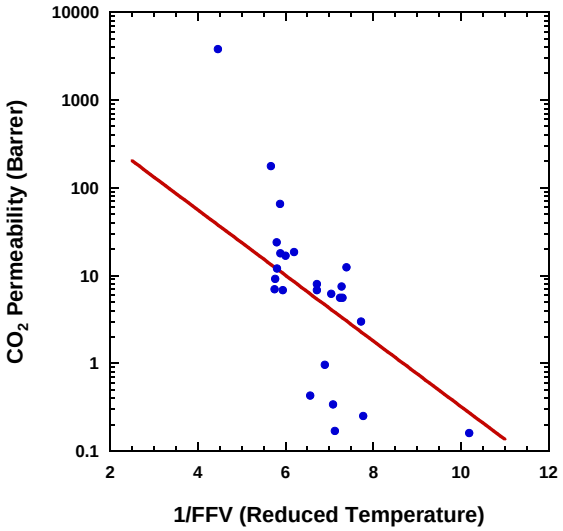
10000
1000
100
10
1
0.1
2
4
6
8
10
12
CO2 Permeability (Barrer)
1/FFV (Reduced Temperature)

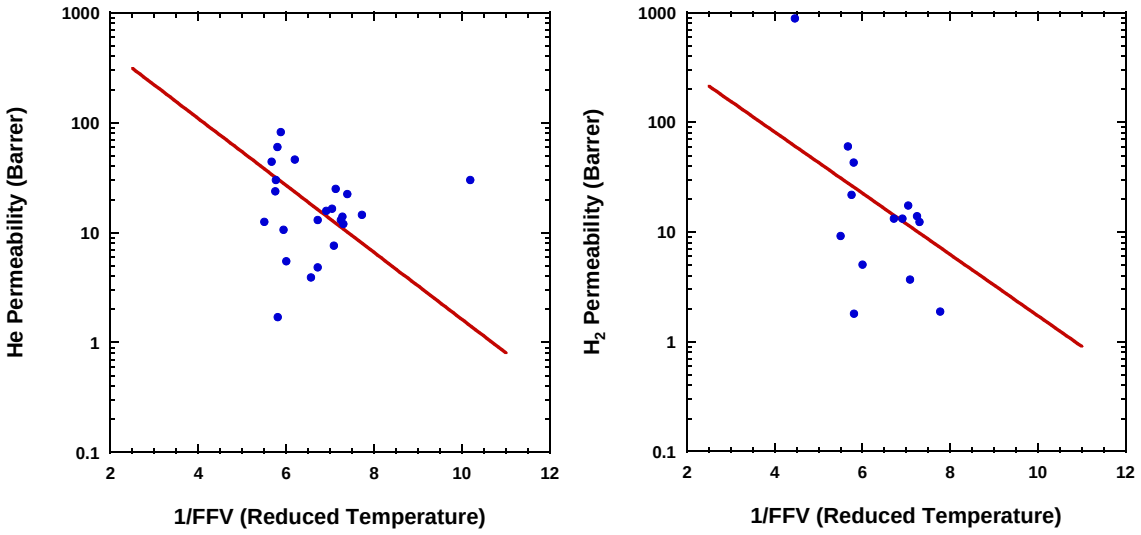

Figure B.5: Gas permeability for various polymers plotted against 1/FFV. Fractional free volume was estimated using the reduced temperature. Solid lines represent Equation B.8 where the *A* and *B* parameters were taken from Park and Paul [14].

The plots do not indicate that alternative methods of estimating free volume correlate better with gas permeability than Park and Paul's method. For the larger gases, the grouping of points seems fairly regular, but for smaller gases such as He or H_2 there is significant scatter. One might speculate that the reduced density and reduced temperature plots suggest a steeper regression line, i.e., the *A* and *B* parameters will increase in absolute value. It may be the case that any of these methods of estimating free volume may result in a useful correlation given sufficient data. Hence, comparisons between polymers could be valid insofar as the same method is used for each polymer. Of course, any correlation derived from this data would still suffer from not using the free volume equation for a mixed system as described earlier.

There are two ways which might adjust and improve this correlation. First, correlating diffusivity with free volume would probably yield better results than permeability, since solubility is thought to be less affected by free volume than diffusivity. Obtaining reliable diffusivity data for so many polymers, though, would be an extraordinarily difficult task. Second, instead of grouping many polymer types together and performing a regression on all of them at once, a smaller group of polymers of a single type might result in a better correlation overall that could more reliably predict the permeability properties of a new polymer of that type. Clearly, free volume is not the only factor in determining gas permeability of polymers. More careful grouping of similar polymers could mitigate some of these issues.

CALCULATING VAN DER WAALS VOLUMES OF SMALL MOLECULES, INCREMENT GROUPS, AND POLYMERS

The van der Waals volume (V_{vdw}) is the space occupied by a molecule that is generally impenetrable by other molecules with ordinary energies. Calculating V_{vdw} requires knowledge of bond distances, bond angles, contact distances, characteristic shapes of atoms (in some cases), and van der Waals radii. For heavy atoms, the van der Waals radius is invariant to the conditions of the atom, i.e., environment, chemical combination, nearest non-bonded neighbor, phase state. The van der Waals radius of some lighter atoms, such as hydrogen, fluorine, etc., may show some variability under certain conditions.

For example, consider a diatomic molecule of two different atoms, having van der Waals radii of R and r, and a bond distance l. Figure B.2 depicts the geometry of this two atom system.

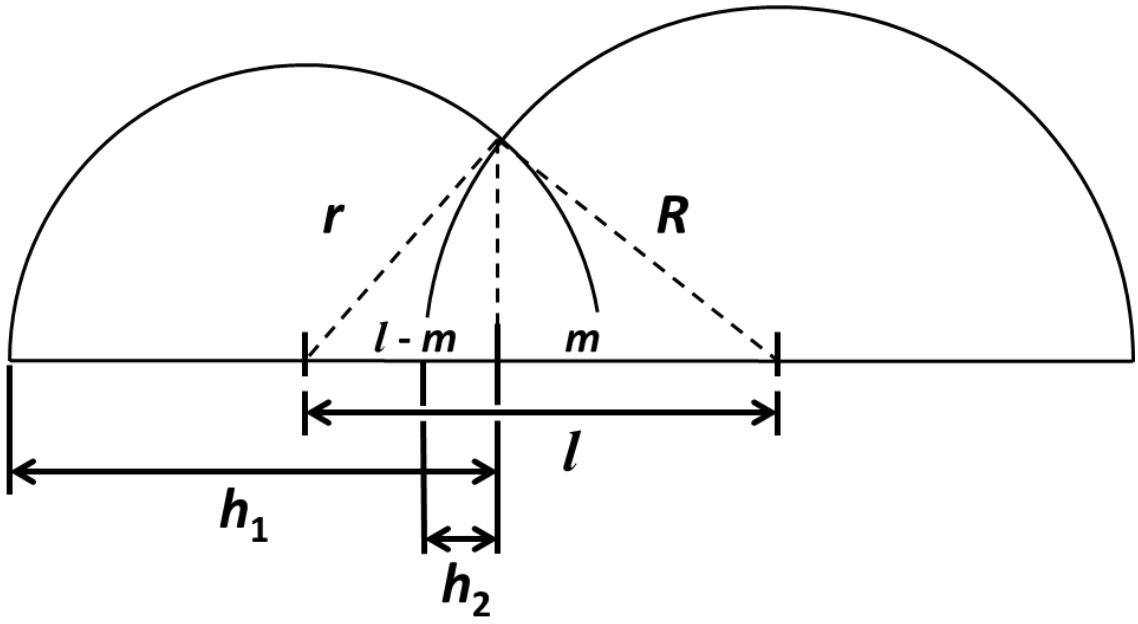

Figure B.6: Schematic of a diatomic system for calculating the van der Waals volume.

The procedure for calculating the volume of the diatomic molecule depicted in Figure B.2 involves summing the contributions of the two atoms and subtracting the overlapping sections with the following equations:

$$m = \frac{(R^2 - r^2 + l^2)}{2l}; h_1 = r + l - m;\ h_2 = R - m \tag{B.9}$$

$$V_1 = \pi {h_1}^2 \left(r - \frac{h_1}{3}\right);\ V_2 = \frac{4}{3}\pi R^3;\ \Delta V_{2-1} = \pi {h_2}^2 \left(R - \frac{h_2}{3}\right) \tag{B.10}$$

$$V_w = V_1 + V_2 - \Delta V_{2-1} \tag{B.11}$$

These equations can be further generalized to calculate the effective contribution of a given atom A with radius *R* to the total van der Waals volume of a structural group, accounting for the connectivity of atom A of each nearest neighbor (having radii r_i and bond distance l_i). Summing the contributions of each atom in the structural group then results in the total van der Waals volume of the group:

$$V_{w,A} = \frac{4}{3}\,\pi R^3 - \sum \pi {h_i}^2 \left(R - \frac{h_i}{3}\right); h_i = R - \frac{l_i}{2} - \frac{R^2}{2l_i} + \frac{{r_i}^2}{2l_i} \qquad \text{(B.12)}$$

CONCLUSIONS

Different methods of estimating occupied volume and fractional free volume have been examined in the context of gas permeability. Van Krevelen's "1.3" approximation should not be abandoned (although perhaps 1.288 would perhaps be more appropriate), but it should only be used in the absence of known values of packing fraction, characteristic mass density, or characteristic temperature. Free volume and other predicted properties can indeed be sensitive to these small but significant assumptions made during calculations.

ACKNOWLEDGEMENTS

The author is very grateful to Lloyd Robeson for generously providing his extensive reference tables of permeability data to assist the correlations of gas permeability with fractional free volume.

REFERENCES

[1] P. E. Mallon, "Application to polymers," in *Positron and Positronium Chemistry*, Y. C. Jean, P. E. Mallon, and D. M. Schrader, Eds. New Jersey: World Scientific, 2003, pp. 253-280.

[2] C. A. Kumins and T. K. Kwei, "Free Volume and Other Theories," in *Diffusion in Polymers*, J. Crank and G. S. Park, Eds. London: Academic Press, 1968, pp. 107-140.

[3] W. M. Lee, "Selection of barrier materials from molecular structure," *Polymer Engineering and Science*, vol. 20, no. 1, pp. 65-69, 1980.

[4] D. W. Van Krevelen, *Properties of Polymers*, 3rd ed. New York: Elsevier, 1990.

[5] A. Bondi, "Van der Waals Volumes and Radii," *Journal of Physical Chemistry*, vol. 68, no. 3, pp. 441-451, 1964.

[6] A. Bondi, *Physical Properties of Molecular Crystals, Liquids, and Glasses*. New York: John Wiley & Sons, 1968.

[7] S. Allen, V. Stannett, and H. Hopfenberg, "Noble gas transport in poly (methyl vinyl ketone) and poly (methyl vinyl ether)," *Polymer*, vol. 22, no. 7, pp. 912–917, 1981.

[8] D. R. Paul, "Personal communication," 2012.

[9] Y. Maeda, *Ph.D. Dissertation, University of Texas at Austin*, 1985.

[10] D. R. Paul, "Gas transport in homogeneous multicomponent polymers," *Journal of Membrane Science*, vol. 18, pp. 75-86, 1984.

[11] Y. Maeda and D. R. Paul, "Effect of antiplasticization on gas sorption and transport. III. Free volume interpretation.," *Journal of Polymer Science, Part B: Polymer Physics*, vol. 25, no. 5, pp. 1005-1016, 1987.

[12] J. E. Mark, *Polymer Data Handbook*, 2nd Edition. Oxford, UK: Oxford University Press, 2009.

[13] I. C. Sanchez and J. Cho, "A universal equation of state for polymer liquids," *Polymer*, vol. 36, no. 15, pp. 2929-2939, 1995.

[14] J. Y. Park and D. R. Paul, "Correlation and prediction of gas permeability in glassy polymer membrane materials via a modified free volume based group contribution method," *Journal of Membrane Science*, vol. 125, no. 1, pp. 23-39, 1997.

[15] L. M. Robeson, "Correlation of separation factor versus permeability for polymeric membranes," *Journal of Membrane Science*, vol. 62, no. 2, pp. 165–185, 1991.

[16] L. M. Robeson, "The upper bound revisited," *Journal of Membrane Science*, vol. 320, no. 1–2, pp. 390-400, 2008.

Bibliography

Aitken, C. L., William J. Koros, and Donald R. Paul. 1992. "Gas transport properties of biphenol polysulfones." *Macromolecules* 25 (14): 3651-58.

Alcoutlabi, Mataz, Lameck Banda, and G. B. McKenna. 2004. "A comparison of concentration-glasses and temperature-hyperquenched glasses: CO_2-formed glass versus temperature-formed glass." *Polymer* 45: 5629-5634.

Alcoutlabi, Mataz, Francesco Briatico-Vangosa, and G. B. McKenna. 2002. "Effect of chemical activity jumps on the viscoelastic behavior of an epoxy resin: Physical aging response in carbon dioxide pressure jumps." *Journal of Polymer Science, Part B: Polymer Physics* 40 (18): 2050-2064.

Allen, SM, V. Stannett, and HB Hopfenberg. 1981. "Noble gas transport in poly (methyl vinyl ketone) and poly (methyl vinyl ether)." *Polymer* 22 (7): 912–917.

Aubert, James H. 1998. "Solubility of carbon dioxide in polymers by the quartz crystal microbalance technique." *The Journal of Supercritical Fluids* 11 (3): 163-172.

Baker, Elizabeth A, Perla Rittigstein, John M Torkelson, and Connie B Roth. 2009. "Streamlined ellipsometry procedure for characterizing physical aging rates of thin polymer films." *Journal of Polymer Science, Part B: Polymer Physics* 47 (24): 2509-2519.

Baker, Richard W, and Kaaeid Lokhandwala. 2008. "Natural Gas Processing with Membranes: An Overview." *Industrial and Engineering Chemistry Research* 47 (7): 2109-2121.

Barillas, Mary Katharine, Robert M. Enick, Michael O'Brien, Robert Perry, David R. Luebke, and Bryan D. Morreale. 2011. "The CO_2 permeability and mixed gas CO_2/H_2 selectivity of membranes composed of CO_2-philic polymers." *Journal of Membrane Science* 372 (1-2): 29-39.

Barsema, J N, S D Klijnstra, J H Balster, NFA van der Vegt, GH Koops, and Matthias Wessling. 2004. "Intermediate polymer to carbon gas separation membranes based on Matrimid PI." *Journal of Membrane Science* 238 (1-2): 93-102.

Berens, A.R. 1977. "Diffusion and relaxation in glassy polymer powders: 1. Fickian diffusion of vinyl chloride in poly (vinyl choride)." *Polymer* 18: 697-704.

———. 1978. "Analysis of transport behavior in polymer powders." *Journal of Membrane Science* 3 (2-3-4): 247-64.

———. 1980. "Gravimetric and Volumetric Study of the Sorption of Gases and Vapors in Poly(Vinyl Chloride) Powders." *Polymer Engineering and Science* 20 (1): 95-101.

———. 1990. "Transport of plasticizing penetrants in glassy polymers." *ACS Symposium Series: Barrier Polymer Structures* 423: 92-110.

Berens, A.R., and H.B. Hopfenberg. 1978. "Diffusion and relaxation in glassy polymer powders: 2. Separation of diffusion and relaxation parameters." *Polymer* 19: 489-96.

———. 1979. "Induction and measurement of glassy state relaxations by vapor sorption techniques." *Journal of Polymer Science, Part B: Polymer Physics* 17: 1757-70.

Bolton, Barbara A., S. Kint, G. F. Bailey, and James R. Scherer. 1986. "Ethanol sorption and partial molar volume in cellulose acetate films." *The Journal of Physical Chemistry* 90 (6): 1207-1211.

Bondi, A. 1964. "Van der Waals Volumes and Radii." *Journal of Physical Chemistry* 68 (3): 441-451.

———. 1968. *Physical Properties of Molecular Crystals, Liquids, and Glasses*. New York: John Wiley & Sons.

Bos, A., I G M Pünt, Matthias Wessling, and H Strathmann. 1998. "Plasticization-resistant glassy polyimide membranes for CO_2/CH_4 separations." *Separation and Purification Technology* 14 (1-3): 27-39.

———. 1999. "CO_2-induced plasticization phenomena in glassy polymers." *Journal of Membrane Science* 155 (1): 67-78.

Bos, A., I. Pünt, H. Strathmann, and Matthias Wessling. 2001. "Suppression of gas separation membrane plasticization by homogeneous polymer blending." *AIChE Journal* 47 (5): 1088-1093.

Budd, P, N Mckeown, B Ghanem, K Msayib, D Fritsch, L Starannikova, N Belov, O Sanfirova, Y Yampolskii, and V Shantarovich. 2008. "Gas permeation parameters and other physicochemical properties of a polymer of intrinsic microporosity: Polybenzodioxane PIM-1." *Journal of Membrane Science* 325 (2) (December 1): 851-860.

Budd, Peter M, Bader S Ghanem, Saad Makhseed, Neil B McKeown, Kadhum J Msayib, and Carin E Tattershall. 2004. "Polymers of intrinsic microporosity (PIMs): robust, solution-processable, organic nanoporous materials." *Chemical Communications* (2): 230-231.

Budd, Peter M, Neil B McKeown, and Detlev Fritsch. 2005. "Free volume and intrinsic microporosity in polymers." *Journal of Materials Chemistry* 15 (20): 1977-1986.

Chen, Chien-Chiang, Wulin Qiu, Stephen J. Miller, and William J. Koros. 2011. "Plasticization-resistant hollow fiber membranes for CO_2/CH_4 separation based on a thermally crosslinkable polyimide." *Journal of Membrane Science* 382 (1-2): 212-221.

Chen, Hongmin, M.L. Cheng, YC Jean, L.J. Lee, and Jintao Yang. 2008. "Effect of CO_2 exposure on free volumes in polystyrene studied by positron annihilation spectroscopy." *Journal of Polymer Science, Part B: Polymer Physics* 46 (4): 388–405.

Chern, R.T., F.R. Sheu, L. Jia, V.T. Stannett, and H.B. Hopfenberg. 1987. "Transport of gases in unmodified and arylbrominated 2,6-dimethyl- 1,4-poly (phenylene oxide)." *Journal of Membrane Science* 35 (1) (December 15): 103-115.

Chern, R.T., and C. N. Provan. 1991. "Gas-induced plasticization and the permselectivity of poly(tetrabromophenolphthalein terephthalate) to a mixture of carbon dioxide and methane." *Macromolecules* 24 (9): 2203-2207.

Chiou, J.S., J.W. Barlow, and Donald R. Paul. 1985. "Plasticization of Glassy Polymers by Co2." *Journal of Applied Polymer Science* 30 (6): 2633-2642.

Chiou, J.S., Yasushi Maeda, and Donald R. Paul. 1985. "Gas and vapor sorption in polymers just below Tg." *Journal of Applied Polymer Science* 30 (10): 4019-4029.

Chiou, J.S., and Donald R. Paul. 1986. "Sorption and transport of CO_2 in PVF2/PMMA Blends." *Journal of Applied Polymer Science* 32 (1): 2897-2918.

———. 1987. "Effects of carbon dioxide exposure on gas transport of properties of glassy polymers." *Journal of Membrane Science* 32: 195-205.

Chung, Tai-Shung, Chun Cao, and Rong Wang. 2004. "Pressure and temperature dependence of the gas-transport properties of dense poly[2,6-toluene-2,2-bis(3,4dicarboxylphenyl)hexafluoropropane diimide] membranes." *Journal of Polymer Science, Part B: Polymer Physics* 42 (2): 354-364.

Chung, Tai-Shung, Sun Sun Chan, Rong Wang, Zhihua Lu, and Chaobin He. 2003. "Characterization of permeability and sorption in Matrimid/C60 mixed matrix membranes." *Journal of Membrane Science* 211 (1): 91-99.

Cui, Lili, Wulin Qiu, D.R. Paul, and William J. Koros. 2011a. "Responses of 6FDA-based polyimide thin membranes to CO_2 exposure and physical aging as monitored by gas permeability." *Polymer* 52 (24): 5528-5537.

Cui, Lili, Wulin Qiu, Donald R. Paul, and William J. Koros. 2011b. "Physical aging of 6FDA-based polyimide membranes monitored by gas permeability." *Polymer* 52: 3374-3380.

Curro, John G, R R Lagasse, and Robert Simha. 1982. "Diffusion model for volume recovery in glasses." *Macromolecules* 15 (6): 1621-1626.

David, OC, Daniel Gorri, Inmaculada Ortiz, and AM Urtiaga. 2011. "Dual-sorption model for H_2/CO_2 permeation in glassy polymeric Matrimid membrane." *Desalination and Water Treatment* 27: 31–36.

David, Oana Cristina, Daniel Gorri, Ana Urtiaga, and Inmaculada Ortiz. 2011. "Mixed gas separation study for the hydrogen recovery from H_2/CO/N2/CO_2 post combustion mixtures using a Matrimid membrane." *Journal of Membrane Science* 378 (1-2): 359-368.

Despotopoulou, M. M., R. D. Miller, J. F. Rabolt, and C. W. Frank. 1996. "Polymer chain organization and orientation in ultrathin films: A spectroscopic investigation." *Journal of Polymer Science Part B: Polymer Physics* 34 (14): 2335-2349.

Dorkenoo, Kokou D, and P.H. Pfromm. 1999. "Experimental evidence and theoretical analysis of physical aging in thin and thick amorphous glassy polymer films." *Journal of Polymer Science, Part B: Polymer Physics* 37 (16): 2239-2251.

———. 2000. "Accelerated Physical Aging of Thin Poly[1-(trimethylsilyl)-1-propyne] Films." *Macromolecules* 33 (10): 3747-3751.

Drozdov, A.D. 2001. "The effect of temperature on physical aging of glassy polymers." *Journal of Applied Polymer Science* 81 (13): 3309-3320.

Efremov, Mikhail Yu., Anna V. Kiyanova, and Paul F. Nealey. 2008. "Temperature-Modulated Ellipsometry: A New Probe for Glass Transition in Thin Supported Polymer Films." *Macromolecules* 41 (16): 5978-5980.

El-Azzami, Louei A, and Eric A Grulke. 2007. "Dual mode model for mixed gas permeation of CO_2, H_2, and N2 through a dry chitosan membrane." *Journal of Polymer Science, Part B: Polymer Physics* 45 (18): 2620-2631.

Emmler, Thomas, Kathleen Heinrich, Detlev Fritsch, Peter M. Budd, Nhamo Chaukura, Dennis Ehlers, Klaus Rätzke, and Franz Faupel. 2010. "Free Volume Investigation of Polymers of Intrinsic Microporosity (PIMs): PIM-1 and PIM1 Copolymers Incorporating Ethanoanthracene Units." *Macromolecules* 43: 6075-6085.

Feynman, Richard P., Robert B. Leighton, and Matthew Sands. 1963. *The Feynman Lectures on Physics*. Reading, MA: Addison-Wesley Publishing Company, Inc.

Forrest, Ja, K Dalnoki-Veress, Jr Stevens, and Jr Dutcher. 1996. "Effect of Free Surfaces on the Glass Transition Temperature of Thin Polymer Films." *Physical Review Letters* 77 (10) (September 2): 2002-2005.

Ghanem, Bader S., Neil B. McKeown, Peter M. Budd, Nasser M. Al-Harbi, Detlev Fritsch, Kathleen Heinrich, Ludmila Starannikova, Andrei Tokarev, and Yuri Yampolskii. 2009. "Synthesis, Characterization, and Gas Permeation Properties of a Novel Group of Polymers with Intrinsic Microporosity: PIM-Polyimides." *Macromolecules* 42 (20): 7881-7888.

Graham, T. 1866. "On the absorption and dialytic separation of gases by colloid septa." *Philosophical Magazine* 32: 401-420.

Guo, Juchen, and Timothy a. Barbari. 2010. "A dual mode interpretation of the kinetics of penetrant-induced swelling and deswelling in a glassy polymer." *Polymer* 51 (22): 5145-5150.

Henis, J., and M.K. Tripodi. 1983. "The developing technology of gas separating membranes." *Science* 220 (4592): 11-17.

Higuchi, Akon, Tadashi Nakajima, Atsushi Morisato, Michiaki Ando, Kazukiyo Nagai, and Tsutomu Nakagawa. 1996. "Estimation of diffusion and permeability coefficients of CO_2 in polymeric membranes by FTIR method." *Journal of Polymer Science, Part B: Polymer Physics* 34 (13) (September 30): 2153-2160.

Hill, Anita J., K J Heater, and C M Agrawal. 1990. "The Effects of Physical Aging in Polycarbonate." *Journal of Polymer Science, Part B: Polymer Physics* 28 (3): 387-405.

Hillock, Alexis M W, Stephen J Miller, and William J. Koros. 2008. "Crosslinked mixed matrix membranes for the purification of natural gas: Effects of sieve surface modification." *Journal of Membrane Science* 314 (1-2): 193-199.

Hong, X., YC Jean, Hsinjin Yang, SS Jordan, and William J. Koros. 1996. "Free-volume hole properties of gas-exposed polycarbonate studied by positron annihilation lifetime spectroscopy." *Macromolecules* 29 (24): 7859–7864.

Horn, Norman R., and D.R. Paul. 2011a. "Carbon dioxide plasticization of thin glassy polymer films." *Polymer* 52 (24): 5587-5594.

Horn, Norman R., and Donald R. Paul. 2011b. "Carbon dioxide plasticization and conditioning effects in thick vs. thin glassy polymer films." *Polymer* 52 (7) (February 12): 1619-1627.

Houde, A. Y., B. Krishnakumar, S. G. Charati, and S. A. Stern. 1996. "Permeability of dense (homogeneous) cellulose acetate membranes to methane, carbon dioxide, and their mixtures at elevated pressures." *Journal of Applied Polymer Science* 62 (13) (December 26): 2181-2192.

Huang, Y., X Wang, and Donald R. Paul. 2006. "Physical aging of thin glassy polymer films: Free volume interpretation." *Journal of Membrane Science* 277 (1-2): 219-229.

Huang, Y., and Donald R. Paul. 2004a. "Physical aging of thin glassy polymer films monitored by gas permeability." *Polymer* 45: 8377-8393.

———. 2004b. "Experimental methods for tracking physical aging of thin glassy polymer films by gas permeation." *Journal of Membrane Science* 244: 167-178.

———. 2005. "Effect of Temperature on Physical Aging of Thin Glassy Polymer Films." *Macromolecules* 38 (24): 10148-10154.

———. 2006. “Physical Aging of Thin Glassy Polymer Films Monitored by Optical Properties.” *Macromolecules* 39 (4): 1554-1559.

———. 2007. “Effect of Film Thickness on the Gas-Permeation Characteristics of Glassy Polymer Membranes.” *Industrial and Engineering Chemistry Research* 46 (8): 2342-2347.

Hutchinson, J M. 1995. “Physical Aging of Polymers.” *Progress in Polymer Science* 20 (4): 703-760.

Ismail, A F, and W Lorna. 2002. “Penetrant-induced plasticization phenomenon in glassy polymers for gas separation membrane.” *Separation and Purification Technology* 27 (3): 173-194.

J.A. Woollam Company. 2001. Ex Situ Data Analysis. In *Guide to Using WVASE32*.

Jordan, SM, William J. Koros, and GK Fleming. 1987. “The effects of CO_2 exposure on pure and mixed gas permeation behavior: comparison of glassy polycarbonate and silicone rubber.” *Journal of Membrane Science* 30 (2): 191–212.

Kanehashi, S, T Nakagawa, K Nagai, X Duthie, S Kentish, and G Stevens. 2007. “Effects of carbon dioxide-induced plasticization on the gas transport properties of glassy polyimide membranes.” *Journal of Membrane Science* 298 (1-2): 147-155.

Keddie, J. L, R. A. L Jones, and R. A Cory. 1994. “Size-Dependent Depression of the Glass Transition Temperature in Polymer Films.” *Europhysics Letters (EPL)* 27 (1) (July 1): 59-64.

Keddie, Joseph L., Richard A. L. Jones, and Rachel A. Cory. 1994. “Interface and surface effects on the glass-transition temperature in thin polymer films.” *Faraday Discussions* 98 (January 1): 219.

Kelman, Scott D, Scott Matteucci, Christopher W Bielawski, and Benny D Freeman. 2007. “Crosslinking poly(1-trimethylsilyl-1-propyne) and its effect on solvent resistance and transport properties.” *Polymer* 48 (23): 6881-6892.

Kim, J.H., William J. Koros, and Donald R. Paul. 2006a. “Physical aging of thin 6FDA-based polyimide membranes containing carboxyl acid groups. Part II. Optical properties.” *Polymer* 47 (9): 3104-3111.

———. 2006b. “Effects of CO_2 exposure and physical aging on the gas permeability of thin 6FDA-based polyimide membranes. Part 2. with crosslinking.” *Journal of Membrane Science* 282 (1-2): 32-43.

———. 2006c. “Effects of CO_2 exposure and physical aging on the gas permeability of thin 6FDA-based polyimide membranes Part 1. Without crosslinking.” *Journal of Membrane Science* 282 (1-2): 21-31.

———. 2006d. “Physical aging of thin 6FDA-based polyimide membranes containing carboxyl acid groups. Part I. Transport properties.” *Polymer* 47 (9): 3094–3103.

Kim, Jae Hyun, Jyongsik Jang, and Wang-Cheol Zin. 2001. "Thickness Dependence of the Melting Temperature of Thin Polymer Films." *Macromolecular Rapid Communications* 22 (6) (March 1): 386-389.

Kim, S, S a Hewlett, C B Roth, and J M Torkelson. 2009. "Confinement effects on glass transition temperature, transition breadth, and expansivity: comparison of ellipsometry and fluorescence measurements on polystyrene films." *The European Physical Journal E, Soft Matter* 30 (1): 83-92.

Koros, William J. 1978. "Personal communication." *Personal communication*.

Koros, William J., Donald R. Paul, M. Fujii, H.B. Hopfenberg, and V. Stannett. 1977. "Effect of Pressure on Co2 Transport in Poly(Ethylene-Terephthalate)." *Journal of Applied Polymer Science* 21 (11): 2899-2904.

Koros, William J., Donald R. Paul, and A A Rocha. 1976. "Carbon dioxide sorption and transport in polycarbonate." *Journal of Polymer Science, Part B: Polymer Physics* 14 (4): 687–702.

Koros, William J., and Donald R. Paul. 1980. "Sorption and Transport of CO_2 Above and Below the Glass Transition of Poly (Ethylene Terephthalate)." *Polymer Engineering and Science* 20 (1): 14-19.

Kovacs, A.J., J M Hutchinson, and J.J. Aklonis. 1977. Isobaric volume and enthalpy recovery in glasses. (I) A critical survey of recent phenomenological approaches. In *The Structure of Non-Crystalline Materials*, 153-163. London: Taylor & Francis.

Kratochvil, Adam M., Shilpa Damle-Mogri, and William J. Koros. 2009. "Effects of Supercritical CO_2 Conditioning on Un-Cross-Linked Polyimide Membranes for Natural Gas Purification." *Macromolecules* 42 (15): 5670-5675.

Kratochvil, Adam M., and William J. Koros. 2010. "Effects of Supercritical CO_2 Conditioning on Cross-Linked Polyimide Membranes." *Macromolecules* 43 (10): 4679-4687.

Van Krevelen, D.W. 1990. *Properties of Polymers*. 3rd ed. New York: Elsevier.

Kumins, C. A., and T. K. Kwei. 1968. Free Volume and Other Theories. In *Diffusion in Polymers*, ed. J. Crank and G. S. Park, 107-140. London: Academic Press.

Lee, Jong Suk, W.C. Madden, and William J. Koros. 2010a. "Antiplasticization and plasticization of Matrimid® asymmetric hollow fiber membranes. Part A. Experimental." *Journal of Membrane Science* 350 (1-2): 232-241.

———. 2010b. "Antiplasticization and plasticization of Matrimid® asymmetric hollow fiber membranes. Part B. Modeling." *Journal of Membrane Science* 350 (1-2): 242-251.

Lee, W. M. 1980. "Selection of barrier materials from molecular structure." *Polymer Engineering and Science* 20 (1): 65-69.

Lide, David R. 1997. *CRC Handbook of Chemistry and Physics*. Ed. David R. Lide. 78th ed. New York: CRC Press.

Lima de Miranda, Rodrigo, Jan Kruse, Klaus Rätzke, Franz Faupel, Detlev Fritsch, Volker Abetz, Peter M. Budd, James D. Selbie, Neil B. McKeown, and Bader S. Ghanem. 2007. "Unusual temperature dependence of the positron lifetime in a polymer of intrinsic microporosity." *Physica Status Solidi (RRL) – Rapid Research Letters* 1 (5): 190-192.

Madden, W.C., David Punsalan, and William J. Koros. 2005. "Age dependent CO_2 sorption in Matrimid® asymmetric hollow fiber membranes." *Polymer* 46 (15): 5433-5436.

Maeda, Yasushi. 1985. *Ph.D. Dissertation, University of Texas at Austin*.

Maeda, Yasushi, and Donald R. Paul. 1985. "Selective gas transport in miscible PPO-PS blends." *Polymer* 26 (13): 2055-2063.

———. 1987a. "Effect of antiplasticization on gas sorption and transport. III. Free volume interpretation." *Journal of Polymer Science, Part B: Polymer Physics* 25 (5): 1005-1016.

Maeda, Yasushi, and Donald R. Paul. 1987b. "Effect of antiplasticization on gas sorption and transport. II. Poly(phenylene oxide)." *Journal of Polymer Science, Part B: Polymer Physics* 25 (5): 981-1003.

Maeda, Yasushi, and Donald R. Paul. 1987. "Effect of antiplasticization on gas sorption and transport. III. Free volume interpretation." *Journal of Polymer Science, Part B: Polymer Physics* 25 (5): 1005-1016.

Mallon, P. E. 2003. Application to Polymers. In *Positron and Positronium Chemistry*, ed. Y. C. Jean, P. E. Mallon, and D. M. Schrader, 253-280. New Jersey: World Scientific.

Mark, James E. 2009. *Polymer Data Handbook*. 2nd Edition. Oxford, UK: Oxford University Press.

Matteucci, Scott, Yuri Yampolskii, Benny D. Freeman, and Ingo Pinnau. 2006. Transport of Gases and Vapors in Glassy and Rubbery Polymers. In *Materials Science of Membranes for Gas and Vapor Separation*, 1-48.

McCaig, M S, Donald R. Paul, and J.W. Barlow. 2000. "Effect of film thickness on the changes in gas permeability of a glassy polyarylate due to physical aging. Part II. Mathematical Model." *Polymer* 41: 639-648.

McCaig, M S, and Donald R. Paul. 2000. “Effect of film thickness on the changes in gas permeability of a glassy polyarylate due to physical aging. Part I. Experimental Observations.” *Polymer* 41: 629-637.

McHattie, J S, William J. Koros, and Donald R. Paul. 1991. “Gas transport properties of polysulphones: 1. Role of symmetry of methyl group placement on bisphenol rings.” *Polymer* 32 (5): 840-850.

McKenna, G. B. 2007. “Glassy states: Concentration glasses and temperature glasses compared.” *Journal of Non-Crystalline Solids* 353 (41-43): 3820-3828.

McKeown, Neil B, Peter M Budd, Kadhum J Msayib, Bader S Ghanem, Helen J Kingston, Carin E Tattershall, Saad Makhseed, Kevin J Reynolds, and Detlev Fritsch. 2005. “Polymers of Intrinsic Microporosity (PIMs): Bridging the Void between Microporous and Polymeric Materials.” *Chemistry - A European Journal* 11 (9): 2610-2620.

Mi, Y., S. Zhou, and S.A. Stern. 1991. “Representation of gas solubility in glassy polymers by a concentration-temperature superposition principle.” *Macromolecules* 24 (9): 2361-2367.

Michels, A., and J. Hamers. 1937. “The effect of pressure on the refractive index of CO_2:: The Lorentz-Lorenz formula.” *Physica* 4 (10): 995–1006.

Mitchell, J.K. 1995. “On the Penetrativeness of Fluids.” *Journal of Membrane Science* 100: 11-16.

Miura, Kei-ichi, Katsuto Otake, Shigeru Kurosawa, Takeshi Sako, Tsutomu Sugeta, Takashi Nakane, Masahito Sato, Tomoya Tsuji, Toshihiko Hiaki, and Masaru Hongo. 1998. “Solubility and adsorption of high pressure carbon dioxide to polystyrene.” *Fluid Phase Equilibria* 144 (1-2): 181-189.

Moore, Theodore T., and William J. Koros. 2007. “Gas sorption in polymers, molecular sieves, and mixed matrix membranes.” *Journal of Applied Polymer Science* 104 (6): 4053–4059.

Morel, G, and Donald R Paul. 1982. “CO_2 sorption and transport in miscible poly(phenylene oxide)/polystyrene blends.” *Journal of Membrane Science* 10 (2-3): 273-282.

Neyertz, S., D. Brown, Sudharsan Pandiyan, and NFA van der Vegt. 2010. “Carbon Dioxide Diffusion and Plasticization in Fluorinated Polyimides.” *Macromolecules* 43 (18): 7813-7827.

Pandiyan, Sudharsan, David Brown, S. Neyertz, and NFA van der Vegt. 2010. “Carbon Dioxide Solubility in Three Fluorinated Polyimides Studied by Molecular Dynamics Simulations.” *Macromolecules* 43 (5): 2605-2621.

Pantoula, Maria, and Costas Panayiotou. 2006. "Sorption and swelling in glassy polymer/carbon dioxide systems. Part I--Sorption." *The Journal of Supercritical Fluids* 37 (2): 254-262.

Park, Ho Bum, Sang Hoon Han, Chul Ho Jung, Young Moo Lee, and Anita J. Hill. 2010. "Thermally rearranged (TR) polymer membranes for CO_2 separation." *Journal of Membrane Science* 359 (1-2): 11-24.

Park, Ho Bum, Chul Ho Jung, Young Moo Lee, Anita J. Hill, Steven J Pas, Stephen T Mudie, Elizabeth Van Wagner, Benny D Freeman, and David J Cookson. 2007. "Polymers with cavities tuned for fast selective transport of small molecules and ions." *Science* 318 (5848): 254-8.

Park, J.Y., and D.R. Paul. 1997. "Correlation and prediction of gas permeability in glassy polymer membrane materials via a modified free volume based group contribution method." *Journal of Membrane Science* 125 (1): 23-39.

Paul, Donald R. 1984. "Gas transport in homogeneous multicomponent polymers." *Journal of Membrane Science* 18: 75-86.

Paul, Donald R. 2010. In *Comprehensive Membrane Science and Technology, Volume 1*, ed. E. Drioli and L. Giorno, 75-90. Oxford: Academic Press.

Paul, Donald R. 2012. "Personal communication."

Peter, J, and Klaus-Viktor Peinemann. 2009. "Multilayer composite membranes for gas separation based on crosslinked PTMSP gutter layer and partially crosslinked Matrimid® 5218 selective layer." *Journal of Membrane Science* 340 (1-2): 62-72.

Pfromm, P.H. 1994. "Gas transport properties and aging of thin and thick films made from amorphous glassy polymers." *PhD Thesis, University of Texas at Austin*.

Pfromm, P.H., and William J. Koros. 1995. "Accelerated physical ageing of thin glassy polymer films: evidence from gas transport measurements." *Polymer* 36 (12): 2379-2387.

Puleo, A. C., N. Muruganandam, and Donald R. Paul. 1989. "Gas sorption and transport in substituted polystyrenes." *Journal of Polymer Science, Part B: Polymer Physics* 27 (11): 2385-2406.

Puleo, A. C., Donald R. Paul, and S. S. Kelley. 1989. "The effect of degree of acetylation on gas sorption and transport behavior in cellulose acetate." *Journal of Membrane Science* 47 (3): 301-332.

Pye, Justin E, Kate A Rohald, Elizabeth A Baker, and Connie B Roth. 2010. "Physical Aging in Ultrathin Polystyrene Films: Evidence of a Gradient in Dynamics at the Free Surface and Its Connection to the Glass Transition Temperature Reductions." *Macromolecules* 43 (19): 8296-8303.

Raegen, A N, M V Massa, J A Forrest, and K Dalnoki-Veress. 2008. "Effect of atmosphere on reductions in the glass transition of thin polystyrene films." *The European Physical Journal E, Soft Matter* 27 (4) (November 20): 375-377.

Robeson, Lloyd M. 1991. "Correlation of separation factor versus permeability for polymeric membranes." *Journal of Membrane Science* 62 (2): 165–185.

Robeson, Lloyd M. 2008. "The upper bound revisited." *Journal of Membrane Science* 320 (1-2): 390-400.

Ronova, Inga a., Egor M. Rozhkov, Alexander Yu. Alentiev, and Yurii P. Yampolskii. 2003. "Occupied and Accessible Volumes in Glassy Polymers and Their Relationship with Gas Permeation Parameters." *Macromolecular Theory and Simulations* 12 (6): 425-439.

Roth, Connie B., and J R Dutcher. 2003. "Glass transition temperature of freely-standing films of atactic poly(methyl methacrylate)." *The European Physical Journal E, Soft Matter* 12 (1): S103-7.

Rowe, Brandon W., Benny D Freeman, and Donald R. Paul. 2007. "Effect of Sorbed Water and Temperature on the Optical Properties and Density of Thin Glassy Polymer Films on a Silicon Substrate." *Macromolecules* 40 (8): 2806-2813.

———. 2009. "Physical aging of ultrathin glassy polymer films tracked by gas permeability." *Polymer* 50 (23): 5565-5575.

Rowe, Brandon W., Benny D. Freeman, and Donald R. Paul. 2010. "Influence of previous history on physical aging in thin glassy polymer films as gas separation membranes." *Polymer* 51 (16): 3784-3792.

Rowe, Brandon W., Steven J. Pas, Anita J. Hill, Ryoichi Suzuki, Benny D. Freeman, and D.R. Paul. 2009. "A variable energy positron annihilation lifetime spectroscopy study of physical aging in thin glassy polymer films." *Polymer* 50 (25): 6149-6156.

Royal, J. Scot, and John M Torkelson. 1993. "Physical aging effects on molecular-scale polymer relaxations monitored with mobility-sensitive fluorescent molecules." *Macromolecules* 26 (20): 5331-5335.

Sanchez, Isaac C, and Junhan Cho. 1995. "A universal equation of state for polymer liquids." *Polymer* 36 (15): 2929-2939.

Sanders, E.S. 1988. "Penetrant-induced plasticization and gas permeation in glassy polymers." *Journal of Membrane Science* 37 (1): 63–80.

Sanders, E.S., William J. Koros, H.B. Hopfenberg, and V.T. Stannett. 1984. "Pure and mixed gas sorption of carbon dioxide and ethylene in poly (methyl methacrylate)." *Journal of Membrane Science* 18: 53–74.

Scherer, J.R., and G.F. Bailey. 1983. “Water in polymer membranes. Part I: Water sorption and refractive index of cellulose acetate.” *Journal of Membrane Science* 13 (1): 29–41.

Scherer, James R. 1987. “The partial molar volume of water in biological membranes.” *Proceedings of the National Academy of Sciences of the United States of America* 84 (22): 7938-42.

Scholes, Colin A, George Q Chen, Geoff W Stevens, and Sandra E Kentish. 2010. “Plasticization of ultra-thin polysulfone membranes by carbon dioxide.” *Journal of Membrane Science* 346 (1): 208-214.

Scholes, Colin A, Wen Xian Tao, Geoff W Stevens, and Sandra E Kentish. 2010. “Sorption of methane, nitrogen, carbon dioxide, and water in Matrimid 5218.” *Journal of Applied Polymer Science* 117 (2): 2284-2289.

Shao, L, Tai-Shung Chung, S Goh, and K Pramoda. 2005. “Polyimide modification by a linear aliphatic diamine to enhance transport performance and plasticization resistance.” *Journal of Membrane Science* 256: 46-56.

Simon, F. 1930. *Ergeg. Exaxt. Naturw.* 9: 222.

———. 1931. *Zeitschrift fur anorganische und allgemeine Chemie* 203: 220.

Simons, Katja, Kitty Nijmeijer, Jordi Guilera Sala, Hans van der Werf, Nieck E. Benes, Theo J. Dingemans, and Matthias Wessling. 2010. “CO_2 sorption and transport behavior of ODPA-based polyetherimide polymer films.” *Polymer* 51 (17): 3907-3917.

Sirard, S M, Peter F Green, and Keith P. Johnston. 2001. “Spectroscopic Ellipsometry Investigation of the Swelling of Poly(Dimethylsiloxane) Thin Films with High Pressure Carbon Dioxide.” *Journal of Physical Chemistry B* 105 (4): 766-772.

Stagg, B. J., and T. T. Charalampopoulos. 1993. “A method to account for window birefringence effects on ellipsometry analysis.” *Journal of Physics D: Applied Physics* 26 (11): 2028-35.

Stamatialis, Dimitrios F., M Wessling, M Sanopoulou, H Strathmann, and J H Petropoulos. 1997. “Optical vs . direct sorption and swelling measurements for the study of stiff-chain polymer-penetrant interactions.” *Journal of Membrane Science* 130: 75-83.

Stern, S.A., and V. Saxena. 1980. “Concentration-dependent transport of gases and vapors in glassy polymers.” *Journal of Membrane Science* 7: 47-59.

Stone, Matthew T., Pieter J. In ’T Veld, Ying Lu, and Isaac C. Sanchez. 2002. “Hydrophobic/hydrophilic solvation: inferences from Monte Carlo simulations and experiments.” *Molecular Physics* 100 (17) (September 10): 2773-2792.

Struik, L. C. E. 1978. *Physical Aging in Amorphous Polymers and Other Materials*. *Physical Aging in Amorphous Polymers and Other Materials*. Vol. 54. Amsterdam, The Netherlands: Elsevier Scientific Publishing Company, April.

Tan, N. C. Beck, W. L. Wu, W. E. Wallace, and G. T. Davis. 1998. "Interface effects on moisture absorption in ultrathin polyimide films." *Journal of Polymer Science, Part B: Polymer Physics* 36 (1) (January 15): 155-162.

Tin, P S, Tai-Shung Chung, Y Liu, R Wang, S L Liu, and Kumari Pallathadka Pramoda. 2003. "Effects of cross-linking modification on gas separation performance of Matrimid membranes." *Journal of Membrane Science* 225: 77-90.

Vieth, W.R., J.M. Howell, and J.H. Hsieh. 1976. "Dual sorption theory." *Journal of Membrane Science* 1: 177-220.

Visser, T., GH Koops, and Matthias Wessling. 2005. "On the subtle balance between competitive sorption and plasticization effects in asymmetric hollow fiber gas separation membranes." *Journal of Membrane Science* 252 (1-2): 265-277.

Visser, T., N Masetto, and Matthias Wessling. 2007. "Materials dependence of mixed gas plasticization behavior in asymmetric membranes." *Journal of Membrane Science* 306 (1-2): 16-28.

Visser, T., and Matthias Wessling. 2007. "When Do Sorption-Induced Relaxations in Glassy Polymers Set In?" *Macromolecules* 40 (14): 4992-5000.

———. 2008. "Auto and mutual plasticization in single and mixed gas C3 transport through Matrimid-based hollow fiber membranes." *Journal of Membrane Science* 312 (1-2) (April 1): 84-96.

Ward, Jason K., and William J. Koros. 2011a. "Crosslinkable mixed matrix membranes with surface modified molecular sieves for natural gas purification: I. Preparation and experimental results." *Journal of Membrane Science* 377 (1-2): 75-81.

———. 2011b. "Crosslinkable mixed matrix membranes with surface modified molecular sieves for natural gas purification: II. Performance characterization under contaminated feed conditions." *Journal of Membrane Science* 377 (1-2): 82-88.

Weber, Jens, Qi Su, Markus Antonietti, and Arne Thomas. 2007. "Exploring Polymers of Intrinsic Microporosity – Microporous, Soluble Polyamide and Polyimide." *Macromolecular Rapid Communications* 28 (18–19): 1871-1876.

Weireld, G De, M Frère, and R Jadot. 1999. "Automated determination of high-temperature and high-pressure gas adsorption isotherms using a magnetic suspension balance." *Meas. Sci. & Tech.* 10 (2) (February 1): 117-126.

Wessling, Matthias, M L Lopez, and H Strathmann. 2001. "Accelerated plasticization of thin-film composite membranes used in gas separation." *Separation and Purification Technology* 24 (1-2): 223-233.

Wessling, Matthias, S. Schoeman, T. van der Boomgaard, and C.A. Smolders. 1991. "Plasticization of gas separation membranes." *Gas Separation and Purification* 5 (4): 222-228.

Wind, John D., Donald R. Paul, and William J. Koros. 2004. "Natural gas permeation in polyimide membranes." *Journal of Membrane Science* 228 (2): 227-236.

Wind, John D., S M Sirard, Donald R. Paul, Peter F Green, Keith P. Johnston, and William J. Koros. 2003a. "Relaxation dynamics of CO_2 diffusion, sorption, and polymer swelling for plasticized polyimide membranes." *Macromolecules* 36 (17): 6442-6448.

Wind, John D., S M Sirard, Donald R. Paul, Peter F. Green, Keith P. Johnston, and William J. Koros. 2003b. "Carbon Dioxide-Induced Plasticization of Polyimide Membranes: Pseudo-Equilibrium Relationships of Diffusion, Sorption, and Swelling." *Macromolecules* 36 (17): 6433-6441.

Wind, John D., Claudia Staudt-Bickel, Donald R. Paul, and William J. Koros. 2002. "The Effects of Crosslinking Chemistry on CO_2 Plasticization of Polyimide Gas Separation Membranes." *Industrial and Engineering Chemistry Research* 41 (24): 6139-6148.

Wonders, A. G., and Donald R. Paul. 1979. "Effect of CO_2 exposure history on sorption and transport in polycarbonate." *Journal of Membrane Science* 5: 63–75.

Wong, Joseph M. 1986. *Ph.D. Dissertation, University of Texas at Austin*.

von Wroblewski, S. 1879. "Ueber die natur der absorption der gase durch flussigkeiten unter hohen drucken." *Ann. Physik. u. Chem.* 8: 29-52.

Zhang, C., B. P. Cappleman, M. Defibaugh-Chavez, and D. H. Weinkauf. 2003. "Glassy polymer-sorption phenomena measured with a quartz crystal microbalance technique." *Journal of Polymer Science, Part B: Polymer Physics* 41 (18) (September 15): 2109-2118.

Zheng, Y., R. D. Priestley, and G. B. McKenna. 2004. "Physical aging of an epoxy subsequent to relative humidity jumps through the glass concentration." *Journal of Polymer Science, Part B: Polymer Physics* 42 (11): 2107-2121.

Zheng, Y., and G. B. McKenna. 2003. "Structural Recovery in a Model Epoxy: Comparison of Responses after Temperature and Relative Humidity Jumps." *Macromolecules* 36 (7): 2387-2396.

Zhou, Chun, Tai-Shung Chung, Rong Wang, Ye Liu, and Suat Hong Goh. 2003. "The accelerated CO_2 plasticization of ultra-thin polyimide films and the effect of surface chemical cross-linking on plasticization and physical aging." *Journal of Membrane Science* 225 (1-2): 125-134.

Vita

Norman Randall Horn was born in Austin, Texas on June 19, 1983. Norman moved to O'Fallon, Missouri in 1995, where his family began homeschooling and continued through high school. He graduated in 2001, and the following semester began attending the University of Missouri-Rolla (now the Missouri University of Science and Technology) to study Chemical Engineering. While an undergraduate, he interned with Science Applications International Corporation for one summer and Honeywell for three summers. He also participated in multiple undergraduate research projects, and is one of few people at UMR to have won undergraduate research awards in both the sciences and the humanities. He graduated from UMR in 2005 with a Bachelor of Science in Chemical Engineering, a second major in Chemistry, and a minor in Music. Norman enrolled in the Chemical Engineering department at the University of Texas at Austin in August, 2005 to purse his doctoral degree with Dr. Don Paul. He completed his Doctor of Philosophy in Chemical Engineering in early 2012. After graduation, Norman will work for Frontier Nanosystems in Austin, Texas as a Chemical Process Engineer and Research Associate.

Permanent email address: norman.horn@gmail.com

This dissertation was typed by the author.